Environmental Earth Sciences (2023) 82:169
https://doi.org/10.1007/s12665-023-10841-2

ORIGINAL ARTICLE

Sedimentary deposits and bioturbation in an Early Cretaceous subarctic stormy greenhouse shelf environment

Stanisław Leszczyński[1] · Michał J. Warchoł[2] · Wojciech Nemec[3]

Received: 2 December 2022 / Accepted: 5 March 2023

Abstract

This study of the Aptian lower part of the Carolinefjellet Formation in Svalbard, Norwegian high Arctic, is based on well cores and outcrop section in the Adventdalen area of Spitsbergen and reports on the deposits and bioturbation structures of an ancient subpolar marine shelf from a well-known period of global greenhouse climate. The study documents the sedimentation conditions and benthic fauna activity on a warm-water aggrading shelf subject to harsh Arctic wave climate and eurybatic base-level changes, with episodic bottom incursions of cold polar water. Lithofacies associations and 38 observed ichnotaxa represent subenvironments ranging from offshore to lower shoreface and hosting the *Cruziana* ichnofacies in its distal to proximal expression, with a brief mid-Aptian encroachment of middle shoreface zone with a distal expression of the *Skolithos* ichnofacies. The ichnofacies are variously impoverished compared to their archetypes. The sediment bioturbation intensity varies, but similar lithofacies associations show a comparable intensity throughout the stratigraphic succession, which indicates an ichnofauna ecology controlled by the seafloor hydraulic regime and oxygenation, and thus mainly by the wave climate and relative sea-level changes. Sandstone tempestites indicate high-frequency storms, commonly exceeding the magnitude of largest modern hurricane events. The study confirms that a change in global climate mode, such as the Early Cretaceous warming, entails extreme weather conditions.

Keywords Aptian · Barents Shelf · Carolinefjellet formation · Spitsbergen · Tempestites · Trace fossils

Introduction

In the last few decades, an integrated sedimentological and ichnological analysis has increasingly proven to be a most useful approach for studying sedimentary successions, as the two types of data supplement and enhance each other (Howard 1975; Savrda and Bottjer 1989, 1991; Pemberton et al. 1992a; Pemberton and Wightman 1992; Uchman 1995, 1998; Gingras et al. 1999; MacEachern et al. 1999a; McIlroy 2004; Uchman et al. 2008; Angulo and Buatois 2012). Ichnological data (Bertling et al. 2006, 2022; Seilacher 2007) allow an assessment of the palaeobathymetry, near-bottom salinity, oxygenation and sediment mobility (Seilacher 1967; Frey et al. 1990; MacEachern et al. 1992; Pemberton et al. 1992a, b; Pemberton and MacEachern 1995, 1997, 2007a; Savdra 1992, 1995; Uchman et al. 2008), whilst the corresponding sedimentological evidence allows recognition of the actual sedimentation processes in the palaeoenvironment hosting particular ichnofauna (Howard and Frey 1984; Raychaudhuri and Pemberton 1992; MacEachern and Pemberton 1992, 1994; MacEachern et al. 1999a, 2005; MacEachern and Løseth 2003; Gouramanis et al. 2003; Taylor et al. 2003; Bann et al. 2004; Uchman et al. 2007). Such integrated interdisciplinary studies have revealed, for example, some strong links between the ichnofauna assemblages and dominant style of bioturbation on the one hand and the substrate type and environment hydrodynamic conditions on the other

This article is part of a Topical Collection in Environmental Earth Sciences on Earth Surface Processes and Environment in a Changing World: sustainability, Climate Change and Society, guest edited by Alberto Gomes, Horacio Garcia, Alejandro Gomez, Helder I. Chamine.

✉ Wojciech Nemec
wojtek.nemec@uib.no

[1] Institute of Geological Sciences, Jagiellonian University, 30-063 Kraków, Poland

[2] Research Centre, Equinor ASA, Sandsli, PO Box 7200, 5020 Bergen, Norway

[3] Department of Earth Science, University of Bergen, 5007 Bergen, Norway

Published online: 23 March 2023

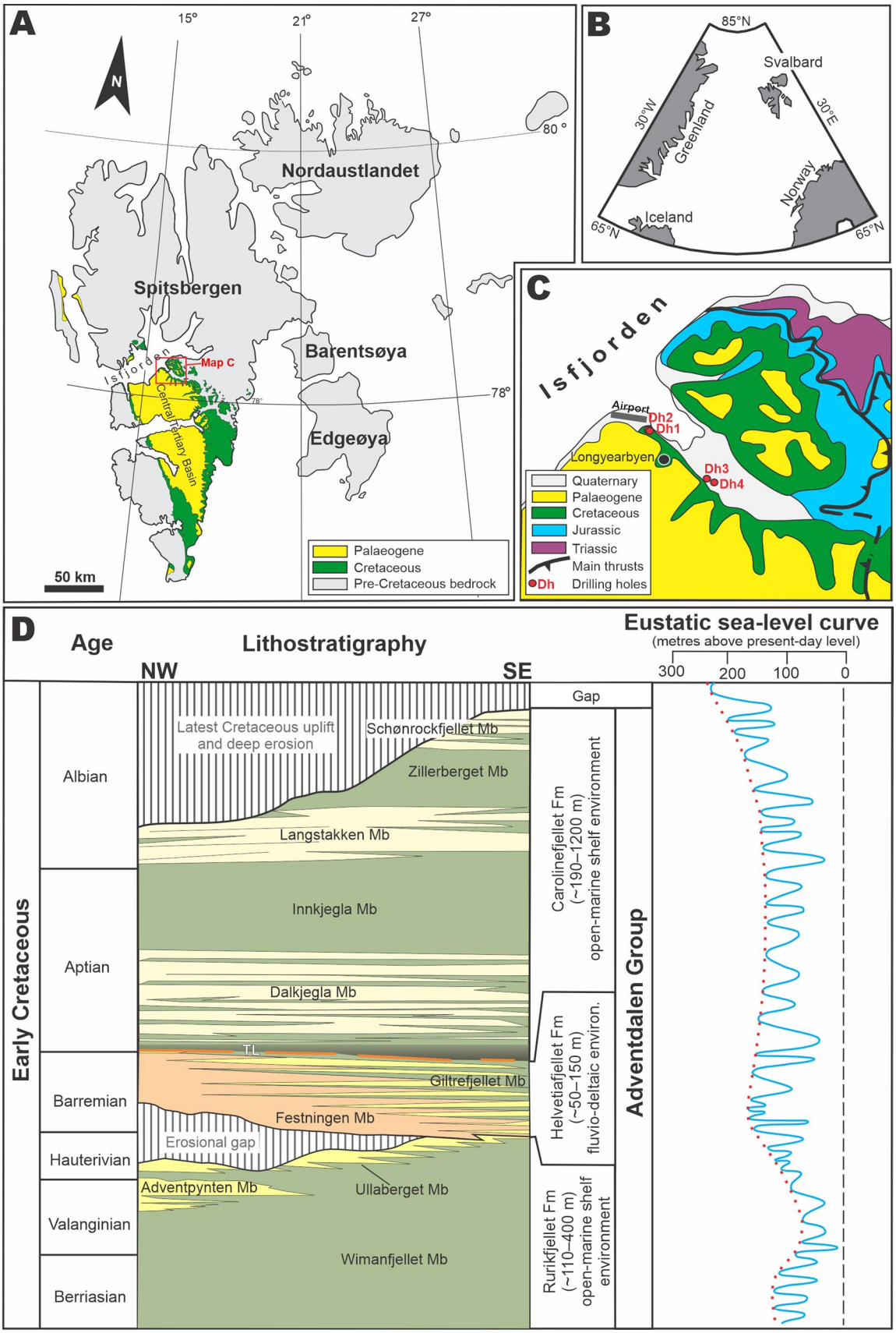
A
15°
21°
27°
N
80 °
Nordaustlandet
Spitsbergen
Barentsøya
Edgeøya
Isfjorden
Map C
Central Tertiary Basin
78°
78°
Palaeogene
Cretaceous
Pre-Cretaceous bedrock
50 km
B
85°N
Svalbard
30°W
30°E
Greenland
Norway
Iceland
65°N
65°N
C
Isfjorden
Airport
Dh2
Dh1
Longyearbyen
Dh3
Dh4
Quaternary
Palaeogene
Cretaceous
Jurassic
Triassic
Main thrusts
Dh Drilling holes
D
Age
Lithostratigraphy
NW
SE
Eustatic sea-level curve
(metres above present-day level)
300
200
100
0
Early Cretaceous
Albian
Aptian
Barremian
Hauterivian
Valanginian
Berriasian
Latest Cretaceous uplift and deep erosion
Schønrockfjellet Mb
Zillerberget Mb
Langstakken Mb
Innkjegla Mb
Dalkjegla Mb
TL
Giltrefjellet Mb
Festningen Mb
Erosional gap
Adventpynten Mb
Ullaberget Mb
Wimanfjellet Mb
Gap
Carolinefjellet Fm (~190–1200 m) open-marine shelf environment
Helvetiafjellet Fm (~50–150 m) fluvio-deltaic environ.
Rurikfjellet Fm (~110–400 m) open-marine shelf environment
Adventdalen Group

◂**Fig. 1** **A** Map of the Svalbard archipelago showing the outcrop of Cretaceous in Spitsbergen (after Hjelle 1993). **B** The present-day location of Svalbard in the arctic part of North Atlantic province. **C** Geological map of the Adventdalen area in central Spitsbergen (after Braathen et al. 2012), showing the location of the town of Longyearbyen and the four boreholes (Dh1–Dh4) referred to in the text; the outcrop section studied is a road-cut cliff extending from the town to its airport. **D** Cretaceous stratigraphy of Spitsbergen (after Mørk et al. 1999; Midtkandal et al. 2008; Grundvåg et al. 2017) and global eustatic curve (after Haq 2014); TL − base-Aptian transgressive lag with global anoxia invasion into Spitsbergen dysoxic estuarine lagoon (cf. Figure 2D)

(Howard and Reineck 1981; Howard and Frey 1984; Pemberton and Frey 1984; Vossler and Pemberton 1989; Frey 1990; MacEachern and Pemberton 1992; Pemberton and MacEachern 1995; MacEachern et al. 1999b; Bann and Fielding 2004; Pemberton et al. 2004; Buatois et al. 2008).

The aim of the present study from the Carolinefjellet Formation (Aptian–Albian) in central Spitsbergen, Svalbard (Fig. 1), is to contribute to this line of interdisciplinary research by shedding more light on the sedimentary facies and ichnofauna communities of ancient stormy marine shelves. The archipelago of Svalbard at the western margin of the Barents Sea Shelf, presently a deglaciated high-Arctic polar desert, was an area located around 63–66 °N in the Early Cretaceous (Torsvik et al. 2002, 2008; Worsley 2008; Grundvåg and Olaussen 2017).

The Cretaceous period is known for its global greenhouse climate and lack of strong latitudinal temperature gradient (Fischer 1981; Ziegler et al. 1987; Wilkinson and Riding 2007; Huang et al. 2012; Moriya 2011; Scotese et al. 2021), with the emerged Svalbard area in the Barremian hosting both high vegetation and a diversified population of herbivore and carnivore dinosaurs. The Early Cretaceous Svalbard had a generally warm-temperate humid climate (estimated mean annual temperatures of 7–10 °C) that supported an ornithopod dinosaur population, deciduous conifers, ginkgos and local peat accumulation forming coal seams (Heintz 1963; Edwards et al. 1978; Steel and Worsley 1984; Nemec 1992; Hurum et al. 2006). However, the Aptian regional marine transgression in Svalbard area opened the Barents Shelf to the adjacent Arctic Ocean (Steel and Worsley 1984; Blakey 2011), whereby the epicontinental sea with its relatively warm waters became subject to a harsh Arctic wave climate and transient incursions of cold bottom water from spells of polar glacial temperatures (Weissert and Lini 1991; Maher et al. 2004; Kessels et al. 2006; Price and Nunn 2010; Price and Passey 2013; Scotese et al. 2021; Wang et al. 2022). These physical conditions amounted to a specific type of shelf environment, thus far little documented in the global stratigraphic record. The present study reports on the sedimentary deposits and ichnofauna assemblages of this subpolar Early Cretaceous greenhouse shelf.

Regional palaeogeographic setting

Spitsbergen is the main island of the Svalbard archipelago (Fig. 1A, B), exposing Precambrian metamorphic basement overlain by a sedimentary rock succession from the Upper Devonian to Neogene, with a notable local lack of the Upper Cretaceous (Parker 1967; Steel and Worsley 1984; Nøttvedt et al. 1992). The Carolinefjellet Formation constitutes the uppermost part of the Jurassic–Lower Cretaceous Adventdalen Group (Fig. 1D; Mørk et al. 1999), which extends over a large area of Spitsbergen as slivers cropping out at the synclinal fringes of the Central Spitsbergen Palaeogene Basin (Fig. 1A, C). The mud-rich open-marine deposits of the Aptian–Albian Carolinefjellet Formation rest transgressively on the sand-rich, coal-bearing Barremian fluvio-deltaic Helvetiafjellet Formation (Fig. 1D; Nemec et al. 1988; Nemec 1992; Gjelberg and Steel 1995) and are overlain unconformably by the coal-bearing Palaeocene fluvio-deltaic deposits of the lowermost Van Mijenfjorden Group (Steel and Worsley 1984; Nøttvedt et al. 1992; Mørk et al. 1999).

The base of the Carolinefjellet Formation is a transgressive surface marking the onset of marine sublittoral sedimentation over the paralic/littoral deposits of the upper Helvetiafjellet Formation (Fig. 1D; Nemec et al. 1988; Gjelberg and Steel 1995; Mørk et al. 1999). The top is an erosional unconformity, with the preserved thickness of Carolinefjellet Formation ranging in outcrop from 220 m in the NW to nearly 1300 m in the SE (Nagy 1970; Mørk et al. 1999). The erosional truncation increases both northwards and westwards, towards the West Spitsbergen Palaeogene strike-slip orogen (Steel et al. 1985). The maturity of organic matter indicates that possibly up to 1000 m of unknown Upper Cretaceous deposits were removed by erosion in the Svalbard area and the adjacent part of the Barents Sea Shelf (Worsley 2008; Midtkandal et al. 2016; Grundvåg et al. 2019). Extensive Upper Cretaceous deposits, including carbonates, are well documented from offshore wells in the southern part of the Barents Shelf (Nøttvedt et al. 1992; Worsley 2008; Grundvåg et al. 2017) and also westwards in the then adjoining northern Greenland and NE Canadian Arctic (Embry 1991; Worsley 2008). The end-Cretaceous erosion of Svalbard was apparently due to an uplift of the Barents Shelf along its rifted northern and western margins, combined with the transpressional West Spitsbergen orogeny (Steel et al. 1985; Ziegler 1988; Torsvik et al. 2002; Worsley 2008).

The Berriasian to lowest Barremian Rurikfjellet Formation (Fig. 1D) consists of shale-dominated offshore deposits passing upwards into sandy, storm-worked lower shoreface deposits with hummocky stratification (Midtkandal et al. 2008; Grundvåg et al. 2019). In the earliest

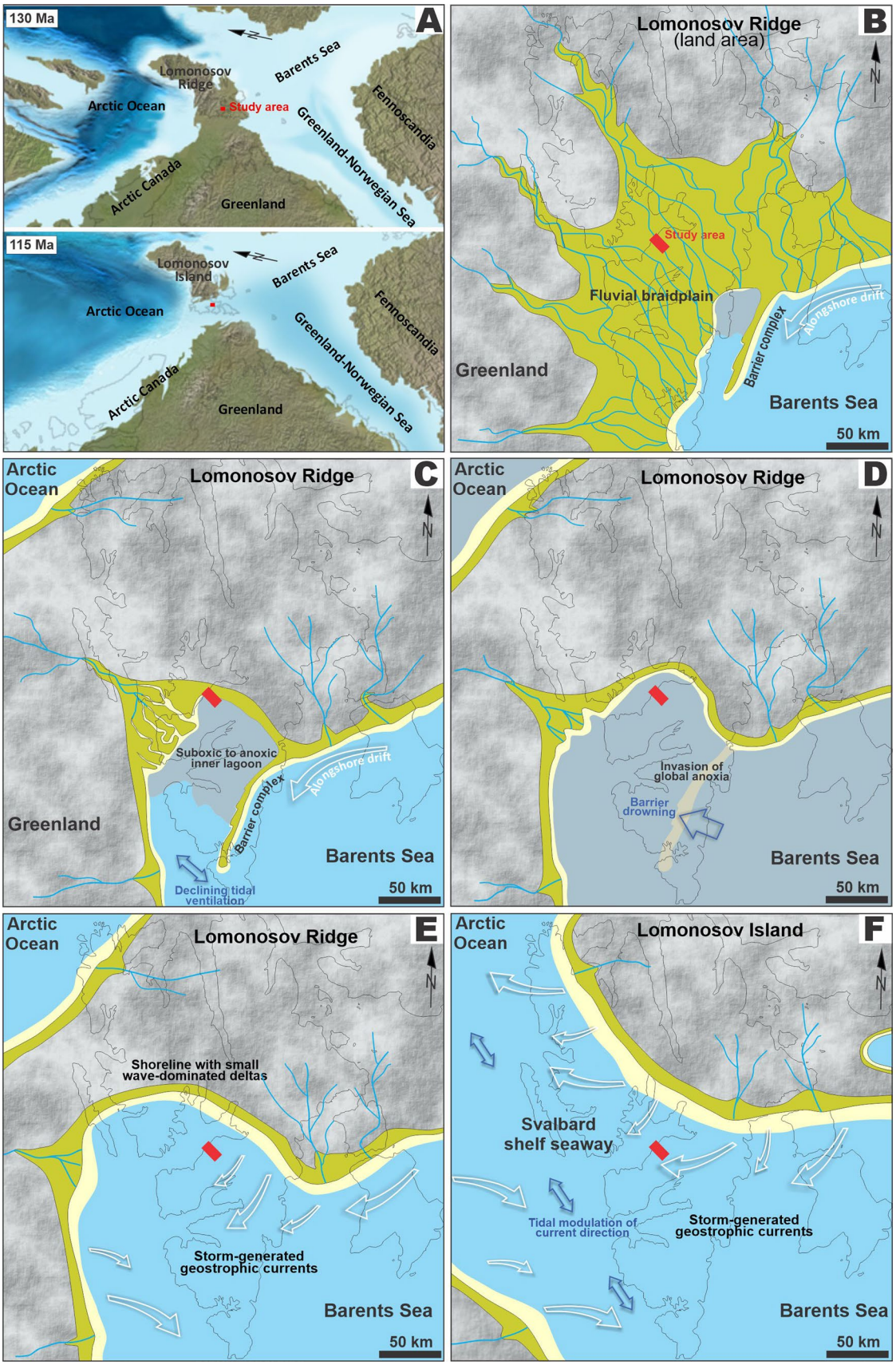
130 Ma
A
Lomonosov Ridge
Barents Sea
Arctic Ocean
Study area
Fennoscandia
Greenland-Norwegian Sea
Arctic Canada
Greenland
115 Ma
Lomonosov Island
Barents Sea
Arctic Ocean
Fennoscandia
Greenland-Norwegian Sea
Arctic Canada
Greenland
Lomonosov Ridge (land area)
B
N
Study area
Fluvial braidplain
Alongshore drift
Barrier complex
Greenland
Barents Sea
50 km
Arctic Ocean
Lomonosov Ridge
C
N
Suboxic to anoxic inner lagoon
Alongshore drift
Barrier complex
Greenland
Barents Sea
Declining tidal ventilation
50 km
Arctic Ocean
Lomonosov Ridge
D
N
Invasion of global anoxia
Barrier drowning
Barents Sea
50 km
Arctic Ocean
Lomonosov Ridge
E
N
Shoreline with small wave-dominated deltas
Storm-generated geostrophic currents
Barents Sea
50 km
Arctic Ocean
Lomonosov Island
F
N
Svalbard shelf seaway
Tidal modulation of current direction
Storm-generated geostrophic currents
Barents Sea
50 km

◂**Fig. 2** Regional setting. **A** Palaeogeography of the western part of subarctic region at the beginning of Barremian (~ 130 Ma BP) and in mid-Aptian (~ 115 Ma BP); spherical (orthographic) reconstructions slightly modified from Blakey (2011). **B**–**F** Hypothetical palaeogeography in Svalbard area (cf. stratigraphy in Fig. 1D), with the background thin black outline of the archipelago's present-day shoreline (cf. Figure 1A). **B** The Helvetjafiellet Fm braidplain delta at its maximum extent (early Barremian). **C** The delta retreat and formation of dysoxic estuarine lagoon (middle to late Barremian). **D** The lagoon drowning by anoxic waters of OAE1a (Barremian/Aptian transition, base of Carolinefjellet Fm). **E** The onset of Dalkjegla Mb deposition in transgressively enlarged embayment (earliest Aptian). **F** The opening of Svalbard seaway and deposition of Carolinefjellet Fm (Aptian–Albian). Reconstructions inspired by Nemec et al. (1988), Nemec (1992) and Grundvåg et al. (2017, 2019, 2021)

Barremian, the Svalbard area emerged as part of the volcanically active Lomonosov Ridge that separated the Barents Shelf from the opening Arctic Ocean (Fig. 2A, B). A broad fluvio-deltaic system of the Helvetiafjellet Formation prograded to the SE across the lowland of Spitsbergen (Figs. 1D, 2C; Steel and Worsley 1984; Nemec et al. 1988; Nemec 1992). This system then receded to the NW in the middle to late Barremian due to a stepwise marine transgression (Fig. 1D; Gjelberg and Steel 1995), which turned the southern Spitsbergen area into a dysoxic muddy estuarine embayment (Fig. 2D). The area was eventually drowned and opened to the Arctic Ocean (Fig. 2E, F), with the onset of the open-marine epicontinental environment of the Carolinefjellet Formation (Fig. 1D).

The invasion of anoxia in Svalbard at the Barremian/Aptian transition (Fig. 1D) is linked to the global oceanic anoxia event OAE1a (Midtkandal et al. 2016). Cretaceous worldwide activity of mantle plumes (Johansson et al. 2018; Müller et al. 2019; Scotese et al. 2021) formed several large igneous provinces (LIPs), including the high-Arctic HALIP of the Lomonosov Ridge (Maher 2001; Torsvik et al. 2006; Polteau et al. 2016). The associated lithospheric degassing of CO_2 is a widely invoked factor for the OAE1a, with an initially doubled atmospheric CO_2 concentration (Ganino and Arndt 2009; Naafs et al. 2016) and possible mass extinctions (Rampino and Self 2015; Scotese et al 2021). The HALIP igneous province, with an area of about 700,000 km^2, could alone release an estimated 1000 s GT CO_2 and significantly contribute to the global OAE1a (Midtkandal et al. 2016; Polteau et al. 2016). The time lag between the anoxic marine invasion and the ultimate opening of the Svalbard shelf seaway (Fig. 2C, D) is hypothetically estimated as possibly no more than 300 to 400 ka (see next paragraph).

The Carolinefjellet Formation

The Carolinefjellet Formation (Harland 1997; Dallmann 1999) consists of dark-grey to blackish mudshales, clayey to silty, intercalated in a variable proportion with thin to thick sandstone sheets. Characteristic features include abundant bioturbation, sporadic shell-debris layers, chamosite ooids, glendonites and siderite concretions (Krajewski and Luks 2003; Mutrux et al. 2008). The basal erosional unconformity (Fig. 1D) is patchily strewn with a transgressive gravelly lag and overlain by a unit of non-bioturbated black mudshales, ~ 15 m thick, correlated to the OAE1a (Midtkandal et al. 2016). The deposition rate of pure black shales is widely estimated as 1–2 mm ka^{-1} (compacted values). However, the basal black shales in the present case have numerous thin sandstone interlayers and vary from laminated to massive (Fig. 3; Midtkandal et al. 2016). Their deposition probably involved abundant dysoxic lagoonal mud of the topmost Helvetiafjellet Formation (Nemec et al. 1988; Nemec 1992), resuspended by the transgression, as well as a spontaneous emplacement of massive fluid-mud layers (Baas et al. 2009). When the rate of mud settling and aggradation into a near-bottom layer exceeds the mud-dewatering rate, the fluid mud tends to flow gravitationally according to the local seafloor gradients (Mehta 1991; Kranenburg and Winterwerp 1997). Assuming a conservative mean rate of 4–5 mm ka^{-1} (compacted values), the deposition of the anoxic muddy unit in Spitsbergen might have taken 300–400 ka.

The Carolinefjellet Formation has been divided into five subunits, referred to in their ascending stratigraphic order as the Dalkjegla, Innkjegla, Langstakken, Zillerberget and Schønrockfjellet members (Fig. 2; Parker 1967; Nagy 1970; Dallmann 1999; Grundvåg et al. 2021). These units have conformable boundaries and differ chiefly in their relative proportion of mudshales and sandstones, but also in some other distinctive features. For example (Dallmann 1999; Krajewski and Luks 2003; Maher et al. 2004; Mutrux et al. 2008): The basal part of Dalkjegla Member consists of black shales nearly devoid of burrows. Chamosite ooids occur only in the Dalkjegla Member, 22–30 m above its base. Siderite concretions form several stratigraphic horizons in the Dalkjegla and Innkjegla members. Glendonites appear in the topmost Dalkjegla Member and recur through most of the Innkjegla Member.

Prior to the modern concepts of shelf sedimentation and tempestites, the heterolithic Carolinefjellet Formation was tentatively considered as tidal-flat deposits (Birkenmajer 1966). Researchers presently agree that the formation represents sedimentation in a wave-dominated, open-marine inner to outer shelf environment affected by relative sea-level changes, with minor direct evidence of tidal influences (Nagy 1970; Steel and Worsley 1984; Nøttvedt and Kreisa 1987; Gjelberg and Steel 1995; Dypvik et al. 2002; Maher et al. 2004; Midtkandal 2007; Worsley 2008; Grundvåg et al. 2019, 2021). The Aptian lower part of the Carolinefjellet Formation (Fig. 1D) is generally regarded as a continued record of

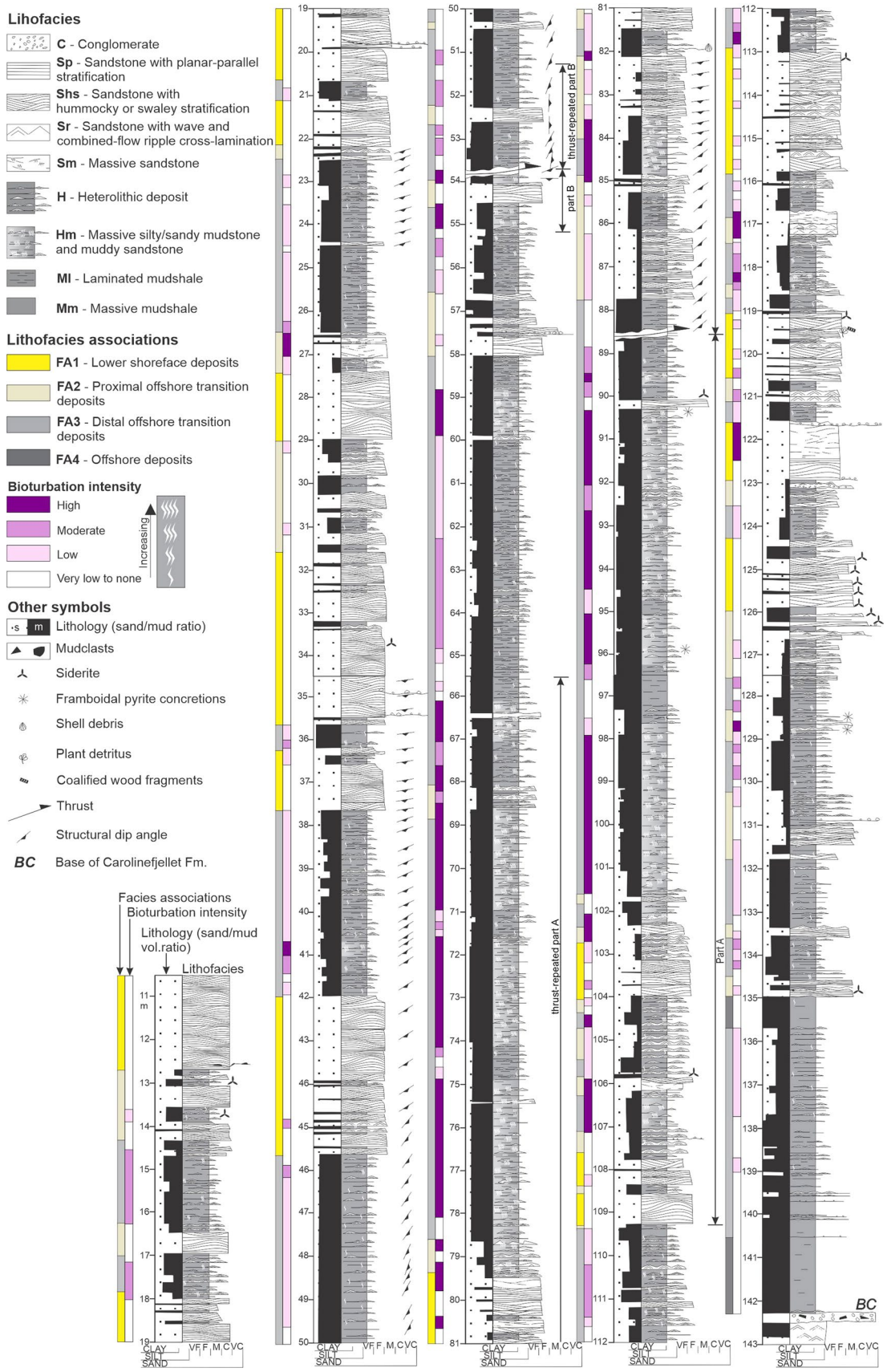
Lihofacies
C - Conglomerate
Sp - Sandstone with planar-parallel stratification
Shs - Sandstone with hummocky or swaley stratification
Sr - Sandstone with wave and combined-flow ripple cross-lamination
Sm - Massive sandstone
H - Heterolithic deposit
Hm - Massive silty/sandy mudstone and muddy sandstone
Ml - Laminated mudshale
Mm - Massive mudshale
Lithofacies associations
FA1 - Lower shoreface deposits
FA2 - Proximal offshore transition deposits
FA3 - Distal offshore transition deposits
FA4 - Offshore deposits
Bioturbation intensity
High
Moderate
Low
Very low to none
Increasing
Other symbols
Lithology (sand/mud ratio)
Mudclasts
Siderite
Framboidal pyrite concretions
Shell debris
Plant detritus
Coalified wood fragments
Thrust
Structural dip angle
BC
Base of Carolinefjellet Fm.
Facies associations
Bioturbation intensity
Lithology (sand/mud vol.ratio)
Lithofacies
thrust-repeated part B
part B
thrust-repeated part A
Part A
BC
CLAY
SILT
SAND
VF F M C VC

◂**Fig. 3** Example log of the Carolinefjellet Fm in central Spitsbergen (well Dh2, Fig. 1C), showing stratigraphic distribution of lithofacies, their associations and the degree of sediment bioturbation

the punctuated regional marine transgression initiated by deposition of the underlying Glitrefjellet Member of the Helvetiafjellet Formation (Nemec et al. 1988; Gjelberg and Steel 1995; Dypvik et al. 2002). The Albian upper part of the Carolinefjellet Formation (Fig. 1D) is considered to represent a punctuated highstand regression, markedly aggradational (Dallmann 1999; Dypvik et al. 2002; Maher et al. 2004; Midtkandal 2007; Grundvåg et al. 2019, 2021).

However, the exact character of the depositional environment and its palaeogeography are uncertain. The Barremian shoreline of the advancing and retreating braidplain delta of the Helvetiafjellet Formation is widely recognized to have had a NE–SW trend (Fig. 2A; Steel and Worsley 1984; Nemec et al. 1988; Nemec 1992; Gjelberg and Steel 1995; Midtkandal 2007; Worsley 2008; Grundvåg et al. 2021). The location and spatial trend of the Aptian–Albian shoreline in Svalbard is less clear, as the coeval coastal deposits are non-preserved. Maher et al. (2004) suggested an E−W shoreline trend with a westward alongshore sediment drift. Dallmann (1999) and Dypvik et al. (2002) considered the Carolinefjellet Formation in Spitsbergen to be a prodelta system advancing towards the SW on a wave-dominated shelf, with the shoreline trending NW–SE and located in the middle of Svalbard, perhaps at the northernmost reaches of inner Isfjorden (Fig. 1A). This interpretation would be consistent with the evidence of transported plant debris and the observed slight decrease in the relative proportion of sandstone beds towards the south (Parker 1967; Nagy 1970), obliquely away from the shoreline. The shoreline might well involve some small wave-dominated deltas, but the notion of a prodeltaic environment per se is questionable. First, the fluvial drainage of the Lomonosov island (Fig. 2F) would be sparse, unlikely to produce any major river deltas. Second, wave-dominated deltas generally lack typical river-fed prodelta zone and are instead fronted by wave-worked shorefaces with a storm-controlled offshore transition (Bhattacharya and Walker 1992; Hampson and Howell 2005).

In the first modern sedimentological study of the Carolinefjellet Formation, Nøttvedt and Kreisa (1987) have recognized its sheet-like sandstone beds as tempestites (see also Grundvåg et al. 2021)—deposits characteristic of a storm-dominated lower shoreface to offshore transition zone, rather than diagnostic of a prodelta environment. Nøttvedt and Kreisa (1987) have recognized also frequent localized stacking of tempestites into mounded, isolated or semi-isolated sandbodies, 1–3 m thick, with a clinoformal bed stacking and anisotropic hummocky cross-strata indicating broadly westward (SW to NW range) direction of sediment transport (see also Grundvåg et al. 2021). For a storm-driven transport influenced by Coriolis effect (Walker 1984b), this evidence would be consistent with a shoreline located to the NE (Birkenmajer 1966; Dallmann 1999; Dypvik et al. 2002). However, these mounded sandbodies have been more recently interpreted by Maher et al. (2004) as low-relief barrier-bar complexes formed on a wave-dominated and tidally influenced inner shelf, accreted by a westward alongshore sediment drift and sheltering brackish tidal lagoons with suboxic bottom conditions. This interpretive scenario of a barred shoreline trending E–W in the midst of Spitsbergen intended to explain a presumed lagoonal origin of the chamosite ooids found in the Dalkjegla Member. Although the interpretation might seem consistent with the southward decrease in the proportion of sandstone beds, several other facts render it questionable. First, the mounded sandbodies occur randomly at all levels of the Carolinefjellet Formation and are found also in its southernmost outcrops in Spitsbergen (Nøttvedt and Kreisa 1987), where—nearly 150 km away from the shoreline postulated by Maher et al. (2004)—hardly any sand should have been delivered and no nearshore barrier bars would be expected. Instead, the sedimentary succession there, in Kvalvågen area (Nøttvedt and Kreisa 1987; Århus 1991; Midtkandal 2007), is only slightly poorer in sand and contains similar mounded sandbodies. Second, the mounded sandbodies in the Carolinefjellet Formation show virtually no facies resemblance to barrier bars (cf. Davies et al. 1971; Reading and Collinson 1996) and are compound tempestite stacks (Grundvåg et al. 2021) known from other mid-shelf areas (Midtgaard 1996). Last, but not least, the iron ooids occur in association with offshore-transition tempestites (cf. Price and Nunn 2010), and hence were either derived by storms from erosion of the lagoonal deposits of the uppermost of Helvetiafjellet Formation or formed directly in the offshore transition area (cf. Boyd et al. 1992; Colin et al. 2005; Boyd 2010).

In summary, researchers generally agree that the sedimentological evidence from the Carolinefjellet Formation is incompatible with the earlier Barremian shoreline and that the Svalbard area must have undergone a dramatic palaeogeographic change in the earliest Aptian (Fig. 2), even though the exact pattern of this change is not quite clear. The present study concurs with the palaeogeographic reconstructions postulating that the Barents Sea Shelf in Barremian was sheltered from the opening Arctic Ocean by a volcanically active peninsular land area of the Lomonosov Ridge (Fig. 2A−C; Ziegler 1988; Brekke et al. 2001; Torsvik et al. 2002; Blakey 2011). The end-Barremian Spitsbergen embayment was sheltered by a prominent sand-barrier complex, ~ 20 m thick (Fig. 2B; Nemec et al. 1988), with the back-barrier lagoonal area hosting dysoxic waters (Nemec

1992). The barrier slightly migrated landwards to the NW, but was drowned by invasion of the OAE1a anoxic water at the Barremian/Aptian transition (Midtkandal et al. 2016). The early Aptian further transgression then opened across Svalbard a wide epicontinental seaway linking the western Barents Sea with the Arctic Ocean (Fig. 2D; Owen 1988; Århus 1991; Nøhr-Hansen 1993; Dypvik et al. 2002; Blakey 2011). The Aptian–Albian local shoreline would then likely assume a NW–SE trend (Fig. 2D; Birkenmajer 1966; Århus 1991; Dypvik et al. 2002), with the island area to the NE being too small to have any extensive fluvial catchments with large deltas. The wave-dominated shorelines of the seaway are unpreserved. The NNW–SSE trend of the Cretaceous outcrop in Spitsbergen, imposed by the Palaeogene foreland syncline (Fig. 1A), would thus be slightly oblique to the Aptian–Albian local shoreline and shelf depositional strike.

High vegetation in the Svalbard area persisted from Barremian until at least the Palaeocene (Steel and Worsley 1984; Nøttvedt et al. 1992; Worsley 2008) and the Arctic isotope data from fossil molluscs indicate a generally warm (≤ 20 °C) seawater during the Cretaceous (Tarduno et al. 1998). However, the isotope thermometry has also indicated that the polar zone probably experienced transient glacial temperatures (Price and Nunn 2010; Price and Passey 2013; Vickers et al. 2019; see also Weissert and Lini 1991; Kessels et al. 2006). The episodic occurrences of glendonites and preservation of plagioclase grains in a sand-starved sublittoral environment of the Carolinefjellet Formation imply cool (4–7 °C) bottom-water conditions (De Lurio and Frakes 1999; Maher et al. 2004; Price and Nunn 2010). This may indicate invasions of deep polar water onto the Barents Shelf prior to the opening of the North Atlantic and development of its modern oceanic circulation (cf. Ziegler 1988; Doré 1991; Mosar et al. 2002; Torsvik et al. 2002). Invasions of polar water might also explain the predominance of a mixture of non-endemic cold-water dinoflagellates in the Aptian and Albian of the Barents Shelf, similar as in the northern Greenland (Århus 1991; Nøhr-Hansen 1993).

Methods and terminology

The data for the present study were derived from four fully cored boreholes (labelled Dh1 to Dh4, Fig. 1C), drilled near the central Spitsbergen town of Longyearbyen under a UNIS project (Braathen et al. 2012), and from a corresponding road-cut outcrop section, about 2.5 km long, between the town and its airport (Fig. 1C). The well cores show the lower to middle part of the Dalkjegla Member of the Carolinefjellet Formation (Fig. 1D), whereas the outcrop shows the member's middle to upper part. The cores were studied by detailed sedimentological logging (scale 1:20), with a special focus on biogenic features. Documentation included photographs. The core samples, stored at the UNIS in Longyearbyen, were non-oriented, hence palaeocurrent directions could only be measured in the outcrop section.

The descriptive sedimentological terminology is after Folk (1980), Harms et al. (1982) and Collinson et al. (2006). The term lithofacies refers to the basic types of sedimentary deposits distinguished on the macroscopic basis of their bulk characteristics (Harms et al. 1975; Walker 1984a). The term facies association denotes an assemblage of spatially and genetically related lithofacies, thought to represent a particular zone (sub-environment) of the depositional system. The distinction of shoreface, offshore transition and offshore zones is based on sedimentary facies and pertains to the prevalent depths of fairweather and storm wave bases (Reading and Collinson 1996). The definition of bioturbation structures and trace fossils is after Bertling et al. (2006, 2022). The simplified four-grade scale for sediment bioturbation intensity used in summary figures refers to the bioturbation index (BI) of Taylor and Goldring (1993) as follows: no bioturbation (BI = 0), low (BI = 1), moderate (BI = 2–3) and high bioturbation (BI = 4–6).

Sedimentary facies

The following lithofacies have been recognized as the basic building blocks of the sedimentary succession in the present study:

C – basal conglomerate, massive to diffusely planar stratified;
Sp – sandstone with planar parallel stratification;
Shs – sandstone with hummocky and/or swaley stratification;
Sr – sandstone with wave and/or combined-flow ripple cross-lamination;
Sm – massive mottled sandstone homogenized by bioturbation;
H – heterolithic facies of thinly interlayered sandstone and mudshale;
Hm – massive silty to sandy mudstone or muddy sandstone homogenized by bioturbation;
Ml – planar parallel laminated silty mudshale;
Mm – homogenous (non-laminated) mudshale.

The sedimentary facies are briefly described and genetically interpreted in Table 1, with an example well-core log in Fig. 3 and lithofacies shown in Figs. 4, 5 and 6. For a more detailed depiction of lithofacies, see Grundvåg et al. (2021).

Table 1 Lithofacies of the Dalkjegla Member of the Carolinefjellet Fortmation in the study area

Facies	Description	Interpretation
C	*Conglomerate*—Poorly sorted, massive to diffusely plane-parallel stratified, granule to fine-pebble conglomerate composed of subrounded to well-rounded clasts, forming a laterally discontinuous solitary layer ≤ 10 cm thick at the formation base. These broad basal conglomerate patches have a sharp, erosional base and sharp top, show weak normal grading. The conglomerate is locally capped with facies Sr and generally covered by mudshales It overlies mudshales or fluvio-deltaic sandstones of the topmost Helvetiafjellet Fm (Figs. 3, 5A, 6B, D). Occasional thin mudclast conglomerate, shell-hash lag or pebbly sandstone underlie beds of facies Sp, Shs and Sm (Figs. 3, 5D, 6B, D, G)	This patchy conglomerate layer is thought to be a basal transgressive lag (Frebold 1930, 1931) derived by erosional stripping from mouth bars of the retreating Helvetiafjellet delta and spread laterally into adjacent muddy areas by storm action (Hwang and Heller 2002; Cattaneo and Steel 2003). The patchy occurrence of this basal conglomerate at widely separated localities (Birkenmajer 1964) may reflect diachroneity of the end-Barremian transgression (Gjelberg and Steel 1995)
Sp	*Sandstone with planar parallel stratification*—Well-sorted, fine-grained to coarse-grained arenitic sandstone, forming beds 2 to 150 cm thick, with occasional stringers/lenses of granule gravel and scattered small pebbles or mud clasts. Sets of planar parallel strata up to a few decimetres thick, separated by subhorizontal or gently undulating erosional surfaces. Typically associated with facies Shs and Sr (Figs. 3, 5D, 6D)	Shoreface-derived sand spread seawards by storm-generated currents and deposited in the upper flow regime (Harms et al. 1982; Arnott and Southard 1990; Arnott 1993b) or by the action of waves with high orbital velocities (Clifton et al. 1971; Komar and Miller 1975; Clifton 1976)
Shs	*Sandstone with hummocky or swaley stratification*—Well-sorted, very fine-grained to medium-grained and rarely coarse-grained arenitic sandstones, commonly with scattered small granules and sporadic pebbles in the basal part of swales. Hummocky and swaley strata sets 10–30 cm thick, with a wavelength of 1–5 m, draped with thin facies Sr or covered by mudshale facies Ml. Composite units up to 1.5 m thick, with intrasets of facies Sp, Sr or Sm and with a preferential westward (WNW) stacking of mounded bed sets (Figs. 3, 4B–F, 5B–C, 6B, D)	Deposition of storm-derived sand in combined-flow conditions, with bedforms ranging from pod-shaped scour-and-fill swales to oval accretionary hummock domes (Bourgeois 1980; Dott and Bourgeois 1982; Duke 1985; Arnott and Southard 1990; Duke et al. 1991; Dumas et al. 2005; Dumas and Arnott 2006)
Sr	*Sandstone with wave and combined-flow ripple cross-lamination*—Well-sorted to moderately sorted, very fine-grained to medium-grained and rarely coarser arenitic sandstone with cross-lamination indicating symmetrical to asymmetrical 2D ripples or dome-shaped 3D ripples ('micro-hummocks' of Kreisa 1981). Sand units 3−5 cm thick (Figs. 3, 5C, 6B, E, H, J)	Deposition of storm-derived sand as ripples by oscillatory waves with noderate orbital velocities (Komar and Miller 1975; Clifton and Dingler 1984) or as 3D ripples by combined flow (Leckie 1988; Cheel and Leckie 1992; Yokokawa et al. 1995; Dumas et al. 2005; Perillo et al. 2014)
Sm	*Massive sandstone*—Well-sorted or moderately sorted, very fine- to medium-grained sandstone, locally with scattered small granules and sporadic pebbles or mudclasts, forming units 10 to 100 cm thick that often cap sandstones Shs/Sr or alternate with them. The massive sandstone is commonly mottled and richer in mud at the upward transition to muddy facies Mm, Ml or Hm (Figs. 3, 6C)	Pervasively bioturbated top parts of originally stratified sand beds or sand-rich heterolithic units. Sharp-based massive lower parts of sand units may be due to a non-tractional dumping of sand from storm-generated current or represent local seafloor liquefaction (Leckie 1988; Jelby et al. 2020)
H	*Heterolithic deposit*—Units of thinly interlayered massive to laminated mudshale and ripple cross-laminated sandstone, very fine- to fine-grained, sporadically coarser with scattered granules and small pebbles. Layers are 0.5 to 5 cm thick. Sandstone layers are often weakly graded, with sharp and slightly erosional bases and with gradational or sharp tops; the thinnest layers show pinch-and-swell geometry (Figs. 3, 4A, 6F–I)	Deposition of 'background' mud (see facies Ml/Mm) punctuated by frequent incursions of wave-worked sand attributed to relatively weak (seasonal?) storms. Lenticular pinch-and-swell layers represent formation of sand-starved wave ripples (De Raaf et al. 1977; Allen 1982)
Hm	*Massive silty/sandy mudstone or muddy sandstone*—Thin (< 5 cm) to thick (> 4 m) units of massive, poorly sorted, dark grey sediment composed of thoroughly intermixed mud and sand, with irregular speckles of sand and silt. Primary depositional structure obliterated by animal burrows, often superimposed (Figs. 3, 6I, 7I, 10D)	Mud-rich deposit (originally facies H and/or Ml) completely bioturbated by benthic fauna (Reineck and Singh 1975; Taylor and Goldring 1993; Seilacher 2007)
Ml	*Laminated mudshale*—Blackish to dark-grey mudshale thinly banded with lighter-grey silt and/or silty mud. The individual silty bands range from single laminae (≤ 0.1 cm thick) to layers up to 0.5 cm in thickness, with sharp to gradational flat boundaries. Common animal burrows (Figs. 3, 6F)	Pulsating 'background' deposition of alternating clayey and silty hemipelagic suspension with a rhythmic shedding from storm-derived suspension plumes (cf. Kerr 1991; Nemec 1995) and/or action of tidal currents (Reineck and Singh 1975)

Table 1 (continued)

Facies	Description	Interpretation
Mm	*Massive mudshale*—Blackish or brownish dark-grey mudshale forming non-laminated, homogenous beds up to 15 cm thick. Animal burrows absent to common. The brownish shale variety is variously sideritized and often shows sideritic 'cannon-ball' concretions (Figs. 3, 6G–H)	'Background' mud deposition by intense fallout of hemipelagic suspension or by local intra-shelf flow of fluid mud (Krajewski and Luks 2003; Baas et al. 2008; Ichaso and Dalrymple 2009)

The lateral discontinuity of the basal conglomerate layer (lithofacies C), interpreted as a transgressive lag, is probably due to the erosional stripping and lateral reshuffling by sea waves of the coarse sediment from accessible fluvial channel belts of the topmost Helvetiafjellet Formation (cf. Nemec 1992). Sandstone beds range in thickness from 1 to 80 cm and have sharp bases and tops. The thinnest beds consist of lithofacies Sr, with the ripple cross-laminae sets commonly flattened and/or loaded by compaction (Fig. 6F−I). Thicker beds consist of lithofacies Sp and/or Sr, whereas the thickest ones show mounded segments with lithofacies Shs (Figs. 4B−E, 5B−D). The internal structure of hummocks ranges from roughly symmetrical solitary sets of dome-shaped parallel strata to multiple sets separated by convex-up truncations (Fig. 4B), and to sporadic unidirectional cross-strata sets underlain by thin lithofacies Sp and draped by lithofacies Sp and/or Sr (Fig. 4A). Structure asymmetry (anisotropy) indicates transport towards the WNW or NW. Amalgamated composite sandstone beds reach locally 2−3 m in thickness (Figs. 3, 4). The tops of non-amalgamated bed, overlain by mudshale, show well-preserved oscillatory wave vortex ripples or combined-flow ripples, often with worm trails (Figs. 6F, I, 7B). All these features support Nøttvedt and Kreisa's (1987) original interpretation of the sandstone beds as tempestites (Table 1; cf. Dott and Bourgeois 1982; Dumas et al. 2005). Bed soles show occasional grooves, small flutes and prod marks indicating flow direction broadly towards the WSW, but often varying by up to 30° on the same bed sole (Birkenmajer 1966). Cross-lamination of combined-flow ripples indicates sand transport in directions ranging between SW and WNW. Asymmetrical wave ripples indicate transport mainly towards the NE or ESE, which may reflect variable wind-modulation of the water oscillatory movement towards the contemporaneous irregular shoreline. Ptygmatic injection dikes, a few centimetres thick and extending above sandstone bed tops (lithofacies Sd; Fig. 6H), are evidence of local post-depositional remobilization of sand by liquefaction, possibly due to seismic events.

The sandstones are predominantly well sorted, fine-grained to medium-grained and quartz-rich sublithic to subarkosic arenites (Maher et al. 2004). The rare scattered small pebbles and basal patchy conglomerate layer similarly consist mainly of rounded quartz and chert clasts (Fig. 6D−E). The textural and mineralogical maturity supports the notion of a wave-worked sediment derived by storms from shoreline zone. However, some of the gravel clasts are merely subrounded. The sand fraction also shows highly varied grain roundness and an admixture of relatively weak mineral grains, such as plagioclase, microcline, chlorite and biotite (Maher et al. 2004). Sediment supply probably involved recycling of older deposits by coastal erosion and local fluvial delivery, with alongshore drift of sediment, its mixing

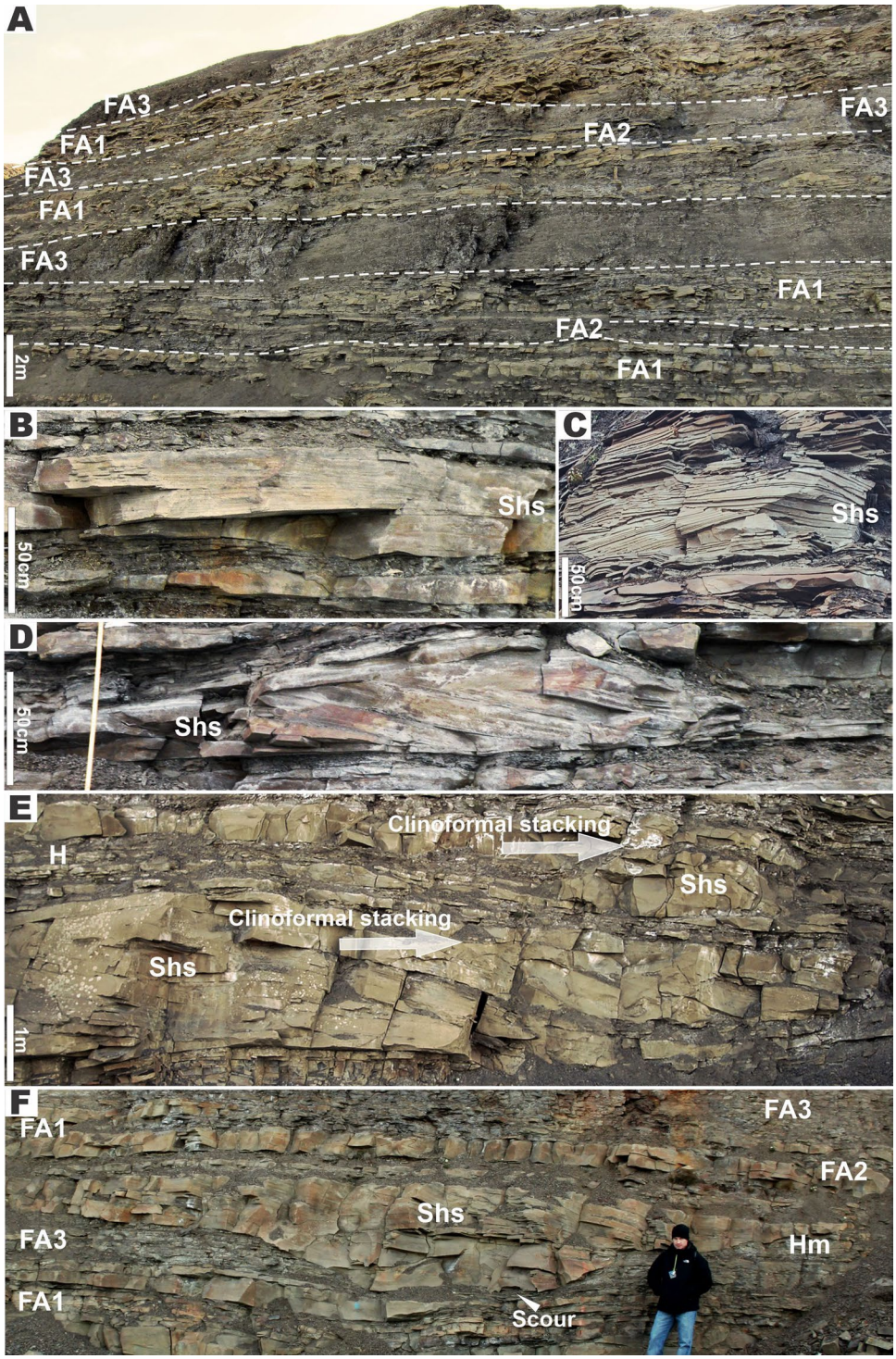

Fig. 4 Outcrop examples of lithofacies (cf. Table 1) and their associations. **A** Broad view of the vertical stacking pattern of lithofacies associations. **B** Isotropic hummock structure in facies Shs bed. **C** Composite isotropic hummock in facies Shs bed. **D** Anisotropic hummock in facies Shs bed. **E** Large storm bar in facies Shs, formed by lateral clinoformal stacking of hummocks. **F** Scour trough (arrow), ~ 0.8 m deep and several metres wide, filled with facies Shs sandstones; note the nearly tabular geometry of the enveloping deposits of FA1–FA3

and variable maturation. Sediment provenance included a contemporaneous volcanic source (Nysæther 1966), linked to the HALIP area in the NE part of the Lomonosov Ridge (Ziegler 1988; Tarduno et al. 1998; Maher 2001; Maher et al. 2004; Mutrux et al. 2008).

Carbonate clasts are rare, including fragments of pelecypod shells, fine-grained contemporaneous hardground limestones and eroded intraformational concretions of microspar calcite or siderite (Maher et al. 2004). In addition to resedimented iron ooids in the lower part the formation, some coalified plant detritus and scattered petrified fragments of driftwood are sporadically found (Mutrux et al. 2008). Early-diagenetic glauconite occurs and increases in abundance upwards in the succession

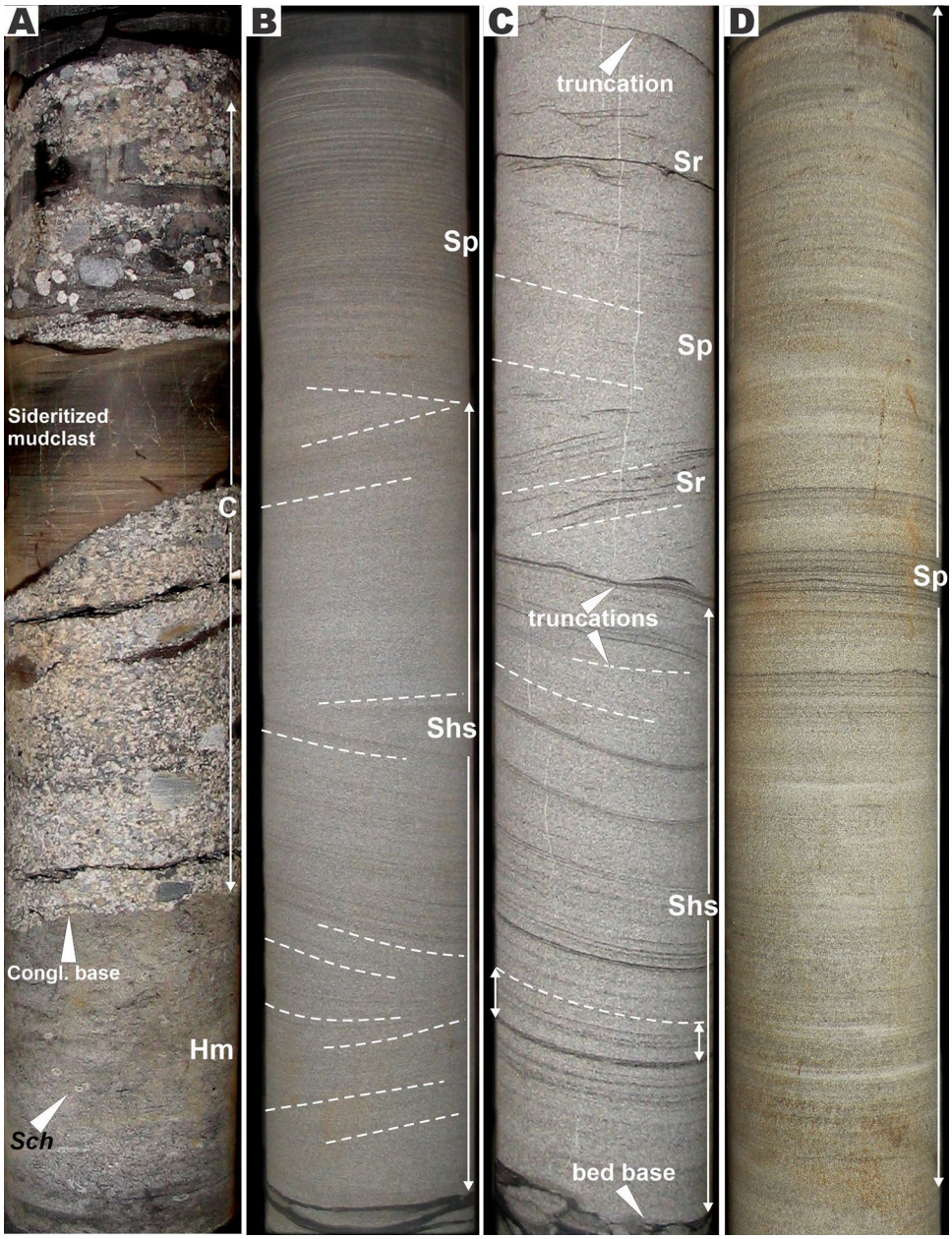

Fig. 5 Well-core examples of lithofacies (cf. Table 1); core diameter 5 cm. **A** Inversely graded basal conglomerate (C) with large sideritized mudclasts, overlying strongly bioturbated muddy sandstone (Hm) with *Schaubcylindrichnus* (*Sch*) burrows. **B** Sandstones of facies Shs passing upwards into facies Sp. **C** Composite bed of facies Shs passing upwards into facies Sr. **D** Thick composite bed of facies Sp

(Maher et al. 2004), which may indicate a decreasing bulk rate of sediment accumulation. Small concretions of bacterial framboidal pyrite tend to be associated with clay pellets and animal burrows. Ball-shaped and strata-bound sideritic ironstone concretions in mudshale beds indicate an early subsurface cementation of uncompacted sediment by non-ferroan calcite in the upper part of sulphite-reduction zone, enriched in framboidal pyrite at the local sites of enhanced bacterial decomposition of organic matter (Krajewski and Luks 2003).

Trace fossils

Trace fossils are common in the studied succession, slightly more abundant in wells Dh1 and Dh2 than in wells Dh3 and Dh4 (Fig. 1C, 3). Only the basal conglomerate (lithofacies C), the overlying black mudshale unit (lithofacies Ml/Mm) and the majority of thick sandstone beds (lithofacies Sp and Shs) are nearly devoid of bioturbation structures (Figs. 6B, D and 8B). The distinct basal unit of

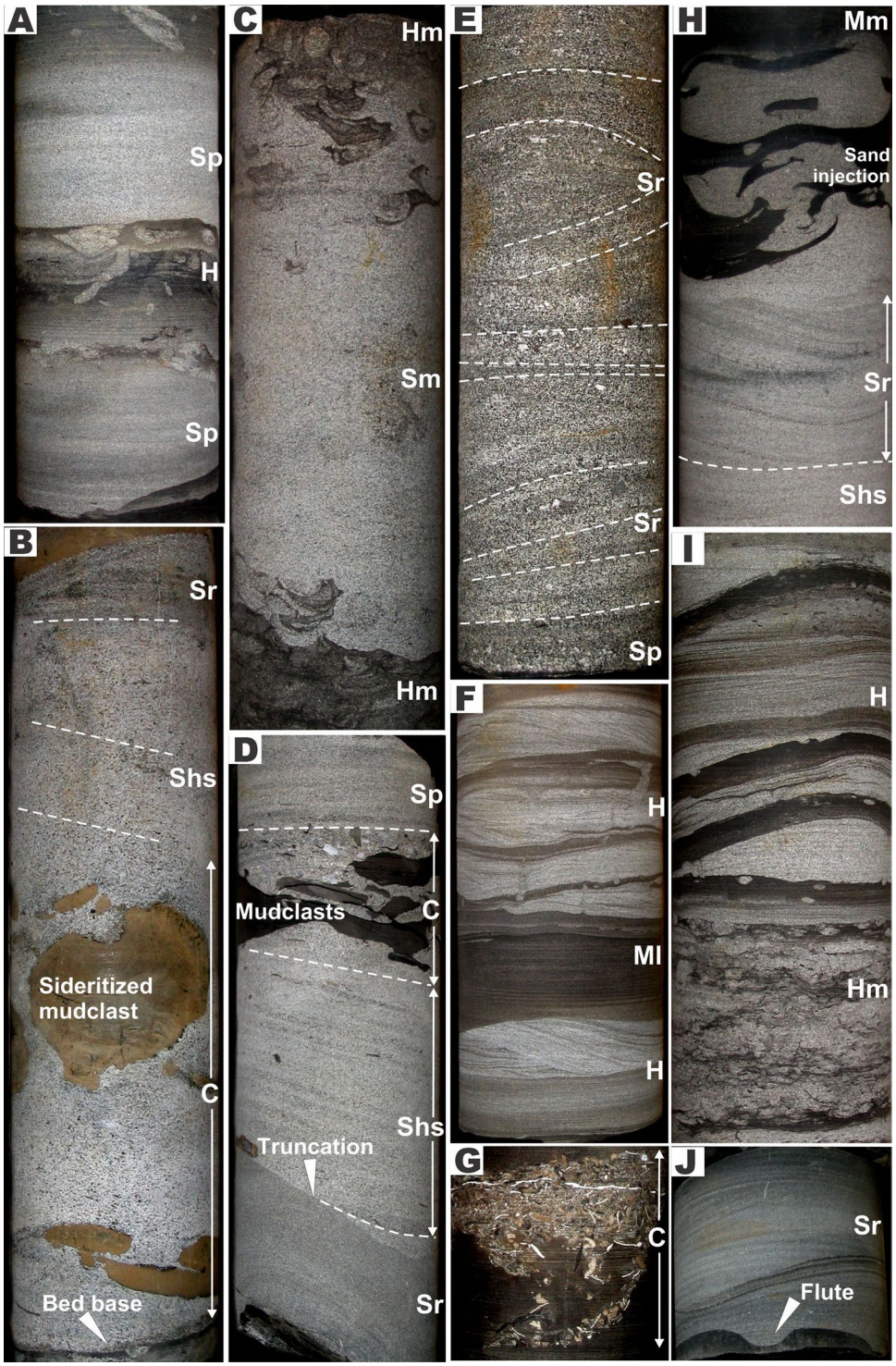

Fig. 6 Well-core examples of lithofacies (cf. Table 1); core diameter 5 cm. **A** Graded beds of facies Sp capped with bioturbated layers of facies H. **B** Facies C bed with large sideritized mudclasts, overlain by facies Shs and Sr. **C** Isolated bed of bioturbated facies Sm sandwiched between layers of facies Hm. **D** Swaley bed of facies Shs underlain by facies Sr and covered by a mudclast conglomerate (C) at the base of facies Sp bed. **E** Facies Sr rich in tiny iron ooids. **F** Beds of facies H, with combined-flow ripples and isolated burrows, separated by facies Ml. **G** Burrowed shelly lag. **H** Sand injectite intrusion in facies Mm, above the sandstone facies Shs and Sr. **I** Facies Hm overlain by facies H, showing marked short-term variation in bioturbation intensity. **J** Sandstone of facies Sr with a flute solemark

lithofacies Ml/Mm shows merely sporadic structures reminiscent of thread-like burrow fills, manifested on the core surface as small spots of lighter-shade very fine-grained sand, 1−2 mm in diameter. In contrast, all units of lithofacies Sm are highly bioturbated (BI = 5–6; Fig. 7C).

The BI varies from 0 to 5 on a bed thickness scale and on the scale of bed packages several metres thick. Burrows are virtually absent in the lower parts of sandstone beds thicker than 5 cm and are increasingly more common in their top parts, at the contact with the overlying mudshale (Fig. 6A, C), which means 'lam-scram' sequences sensu Bromley (1990). Burrows are also relatively rare or absent in the heterolithic deposits of lithofacies H and in sideritized mudshales (Fig. 6B, F). On a larger stratigraphic scale, burrows

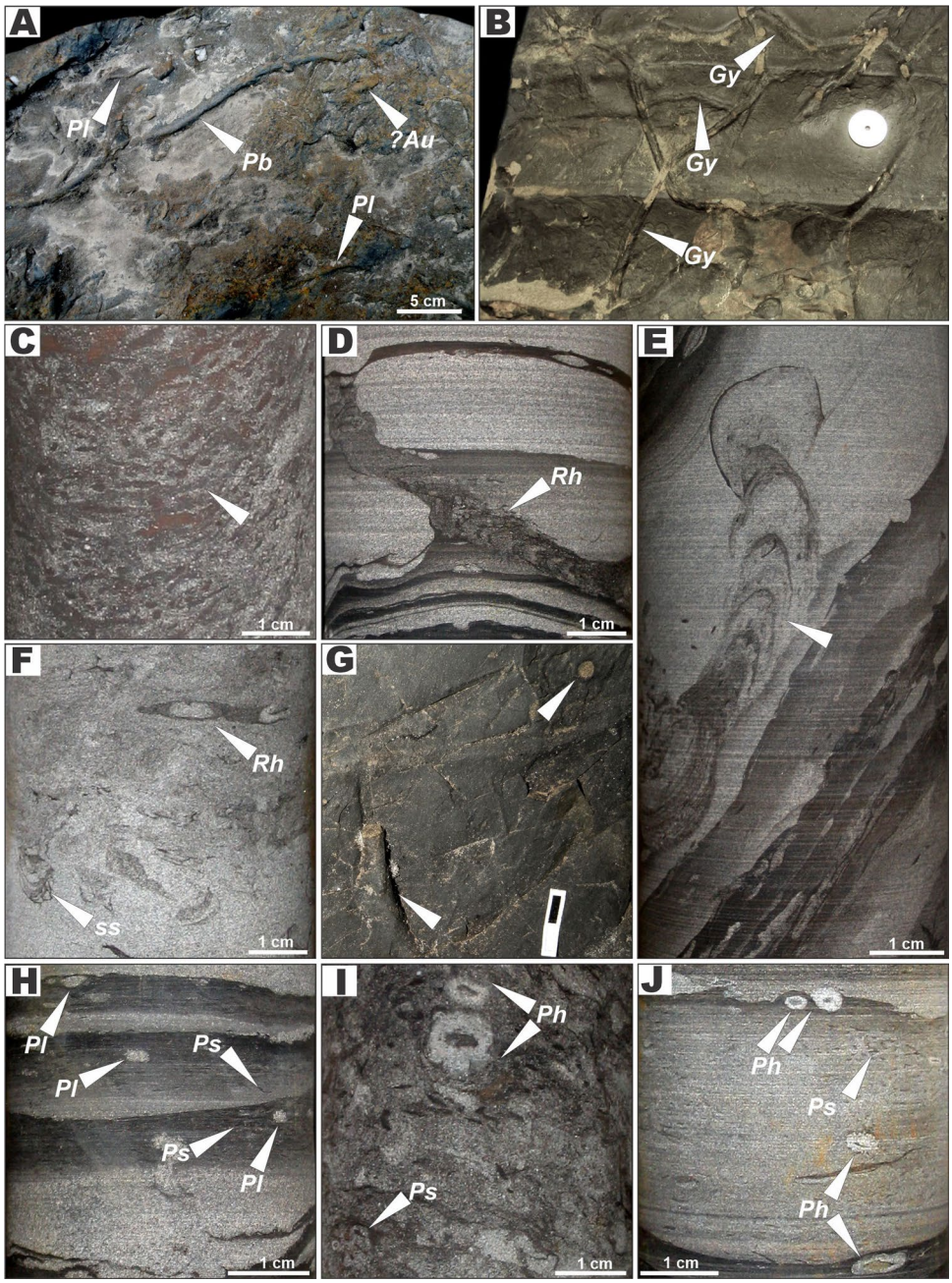

Fig. 7 Trace fossils in the Dalkjegla Mb of Carolinefjellet Fm. **A** Strogly bioturbated top of sandstone bed showing ?*Aulichnites* isp. (*Au*), *Planolites beverleyensis* (*Pb*), *P. montanus (Pm*) and *Planolites* isp. (*Pl*). Loose slab from the outcrop in Longyearbyen. **B** *Gyrochorte comosa* (*Gy*) on wave-rippled top of sandstone bed in Longyearbyen outcrop; the coin (scale) is 2 cm in diameter. **C** Sandstone with crowded traces ?*Helminthopsis* isp. (arrow); well Dh2, depth 64–65 m. **D** Moderately bioturbated facies H, showing vertical cross-section of bedding-oblique, protrusive *Rhizocorallium* isp. (*Rh*); well Dh2, depth 123.83–123.88 m. **E** Vertical cross-section of bedding-parallel spreiten burrow resembling *Rhizocorallium* (arrow); well Dh1, depth 69.07–69.14 m. **F** Sandstone with upward-increasing bioturbation intensity, including ?*Rhizocorallium* isp. (*Rh*) and funnel-shaped laminated burrow (*ss*); well Dh1, depth 102–103 m. **G** Bedding-parallel and vertical *Planolites beverleyensis* (*Pb*) at transition from sandstone to mudstone; loose rock slab in Longyearbyen outcrop; scale bar 1 cm. **H** Facies H showing cross-sections of *Planolites* isp. (*Pl*) and poorly visible *Phycosiphon incertum* (*Ps*); well Dh1, depth 80–81 m. **I** Heavily bioturbated muddy sandstone showing vertical cross-section of *Phycosiphon ?incertum* (*Ps*), *Palaeophycus heberti* (*Ph*) and mud filled small, vermicular, taxonomically undetermined burrows (?*Helminthopsis*, ?*Cosmorhaphe*); well Dh2, depth 51–52 m. **J** Small forms of *Palaeophycus heberti* (*Ph*) with differing thicknesses of burrow lining, and small hallowed burrows resembling *Phycosiphon incertum* (*Ps*); well Dh1, depth 132–133 m

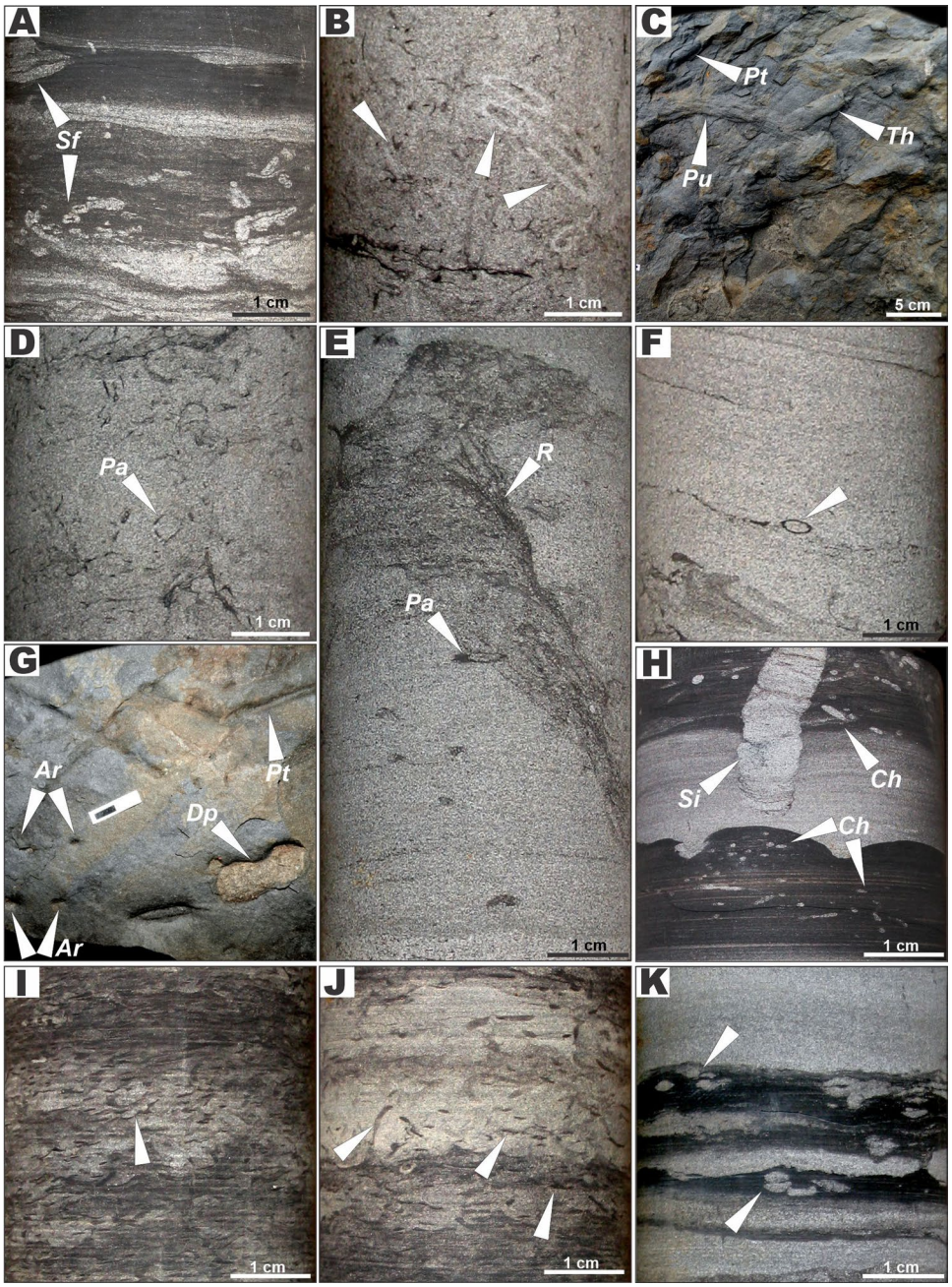

Fig. 8 Trace fossils in the Dalkjegla Mb of Carolinefjellet Fm. **A** *Schaubcylindrichnus freyi* (*Sf*, arrows), variably oriented, in lithofacies H; well Dh3, depth 140–141 m. **B** *Schaubcylindrichnus coronus* (arrows) in oblique section in lithofacies Sm; well Dh1, depth 124–125 m. **C** *Palaeophycus ?sulcatus* (*Pu*), *P. tubularis* (*Pt*) and *Thalassinoides ?suevicus* (*Th*) on mudstone bedding surface; loose rock slab in Longyearbyen outcrop. **D** Strongly bioturbated lithofacies Sm showing mud-lined, variably oriented burrows interpreted as *Palaeophycus* isp. (*Pa*); well Dh1, depth 124–125 m. **E** Ichnotraces ?*Rosselia* isp. (*R*) and *Palaeophycus* isp. (*Pa*) in lithofacies Sp; well Dh1, depth 120–121 m. **F** Mud-lined *Palaeophycus* isp. (arrow) in sandstone lithofacies; well Dh1, depth 124–125 m. **G** Ichnotraces *Arenicolites* isp. (*Ar*), *Diplocraterion* isp. A (*Dp*) and *Palaeophycus tubularis* (*Pt*) in lithofacies H; loose rock slab in Longyearbyen outcrop; scale bar 1 cm. **H** Ichnotraces ?*Chondrites targionii* (*Ch*) and *Siphonichnus* isp. (*Si*) in lithofacies H; well Dh2, depth 20–21 m. **I** Lithofacies Hm with ?*Phycosiphon* isp. (arrow); well Dh1, depth 95–96 m. **J** Lithofacies Hm with ?*Phycosiphon* isp. (arrows); well Dh2, depth 81–82 m. **K** Clusters of sand-filled burrows (arrows) in lithofacies H, interpreted as vertical section of spiral burrows resembling *Gyrolithes*; well Dh1, depth 117–118 m

are most abundant in the interval from 30 to 55 m above the formation base, whereas the higher part of the Dalkjegla Member shows marked fluctuations in bioturbation intensity (Fig. 3).

The burrows indicate a range of seafloor animal ethological activities, mainly feeding, dwelling, grazing, resting and crawling. Most bioturbation structures visible in non-slabbed core samples are small portions of burrow systems of unclear taxonomic affiliation. Many of them were produced by sediment scrambling, often multiple, or by scrambling of a soupy-state sediment substrate, which renders them taxonomically non-classifiable. In general, an exact taxonomic classification of trace fossils at ichnospecies level was seldom possible, but 38 ichnotaxa were inferred in the sedimentary succession (Figs. 7, 8, 9, 10 and 11), with three undetermined and 14 uncertain (labelled with question marks). A systematic ichnological description of the trace fossils is given in Table 2.

The occurrence and stratigraphic distribution of particular ichnotaxa and trace-fossil assemblages is generally related to lithofacies. For example, the ichnotaxa found in the thick sandstone beds of lithofacies Sp, Shs and Sr are different from those in lithofacies Sm or Hm. These differences entail variation in ichnofabric. An ichnofabric

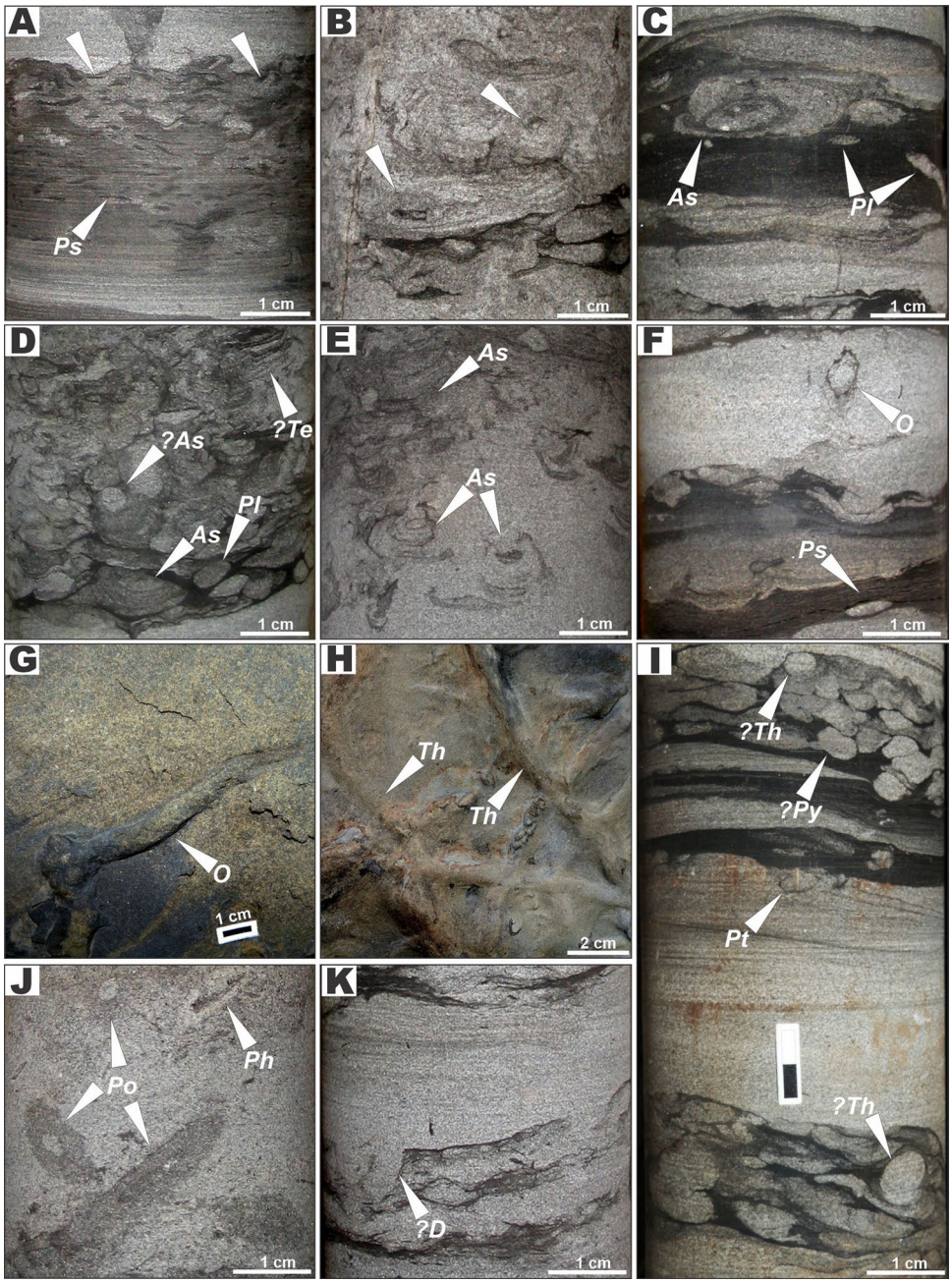

Fig. 9 Trace fossils in the Dalkjegla Mb of Carolinefjellet Fm. **A** Hallowed burrows resembling large *Phycosiphon incertum* (arrows) in strongly bioturbated silty upper part of lithofacies Sp graded bed; the dark triangular structure in overlying Sp bed seems to represent a dwelling bivalve burrow (domichnion); well Dh1, depth 94–95 m. **B** Strongly bioturbated bed of lithofacies Sm with distinct *Asterosoma* isp. (arrows); well Dh1, depth 79–80 m. **C** Moderate bioturbation with *Asterosoma* (*As*) and ?*Planolites* isp. (*Pl*) in lithofacies H; well Dh1, depth 30–31 m. **D** Strongly bioturbated lithofacies Hm with *Asterosoma* isp. (*As*), *Planolites beverleyensis* (*Pl*) and structures resembling *Teichichnus* isp. (?*Te*); well Dh1, depth 111–112 m. **E** *Asterosoma* isp. (*As*) in lithofacies Sm; well Dh1, depth 80–81 m. **F** *Ophiomorpha* cf. *rudis* (*O*), *Phycosiphon incertum* (*Ps*) and undetermined burrows in lithofacies H; well Dh1, depth 30–31 m. **G** Sandstone bedding plane showing *Ophiomorpha* cf. *rudis* (*O*); loose rock slab in Longyearbyen outcrop. **H** Sandstone bed sole showing *Thalassinoides suevicus* (*Th*); loose rock slab in Longyearbyen outcrop. **I** Strongly bioturbated mud and sparsely bioturbated sand in lithofacies H with ?*Phycodes* isp. (?*Py*) *Palaeophycus tubularis* (*Pt*) and *Thalassinoides* isp. (?*Th*); well Dh3, depth 79–80 m. **J** Thickly mud-mantled sand-filled tubes interpreted as *Phoebichnus* isp. (*Po*) and *Palaeopycus heberti* (*Ph*); well Dh1, depth 107–108 m. **K** Structure resembling lower part of *Diplocraterion* isp. (?*D*); well Dh1, depth 129–130 m

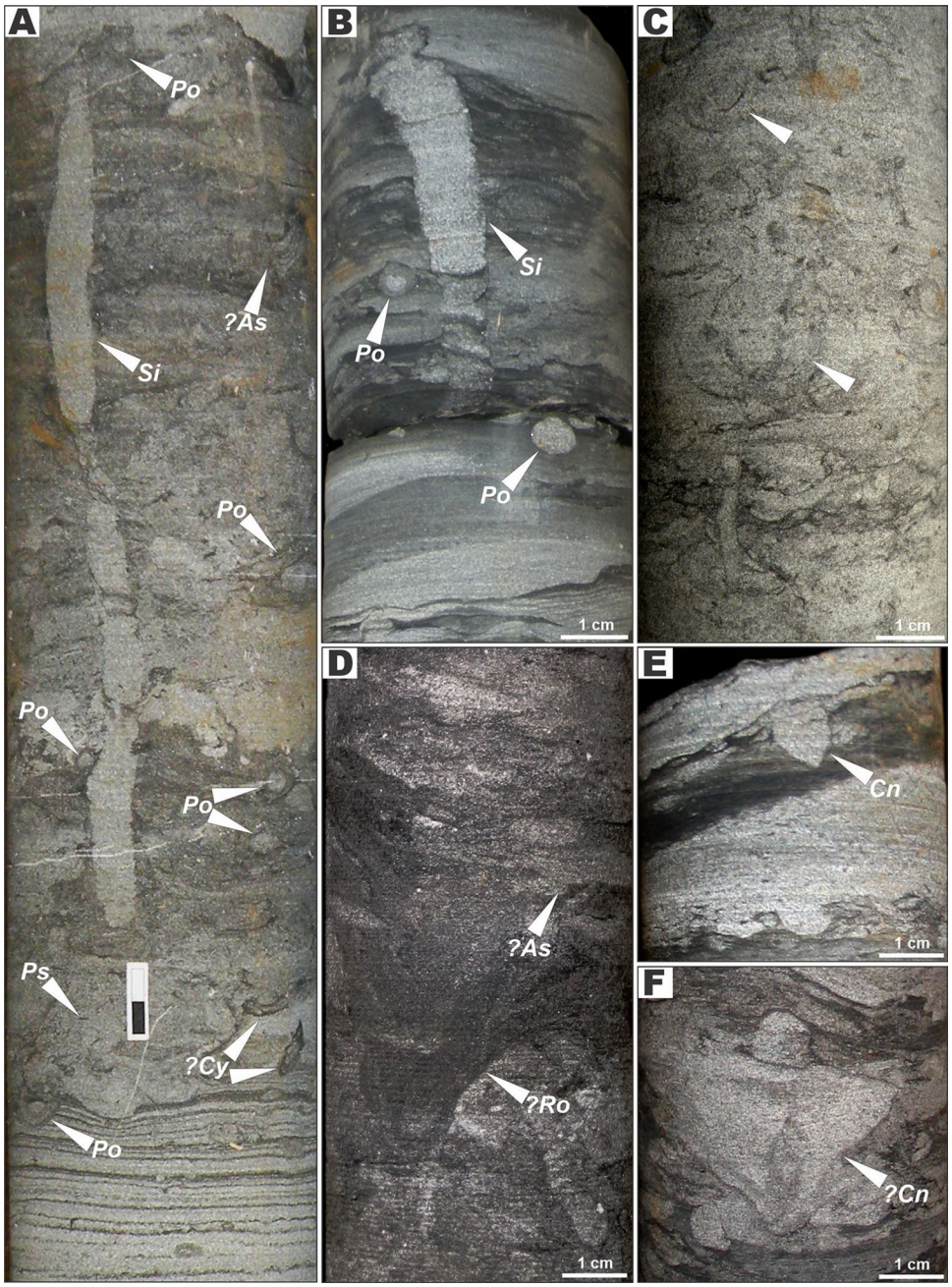

Fig. 10 Trace fossils in the Dalkjegla Mb of Carolinefjellet Fm. **A** Moderately bioturbated lithofacies H with ?*Astreosoma* isp. (?*As*), ?*Cylindrichnus* isp. (?*Cy*), *Phoebichnus* isp. (*Po*), *Phycosiphon* (*Ps*) and *Siphonichnus* isp. (*Si*); scale 1 cm, well Dh3, depth ~ 66.5 m. **B** Weakly bioturbated lithofacies H with *Phoebichnus* isp. (*Po*) and *Siphonichnus* isp. (*Si*); well Dh3, depth 72.0–72.1 m. **C** *Arenicolites* isp. (arrows) in moderately bioturbated lithofacies H; well Dh3, depth 95–96 m. **D** Strongly bioturbated lithofacies H with ?*Rosselia* isp. (?*Ro*) and ?*Asterosoma* isp. (?*As*); well Dh1, depth 108–109 m. **E** Moderately bioturbated lithofacies H with *Conichnus* aff. *papillatus* (arrow); well Dh1, depth 130–131 m. **F** Strongly bioturbated lithofacies Sm with presumed *Conichnus* isp. (arrow); well Dh1, depth 114–115 m

dominated by *Phycosiphon*-like burrows (*Phycosiphon incertum*, ?*Phycosiphon* isp., *Helminthopsis* isp.) is characteristic of lithofacies Sm (Figs. 7C, I, J, 8I, J) and locally Mm/Ml, and of the bioturbated divisions of lithofacies H (Fig. 7H). An ichnofabric dominated by *Asterosoma*, locally accompanied by *Teichichnus*, *Thalassinoides* and plug-shaped equilibrium structures (cf. Bromley and Uchman 2003), characterizes the top parts of the thick sandstone beds of lithofacies Sp, Shs and Sr, subsequently covered with the mudshales of lithofacies M (Fig. 9B, D, F). Bedding surfaces in the outcrop show also ?*Aulichnites* isp., *Gyrochorte comosa*, *Palaeophycus sulcatus*, ?*Phycodes* isp. and *Thalassinoides suevicus* (Fig. 7G, H). A package of sandstone lithofacies 20–26 m above the base of the formation in well cores (Fig. 3) shows an ichnofabric dominated by *Skolithos*, *Palaeophycus* isp. and *Arenicolithes* burrows (Figs. 10C, 11F).

The studied succession as a whole bears a mixed *Cruziana–Skolithos* ichnofacies (cf. Seilacher 1964, 1967, 2007; Bromley 1990; MacEachern et al. 2007a). The trace fossil suite in the above-mentioned sandstone package in well profiles represents the *Skolithos* ichnofacies, with the highly burrowed (scrambled) sediment indicating a distal variety of this ichnofacies. Trace fossils in the remaining part of the

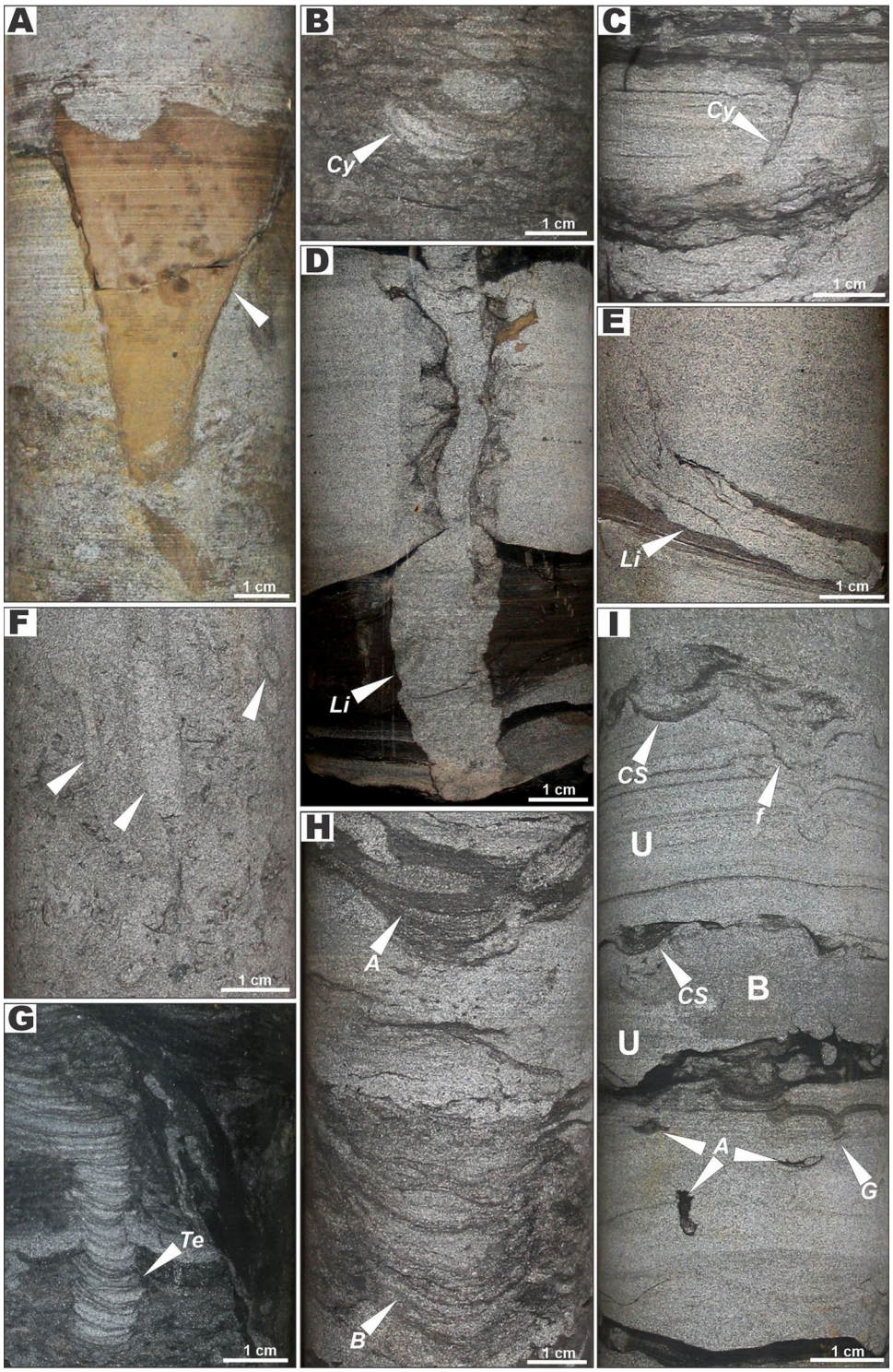

Fig. 11 Trace fossils in the Dalkjegla Mb of Carolinefjellet Fm. **A** Moderately bioturbated sandstone with sideritized structure resembling *Conichnus* isp. (arrow); well Dh1, depth 106–107 m. **B** Strongly bioturbated lithofacies Hm with ?*Cylindrichnus concentricus* aff. (*Cy*); well Dh2, depth 106–107 m. **C** ?*Cylindrichnus concentricus* aff. (*Cy*) in moderately bioturbated lithofacies H; well Dh1, depth 129–130 m. **D** Vertical section of *?Lingulichnus* isp. (*Li*) in lithofacies D; well Dh2, depth 22–23 m. **E** Vertical section of ?*Lingulichnus* isp. (*Li*) extending from mudstone interlayer into sandstone; well Dh1, depth 102–103 m. **F** Vertical section of lithofacies Sm with irregularly aligned *Skolithos* isp. (arrows); well Dh1, depth 123–124 m. **G** Vertical section of *Teichichnus* isp. (*Te*) in lithofacies Hm; well Dh3, depth 68.7–68.9 m. **H** Meniscoid laminated structures (?equilibrichnia) in lithofacies H: a shallow cup-shaped structure with sharp irregular margins (*A*) and a deeper, post-shaped laminated structure with frayed muddy margins (*B*); well Dh1, depth 113–114 m. **I** Sand-dominated lithofacies H with strongly bioturbated (B) and unbioturbated (U) parts, showing vertical sections of cup-shaped trace fossil with differing sizes and pattern (*CS*), a funnel-shaped fugichnion or equilibrichnion (*f*), a trace fossil resembling *Cylindrichnus* isp. (*A*), and a bilobate repichnion considered to be *Gyrochorte* isp. (*G*); well Dh1, depth 113–114 m

succession represent the *Cruziana* ichnofacies, which varies between the following two suites:

- A proximal to archetypal variety of the *Cruziana* ichnofacies (MacEachern et al. 2007a, c) dominated by *Asterosoma* isp., *Cylindrichnus* isp., ?*Phoebichnus* isp. and *Teichichnus* isp., often accompanied by *Schaubcylindrichnus coronus*, *Rosselia* isp., *Palaeophycus heberti, Thalassinoides* ?div. isp., *Rhizocorallium (?Taenidium), Diplocraterion* div. isp., *Conichnus* div. isp., plug-shaped equilibrium structures and undetermined cup-shaped burrows (Table 2).
- A distal variety of the *Cruziana* ichnofacies (MacEachern et al. 2007a, c) dominated by *Phycosiphon*-like trace

Table 2 Taxonomy of bioturbation structures in the Dalkjegla Mb of the Carolinefjellet Fm in the study area, with ichnogenera ordered alphabetically

Ichnogenus/ichnospecies	Description (incl. orientation, branching, shape, fill, lining and preservation)	Ethology	Inferred producer	Remarks	References
Arenicolites isp. (Figs. 8G, 10C)	U-shaped, vertical, tubular, smooth-walled structure 3 mm in diameter, distance between limbs up to 30 mm	Domichnion, fodinichnion	Worm-like animal	Observed as several poorly exposed specimens on core surface in one sandstone bed and on a bedding surface in outcrop	MacEachern and Pemberton (1992)
Asterosoma isp. (Fig. 9B–E)	Branched(?), bifurcated(?), radial(?), spindle-form horizontal to oblique endichnial burrow recorded in vertical section as semicircular to elliptical structure, 5−30 mm across, showing concentric sand and mud laminae packed about a central tube. The thickest and most numerous laminae occur in the burrow bottom part	Fodinichnion	?Worm-like animal	Many specimens observed in different cross-sections on core surface. The spindles are solitary or crowded. Specimens in Fig. 9B, D, E, may represent vertical sections of the lower, non-vertical segments of *Scalichnus* isp.	MacEachern et al. (2007a), Gani et al. (2007) and Knaust (2015)
?Aulichnites isp. (Fig. 7A)	Positive, bilobate, unlined, unbranched, actively filled epirelief recorded on bedding surfaces as straight to sinuous, bedding-parallel, unornamented, 3–5 mm wide. Median furrow narrow in small forms and wide in large specimens	Repichnion	Gastropod	Observed exclusively in outcrop, poorly preserved. Small forms show some similarity to *Gyrochorte,* but are much smaller	Frey and Howard (1990)
?*Chondrites targionii* (Fig. 8H)	Branched, straight endorelief recorded in vertical section as clusters of light-grey circular to elliptical spots and veins ~ 1–1.5 mm in diameter, built of silt	Chemichnion, agrichnion	?Worm-like animal	Clustered spots and veinlets observed on core surface in several horizons in the top part of succession	Fu (1991), Seilacher (2007)
Conichnus isp. A (Fig. 10E)	Amphora-shaped, vertical positive hyporelief recorded in vertical section as sand-filled body 10 mm high, 7 mm in diameter, acute basal apex. Burrow outline as in *Conichnus papillatus*, but the latter is much larger and shows a distinct bump on the apex	Domichnion?	Sea anemone, ?bivalve	Single specimen observed on core surface. Possible affiliation with the ichnogenus *Lockeia*	Mänill (1966), Pemberton et al. (1988), Pacześna (2010)

Table 2 (continued)

Ichnogenus/ichnospecies	Description (incl. orientation, branching, shape, fill, lining and preservation)	Ethology	Inferred producer	Remarks	References
?*Conichnus* isp. B (Fig. 10F)	Conical, vertical positive hyporelief recorded in vertical section as sand-filled body 10–20 mm high, 15–30 mm wide at its upper extremity. It tapers downwards at 40–70º smooth as sharply rounded basal apex. The infill shows inhomogeneity reminiscent of burrow draping	Domichnion, cubichnion	?Bivalve	Recorded on core surface as two specimens with different tapering angles (40º and 70º)	Frey and Howard (1981)
?*Conichnus* isp. C (Fig. 11)	Conical, vertical, positive hyporelief recorded in vertical section as siderite-filled body, 65 mm high, 40 mm wide at its upper extremity, with smooth, rounded basal apex. Sideritized infill reminiscent of smaller burrows	Domichnion, cubichnion	Unknown	Recorded on core surface as one specimen, which is much higher than isp. A and B, and tapers downwards at an angle of 25º	Frey and Howard (1981)
?Cylindrichnus concentricus aff (Fig. 11B, C)	Straight to bow-shaped, horizontal to oblique endorelief, cylindrical in section perpendicular to elongation, 5−8 mm in diameter, concentrically layered inside. The layered structure marked by alternating darker and lighter layers	Domichnion	Terebellid polychaete	Recorded on core surface as many specimens in vertical and oblique sections. Smaller than specimens described by Belaústegui and Gibert (2013)	Belaústegui and Gibert (2013)
Diplocraterion isp. A (Fig. 8G)	U-shaped, vertical sand-filled structure recorded on bedding surface as two joined, vertical, unlined, sand-built cylinders (dumbbell shape), 8 mm in diameter, 7 mm apart. Spreite between the arms poorly discernible, of retrusive type	Domichnion	Corophiid amphipod	Paired, dumbbell-shaped sand-built cylinders suggestive of a U-shaped burrow. One specimen on bedding surface of a loose sandstone slab at outcrop foot	Fillion and Pickerill (1990) and Šimo and Olšavský (2007)

Table 2 (continued)

Ichnogenus/ichnospecies	Description (incl. orientation, branching, shape, fill, lining and preservation)	Ethology	Inferred producer	Remarks	References
?Diplocraterion isp. B (Fig. 9K)	U-shaped, vertical, tubular, sand-filled structure 4 mm in diameter with spreite between limbs. Limbs up to 6 mm apart in vertical section parallel to burrow extension. In perpendicular section, seen as a column of vertically stacked menisci underlain by rounded sand body 4 mm in diameter	Domichnion	Corophiid amphipod	Observed as three specimens on core surface, in wavy to lenticularly bedded heterolithic facies H. Spreite indistinct in one specimen	Fillion and Pickerill (1990)
Gyrochorte comosa (Fig. 7B)	Positive, bilobate, unlined, unbranched, actively filled epirelief, recorded on bedding surfaces as ridges (lobes) 4–5 mm wide, showing plaited ornamentation, winding, intersecting itself	Fodinichnion	Endobenthic worm-like animal	Ornamentation poorly preserved. Observed in two thin sandstone slabs with oscillatory rippled top and no other burrows	Gibert and Benner (2002) and Cabrera et al. (2008)
?Gyrolithes isp. (Fig. 8K)	Spiral, unbranched endorelief recorded in vertical section as cluster of sand-filled, vertically stacked burrows, showing elliptical cross-section, 3 mm in diameter	Domichnion, fodinichnion	Decapod crustacean	Two specimens recorded on core surface in mudstone as cluster of 4 sand-filled, vertically stacked burrows. The structure suggests to represent one coil	Netto et al. (2007), Buatois et al. (2005) and Lettley et al. (2007)
?Helminthopsis isp. (Fig. 7C)	Positive, winding, unlined, unbranched hyporelief and endorelief recorded in vertical section as densely distributed, black, lenticular spots, 1 mm in diameter and as horizontal to oblique veins, up to 10 mm long and 0.5 mm thick. Winding black strings on bedding surfaces. Locally with light halo	Fodinichnion	Endobenthic worm-like animal	Recorded on core surface, frequently as a common trace fossil, except for the lower part of succession	Fillion and Pickerill (1990), Han and Pickerill (1995) and Coates and McEachern (2007)

Table 2 (continued)

Ichnogenus/ichnospecies	Description (incl. orientation, branching, shape, fill, lining and preservation)	Ethology	Inferred producer	Remarks	References
?*Lingulichnus* isp. (Fig. 11D, E)	Straight to curved in the lower part, vertical endorelief recorded as sand-filled shafts, usually surrounded by fluid-state deformed sediment. The fill occasionally shows subtle annulation	Fugichnion, equilibrichnion	Lingulid Brachiopod	Several specimens in core samples. The lack of distinct aureole of fluidal sediment resembles burrows interpreted as lingulid pedicle traces	Zonneveld and Pemberton (2003) and Zonneveld et al. (2007)
Ophiomorpha cf. *rudis* (Fig. 9F, G)	Straight to slightly curved, branched endorelief, positive hyporelief recorded as circular to elliptical elongate sand-filled bodies in vertical section and as cylindrical, gently winding sand-filled tunnels, 4–6 mm in diameter, irregularly lined with flame-like deformed mud pellets. Lining preserved fragmentarily, with granular texture	Domichnion, fodinichnion	Crustacean	Observed on core surface as several bedding-oblique to horizontal specimens, and as single bedding- parallel specimen in a loose sandstone slab at outcrop foot	Howard and Frey (1984), Gani et al. (2007) and Uchman (2009)
Palaeophycus heberti (Fig. 7I, J)	Gently curved, unbranched endorelief and epirelief with elliptical shape on core surface, thickly grain-lined, 3–10 mm in diameter. Lining 0.9–1.5 mm thick, made of structureless light-coloured sand. Cross-sectional views indicate that the trace fossil has a form of horizontal and subhorizontal, lined cylinder. Some specimens show lining thicker than the tunnel	Fodinichnion	Endobenthic worm-like animal	The trace fossil seems to occur solitarily, and this feature – together with the simple lining – renders *P. heberti* different from *Schaubcylindrichnus*	Pemberton and Frey (1982), Howard and Frey (1984) and Nara (2006)
Palaeophycus ?*sulcatus* (Fig. 8C)	Bedding-parallel, straight to slightly curved endichnial and epichnial tubular burrow, 7 mm in diameter, sculpted by small, interwoven longitudinal to slightly oblique ridges	Fodinichnion	Endobenthic ?worm-like animal	Recorded in a loose sandstone slab at outcrop foot	Pemberton and Frey (1982)

Table 2 (continued)

Ichnogenus/ichnospecies	Description (incl. orientation, branching, shape, fill, lining and preservation)	Ethology	Inferred producer	Remarks	References
Palaeophycus tubularis (Fig. 8C, F, G)	Bedding-parallel, straight to slightly curved epichnial tubular burrow, 7 mm in diameter, sculpted by small, interwoven longitudinal to slightly oblique ridges	Fodinichnion	Endobenthic ?worm-like animal	Recorded as short segments on bedding plane of loose sandstone slabs at outcrop foot and on core surface	Pemberton and Frey (1982)
Palaeophycus isp. (Fig. 8D, E)	Bedding-parallel, straight to slightly curved endichnial and epichnial tubular burrow 4 mm in diameter, mud lined, made of sand, observed on bedding plane	Fodinichnion	Endobenthic ?worm-like animal	Several specimens recorded on core surface	Pemberton and Frey (1982)
?*Phoebichnus* isp. (Figs. 9J, 10B)	Straight, cylindrical endorelief 5–12 mm in diameter, representing complex stellate system, circular to elliptical in vertical section, marked with sand-built centre 3−4 mm in diameter, surrounded by mud lining 1−2 mm thick	Fodinichnion	Endobenthic?echiuran worm	Found on core surface as several bedding-oblique to horizontal specimens. Relatively thick mud lining indicates *Phoebichnus* affinity	Bromley and Asgaard (1972), Kotake (2003) and McEachern et al. (2007a)
?*Phycodes* isp. (Fig. 9I)	Bundle of cylindrical endichnial burrows, circular to elliptical and lenticular in vertical section, made of homogeneous sand and showing slightly irregular outline, 7−12 mm in diameter	Fodinichnion	Endobenthicworm-like animal	Found as several bedding-parallel specimens on core surface. Bundled occurrence suggests *Phycodes* affinity	Frey and Pemberton (1985) and Fillion and Pickerill (1990)
Phycosiphon incertum (Fig. 9)	Complex, lobate, U-shaped, unbranched epirelief and endorelief recorded in vertical cross-section as elliptical to elongated, vermiform black spots surrounded by a pale-grey halo (frogspawn texture). The black spots are 1−1.5 mm in diameter and the mantle is 1−2 mm thick	Fodinichnion	Endobenthic worm-like animal	Observed in lithofacies H and Hm. No visible spreiten. Occurrence of U-shaped lobes is inferred from frequent occurrence of elongate spots up to 3 mm long. Occurs gregariously in many horizons	Wetzel and Bromley (1994), Bednarz and McIlroy (2009, 2012) and McEachern et al. (2007a, c, d)

Table 2 (continued)

Ichnogenus/ichnospecies	Description (incl. orientation, branching, shape, fill, lining and preservation)	Ethology	Inferred producer	Remarks	References
?Phycosiphon isp. (Fig. 8I, J)	Horizontal to oblique, curved endorelief marked in vertical section as dark-grey to black, highly curved streaks and spots up to 1 mm thick surrounded by a faint halo	Chemichnion, fodinichnion	Endobenthicworm-like animal	Recorded as crowds on core surface, represents compactionally flattened mud-filled tunnels. Differs from *Phycosiphon incertum* by less distinct, diffuse, flame-like halo similar to ichnogenus *Multina*	Bednarz and McIlroy (2009), McEachern et al. (2007a, c, d) and Kotlarczyk and Uchman (2012)
Planolites beverleyensis (Fig. 7A)	Straight to irregularly curved, unbranched endorelief, epirelief and hyporelief seen on bedding planes as cylindrical and in vertical section as circular, 5–6 mm in diameter, made of homogeneous sand, with smooth to slightly irregular walls	Fodinichnion	Endobenthic worm-like animal	Observed both in cross-section on core surface and on bedding planes in outcrop	Pemberton and Frey (1982) and Uchman (1995)
Planolites montanus (Fig. 7A)	Gently irregularly curved, rarely branched, smooth endorelief, epirelief and hyporelief recorded on bedding planes as tubular and in vertical section as circular, 1.5–2 mm in diameter, made of sand	Fodinichnion	Endobenthic worm-like animal	Recorded both in cross-section on core surface and on bedding planes. Locally quite common on bedding planes in sandstone lithofacies	Pemberton and Frey (1982) and Fillion and Pickerill (1990)
Planolites isp. (Fig. 7A, H)	Gently irregularly curved, unbranched, unlined endorelief, epirelief and hyporelief recorded in vertical section as circular and elliptical spots, 2.5−5 mm in diameter, marked by sand in mudstone layers. Cross-sections show a horizontal or subhorizontal, curved, unlined cylinder infilled with homogeneous sand	Fodinichnion	Endobenthic worm-like animal	Recorded both in cross-section on core surface and on bedding planes	Pemberton and Frey (1982)

Table 2 (continued)

Ichnogenus/ichnospecies	Description (incl. orientation, branching, shape, fill, lining and preservation)	Ethology	Inferred producer	Remarks	References
Rhizocorallium isp. (Fig. 7D–F)	U-shaped in planar view, actively filled endorelief recorded in vertical section as a meniscated stripe 5 mm thick, indicative of spreite structure. Spreite arrangement protrusive or retrusive	Fodinichnion	Polychaete	Recorded as several specimens on core surface	Fielding et al. (2007) and Seilacher (2007)
Rosselia isp. (Figs. 8E, 10D)	Chalice-shaped, unbranched, vertical endorelief seen in vertical section as vertically or obliquely elongate, horn-shaped to conical structure 25−40 mm in diameter, 30–50 mm high, filled with faintly laminated mud. Laminae arrangement reminiscent of concentric sheaths	Fodinichnion	Unknown	Recorded as a few specimens on core surface	Miller and Aalto (2008), Coates and MacEachern. (2007), Hansen and MacEachern (2007) and Davison and MacEachern (2007)
Schaubcylindrichnus coronus (Fig. 8B)	Straight, oblique to bedding, unbranched endorelief seen in vertical section as clusters of tubular burrows, 3 mm in diameter, showing relatively thick, distinctive light-coloured lining (0.5–0.9 mm thick)	Domichnion	Endobenthicsessile ?polychaet	Recorded as many specimens on core surface only. The trace similar to *S. freyi* in the type of lining but its tubes are much larger and show only bedding-oblique alignment. Clustering distinguishes it from *Palaephycus heberti*	Frey and Howard (1981) and Nara (2006)
Schaubcylindrichnus freyi (Fig. 8A)	Straight to gently curved, horizontal to oblique, unbranched endorelief seen in vertical section as clusters of well-lined and usually flattened tubes, 2–5 mm in diameter. Light-coloured wall lining 0.5−1 mm thick	Domichnion	Endobenthicsessile ?polychaet	Recorded as many specimens on core surface. *S. freyi* may represent the lower part of the *S.* burrowing system where the individual tubes tend to converge	Miller (1995)

Table 2 (continued)

Ichnogenus/ichnospecies	Description (incl. orientation, branching, shape, fill, lining and preservation)	Ethology	Inferred producer	Remarks	References
Siphonichnus isp. (Fig. 10A, B)	Straight to slightly curved, vertical endorelief seen on core surface as columnar, cylindrical sand body 10 mm wide, showing faint meniscate backfill structure accentuated by delicate, irregular rippling of walls	Fugichnion, equilibrichnion	Endobenthic bivalve	Recorded as several evident specimens on core surface and bedding plane	Stanistreet et al. (1980), Zonneveld and Gingras (2013) and Knaust (2015)
Skolithos linearis (Fig. 11F)	Straight to slightly curved, vertical to subvertical endichnial shafts 5–7 mm in diameter, filled with homogeneous sand, show wall lining 1–2 mm thick, slightly darker than the shaft infill	Domichnion	Annelid, phoronid	Observed on core surface, with longest specimen up to 6 cm. Resembles stem tunnels of *Rosselia socialis* (cf. Miller and Aalto 2008)	Haldeman (1840), Alpert (1974), McEachern et al. (2007a) and Schlirf and Uchman (2005)
Teichichnus rectus (Fig. 11G)	Columnar to lobate vertical endorelief with stacked concave-up spreite, 5–20 mm wide, up to 30 mm high and ≥ 40 mm long. Long, wavy, down-bowed laminae tending to merge upwards at their ends. Oblique sections show shorter, truncated laminae	Fodinichnion	Crustacean ?worm-like animal	Recorded as many specimens on core surface	Seilacher (1955, 2007) and Coates and MacEachern. (2007)
Thalassinoides suevicus (Figs. 8C, 9H)	Cylindrical, unlined boxwork endorelief, positive hyporelief, 10−20 mm in diameter, slightly enlarged at points of branching, filled with sand. Smooth walls and T- or Y-shaped ramifications	Domichnion, fodinichnion	Crustacean	Several specimens on bedding surface of loose sandstone slabs at outcrop foot	Frey et al. (1984) and Frey (1990)
?*Thalassinoides* isp. (Fig. 9I)	Cyllindrical, unlined to delicately mud-lined endorelief, positive hyporelief, 10–20 mm in diameter, filled with sand, showing Y-shaped branching	Domichnion, fodinichnion	Crustacean	The fill is occasionally laminated, with thickest laminae at the bottom. Ichnotaxon noted on bedding surface of several sandstone slabs at outcrop foot	Frey et al. (1984), Bromley and Uchman (2003) and MacEachern et al. (2005)

Table 2 (continued)

Ichnogenus/ichnospecies	Description (incl. orientation, branching, shape, fill, lining and preservation)	Ethology	Inferred producer	Remarks	References
Undetermined ichnotaxa					
Cup-shaped isp. (Fig. 11H, I)	Endorelief with a copular lower outline, pointing downwards centrally and having sharp, uneven margin. Structure 0.5−1.5 cm deep and 1.0−3.5 cm wide in its broadest part, with irregularly streaked, down-bent sandy infill	Cubichnion, equilibrichnion	Sea ?anemone, ?bivalve	Structure seen as many specimens on vertical core surface	None
Funnel-shaped isp. (Figs. 7F, 13I)	Epirelief with sheath-shaped lower outline, pointing downwards centrally, 7−10 mm deep and 10−15 mm wide in its broadest part. Irregularly laminated infill with sharply down-bent laminae	Fodinichnion, equilibrichnion	Sea ?anemone	Structure seen as many specimens on vertical core surface	None
U-shaped isp. (Fig. 11H)	Endorelief with irregular U-shaped lower outline, pointed downwards centrally. Spreite-type infill and a fringed margin. Structure 4 cm deep and ~ 3.5 cm wide. Margins marked by muddy shreds protruding outwards from the trace body	Domichnion, equilibrichnion	Sea ?anemone	Apart from its fringed margin, the structure resembles *Teichichnus*. Observed one specimen on core surface. May represent downward extension of the cup-shaped isp.	None

fossils (*Phycosiphon incertum*, ?*Phycosiphon* isp., ?*Helminthopsis* isp.) with some *Planolites* isp., *Diplocraterion* div. isp., plug-shaped equilibrium structures, ?*Lingulichnus* isp., *Siphonichnus* isp. and rarely some other ichnotaxa.

The first suite occurs in the top parts of medium to thick sandstone beds overlain by mudshale and in some packages of the heterolithic deposits of lithofacies H. The second suite occurs in lithofacies Sm and in some beds of lithofacies H.

Notably, both the *Skolithos* and *Cruziana* ichnofacies here show quite specific composition in comparison to that commonly reported from similar sublittoral deposits in other regions (cf. Buatois and Angriman 1991; MacEachern and Pemberton 1992). The *Skolitho*s ichnofacies differs from its 'classic variety' by nearly lacking such trace fossils as *Ophiomorpha*, *Bergaueria*, *Taenidium* and *Macaronichnus* (cf. MacEachern et al. 2007a, 2012; Buatois and Mangano 2011), whereas the *Cruziana* ichnofacies lacks its most characteristic arthropod tracks and *Zoophycos* burrows (cf. Buatois and Mangano 2011). Moreover, the facies-crossing ichnogenus *Chondrites,* so commonly reported from such deposits, has not been evidenced in the present case. Its absence is particularly remarkable in the lower part of the succession, in the blackish to brownish dark-grey mudshales of lithofacies Mm overlying the non-bioturbated basal lithofacies Ml, where other trace fossils begin to appear, such as *Phycosiphon*-like burrows and *Schaubcylindrichnus freyi*.

Lithofacies associations

The lithofacies (Table 1) have been recognized to form four main associations, labelled FA1 to FA4, which range from sand-rich to muddy and are vertically alternating with one another in the stratigraphic succession (Fig. 3). The extensive outcrop section of gently-inclined deposits and the two pairs of closely-spaced wells (Fig. 1C) show also considerable lateral changes over the distances of a few hundred metres, with some lithofacies pinching out and with one lithofacies association passing laterally into another.

The lithofacies associations and their ichnofauna assemblages are described and interpreted below. The lithofacies associations are thought to represent different inner to outer shelf zones and for simplicity are given interpretive environmental labels, but their descriptions are separated from interpretations in the text. The stratigraphic alternation of lithofacies associations (Fig. 3) is attributed to the lateral shifting of shelf zones in response to relative sea-level fluctuations accompanied by morphodynamic changes of the shoreface–shelf profile (cf. Hampson 2000; Hampson and Storms 2003; Grundvåg et al. 2021).

FA1: Lower shoreface deposits

The deposits of lithofacies association FA1 occur several times in the stratigraphic succession (Fig. 3), forming packages up to 6 m thick, enveloped by the mud-richer association FA2 and passing laterally into the latter. Their boundaries are mainly gradational, marked by a rapid upward change in the thickness and relative proportion of sandstone and mudstone beds, but the basal contact of FA1 in some cases is sharp and recognizably erosional.

Description

This lithofacies assemblage (Figs. 3, 4) consists mainly of lithofacies Sp and Shs, with drapes or intercalations of lithofacies Sr and subordinate thin interbeds of lithofacies Sm, Hm and/or Mm, rarely Ml. Lithofacies Shs volumetrically dominates, as the sandstone beds with hummocky stratification are the thickest. Beds of sandstone lithofacies tend to be amalgamated by erosion, whereby the interbeds of muddy lithofacies are commonly truncated, discontinuous or virtually removed. Mudclasts, up to 7 cm in length, occur scattered along internal erosional surfaces.

Sandstone beds in the outcrop are generally extensive sheets, but their geometry varies from tabular to irregularly mounded or lenticular (Fig. 3; see also Grundvåg et al. 2021). Some beds show a uniform thickness over lateral distances of several tens of metres, before thinning markedly or pinching out within a few metres. Other sandstone beds, particularly the thickest ones, show irregular mounds in the form of simple low-amplitude domes (isotropic to anisotropic hummocks) or compound, broader and thicker (≤ 1.5 m) domes with a clinoformal lateral stacking of the successive units of lithofacies Shs and subordinate Sr, mainly towards the W or WSW (Fig. 3). The amalgamated clinoforms are convex-upwards to sigmoidal, inclined at 5–20°. Most of the sand mounds have erosional bases with an irregular low relief (< 10 cm), but reaching a relief of up to 50 cm where forming a sharp lower boundary of FA1 package (Fig. 3). There are also solitary channel-like scours (Fig. 3F), up to 1.5 m deep and a few tens of metres wide, trending towards the W or WSW and filled with vertically accreted packages of lithofacies H or obliquely inclined (10−15°) packages of lithofacies Sp and Sr (see Birkenmajer 1966, Figs. 3, 4).

Animal burrows in lithofacies association FA1 are relatively uncommon and limited mainly to infrequent bioturbated horizons, generally corresponding to the mudshale-covered top parts of sandstone beds or their amalgamated packages. The degree of bioturbation thus varies from none to high (BI = 0 to 6) on the thickness scale of a bed or a bed package. The following ichnotaxa have been recognized: *Arenicolithes* isp., *Asterosoma* isp., *Paleophycus tubularis*,

Palaeophycus isp., ?*Phoebichnus* isp., *Planolites* isp., *Rosselia* isp., *Schaubcylindrichnus coronus*, *Skolithos* isp. and *Teichichnus rectus*, with accompanying ?*Helminthopsis*-like traces and sporadic *Ophiomorpha* cf. *rudis* and *Diplocraterion* isp. (Table 2).

The FA1 packages are generally hosting a proximal variety of the *Cruziana* ichnofacies (cf. MacEachern et al. 2007a), dominated by either *Asterosoma* or undefined scrambled ichnofabric overprinted by other taxa as deeper tiers. Only one sandstone package, about 1 m thick and located 20–26 m above the base of Carolinefjellet Formation in the wells (Fig. 12), hosts a distal variety of the *Skolithos* ichnofacies (cf. MacEachern et al. 2007a) dominated by suspension-feeder traces and comprising *Skolithos* isp., *Arenicolithes* isp., *Palaeophycus tubularis*, *Palaeophycus* isp. and sporadic *Ophiomorpha* and *Diplocraterion* (Figs. 10C, 11F).

Interpretation

The assemblage of sandstone lithofacies Sp, Shs and Sr indicates the action of littoral waves with variable orbital velocities, punctuated by storm combined-flow events (Table 1). The clinoformal stacking of amalgamated sandstone units suggests broad subaqueous sand bars formed by series of high frequency storms, with the geostrophic currents deviated from shoreline by the Coriolis effect (Walker 1984b) and with the initial hummocks instigating subsequent deposition in their hydraulic shadow. Midtgaard (1996) described similar sandbodies, accreted seawards at ~ 70° away from shoreline, from the Lower Cretaceous mid-shelf deposits in western Greenland. The channel features, limited to FA1, were originally attributed to tidal currents (Birkenmajer 1966), but this lithofacies association represents sedimentation dominated by waves and storm-generated currents. These features are likely storm-current elongate scours (cf. Bentley et al. 2002, Fig. 19) or bypass troughs formed by storm-boosted rip currents (cf. Gruszczyński et al. 1993; Stone et al. 1995; Mathers and Zalasiewicz 1996), filled in directly by the storm and/or subsequent fairweather sedimentation.

The scarcity of burrows in sandstone beds implies seafloor conditions of high and quasi-perennial sediment mobility, and hence deposition mainly above the fairweather wave base. The numerous internal truncation and amalgamation surfaces imply that a considerable part of fairweather sand (lithofacies Sp and Sr) was probably removed by erosive storms and transferred seawards. The interbeds of muddy facies and isolated bioturbation horizons represent episodes when the wave base stayed above the seafloor. The evidence as a whole indicates deposition between the maximum and mean depth of fairweather wave base, which means a lower shoreface zone (Clifton 1981; Brenchley 1985; Tillman 1985; Reading and Collinson 1996; Hampson 2000).

Deposition below the mean fairweather wave base is consistent with the occurrence of *Cruziana* ichnofacies and with the bioturbation horizons indicating distinct time-windows for benthic colonisation (Pollard et al. 1993; Goldring et al. 2004, 2007). The solitary sandstone package with *Skolithos* ichnofacies (Fig. 12) indicates a highly mobile sandy substrate and low sedimentation rate (cf. MacEachern et al. 2007a; MacEachern and Bann 2008), which would suggest deposition around the mean fairweather wave base in a middle shoreface zone and imply the maximum fall of relative sea level recorded within the sedimentary succession. This episode might either signify the greatest shoreline advance or represent brief opportunistic colonization of lower shoreface by *Skolithos* ichnofauna following an exceptionally high delivery of sand by a series of strong storms (e.g., Vossler and Pemberton 1988, 1989; Pemberton et al. 1992b, 2012; Pemberton and MacEachern 1997). In either case, the sparsity of bioturbation in this sandstone package would reflect the short duration of inter-storm benthic colonisation windows (MacEachern and Pemberton 1992; Dashtgard et al. 2012; Pemberton et al. 2012).

FA2: Proximal offshore-transition deposits

Lithofacies association FA2 shows a comparable thickness proportion of alternating sandy and muddy deposits, forming packages about 1 to 4 m thick. They underlie and overlie lithofacies association FA1 or occur in isolation from the latter (Fig. 3). The outcrop section also shows FA1 passing laterally into FA2 by the lateral thinning or pinch-out of sandstone beds and an increase in the relative proportion of muddy deposits.

Description

This lithofacies assemblage (Figs. 3, 4) consists of the heterolithic deposits of lithofacies H and mudshale lithofacies Mm interspersed with discrete sheet-like sandstone beds showing various combinations of lithofacies Sp, Shs and Sr (Table 1; Fig. 5B–D). Subordinate are beds of lithofacies Sm or intervals of Hm. The muddy and sandy beds are up to 50 cm thick, but mainly 10–20 cm. Sandstone beds have mainly flat bases, sharp to slightly erosional, whereas their tops in the outcrop section show broad undulations on a lateral scale of several to a few tens of metres. The undulations render some of the thinner beds discontinuous, split into irregular broad lenses (probably 3D patches). Erosional amalgamation of sandstone beds is uncommon and only local.

Bioturbation in lithofacies association FA2 is more common than in FA1 and ranges from isolated to clustered burrows, but occurs mainly in the muddy facies and reaches

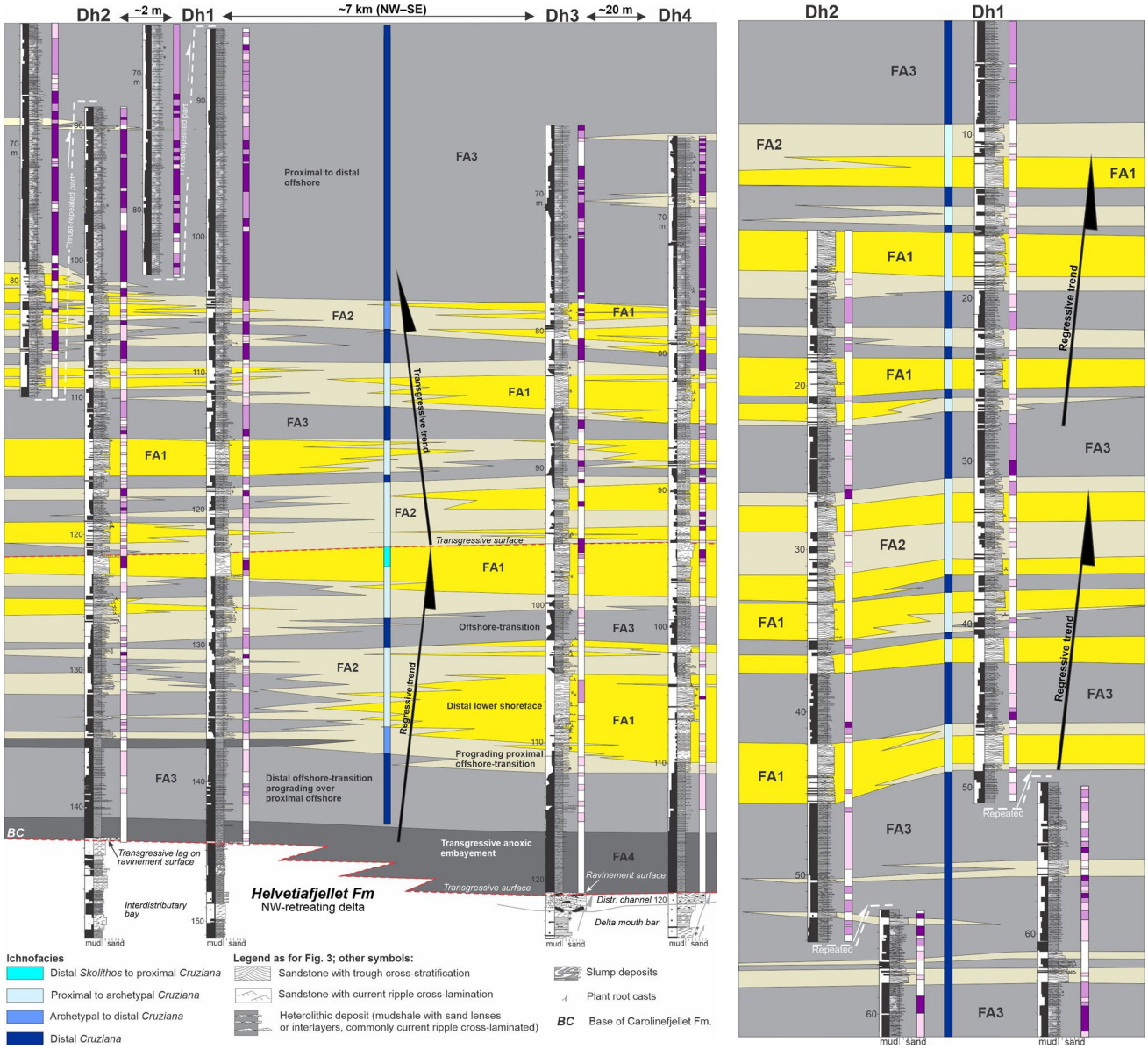

Fig. 12 Well-log correlation panel showing the interpretive depositional architecture of the Dalkjegla Mb of Carolinefjellet Fm in the study area (Fig. 1C) and the vertical distribution of its lithofacies and ichnofacies associations. Legend as in Fig. 3. The panel shows the lower part of the Carolinefjellet Fm and its basal contact with the Helvetiafjellet Fm. Note the stratigraphic repetition due to tectonic thrusting in logs Dh1 and Dh2. The right-hand continuation of the figure shows the topmost part of the succession in wells Dh1 and Dh2, lacking in wells Dh3 and Dh4; note again the slight stratigraphic repetition due to thrusting

its highest intensity in distinct horizons of unknown lateral extent (observation from well cores). The trace fossils include *Asterosoma* isp., *Paleophycus tubularis*, *Palaeophycus* isp., ?*Cylindrichnus concentricus*, *Teichichnus rectus*, *Thalassinoides* isp., *Rosselia* isp., *Conichnus* div. isp., *Planolites* isp., *Arencolites* isp., ?*Helminthopsis* isp., ?*Phycosiphon incertum* and various plug-shaped equilibrium structures, with sporadic *Diplocraterion* ?div. isp., *Rhizocorallium* isp. (?*Taenidium* isp.), ?*Lingulichnus* isp., *Siphonichnus* isp., ?*Phoebichnus* isp., ?*Phycodes* isp. and ?*Chondrites targionii* (Table 2). In addition, *Planolites montanus, P. beverleyensis, Palaeophycus sulcatus, Gyrochorte comosa* and ?*Aulichnites* isp. were found on sandstone bedding surfaces in the outcrop (Fig. 9A, B, G).

The bioturbation intensity in FA2 varies from none to high (BI = 0 to 6). Most common are stratigraphic intervals with no or little bioturbation (BI = 1), hosting isolated burrows (Figs. 6A, E, F, H, I, 7D). Similarly varied is ichnofabric, dominated by horizontal burrows. The rare strongly bioturbated horizons show a scrambled fabric intersected

by *Asterosoma* and/or *Teichichnus,* rarely other ichnotaxa. The less bioturbated deposits show a full range of isolated burrows, rarely intersecting one another.

Interpretation

Compared to FA1, this lithofacies association contains thinner sandstone beds and a higher proportion of muddy facies, which suggests a more distal depositional zone relative to palaeoshoreline. The discrete sandstone sheets with wave-generated and combined-flow structures indicate sand emplacement by brief events, considered storms. The thicker beds of muddy facies and greater abundance of bioturbation indicate considerably longer periods of sand-starved seafloor conditions below the fairweather wave base. Such conditions characterize the lowermost shoreface to upper offshore-transition zone, at a water depth range from around the maximum fairweather wave base to the mean storm wave base, where sand is delivered and spread mainly by storms (Howard and Reineck 1981; Kreisa 1981; Reading and Collinson 1996; Hampson 2000). The lenticularity of sandstone beds on a lateral scale of up to a few hundred metres (Nøttvedt and Kreisa 1987; Grundvåg et al. 2021) probably reflects a patchy style of the spatial distribution of sand by storms (cf. Bentley et al. 2002; Keen et al. 2004).

The ichnofauna assemblage in FA2 indicates environmental conditions hospitable to a wide range of benthic animals, but also reflects the ecological stress imposed by episodic sand emplacement (cf. Pemberton et al. 1992b; Pemberton and MacEachern 1997; MacEachern et al. 2007b; Bann et al. 2008; MacEachern and Bann 2008). The predominance of horizonal burrows indicates a deposit-feeding benthic fauna (cf. Pemberton et al. 2012), which implies relatively long periods of low-energy bottom water conditions. The scarcity of suspension-feeding fauna indicates a quick burial of the episodically emplaced sand layers by ubiquitous mud, which disfavoured seafloor colonization by organisms preferring a sandy substrate (Pemberton et al. 2012). The event sedimentation and variable time-windows for benthic colonisation may explain the varying bioturbation degree of the deposits (Pemberton et al. 1992b, 2012).

FA3: Distal offshore-transition deposits

Lithofacies association FA3 contains a much higher thickness proportion of muddy lithofacies, with sandstone beds generally thinner and finer-grained. These mud-dominated deposits form packages up to ~ 20 m thick, both underlying and overlying lithofacies association FA2 (Fig. 3). The contacts of these two associations are conformable and transitional, marked by changes in the relative proportion of sandy and muddy lithofacies. In the outcrop section, FA2 is also passing laterally into FA3 within a few hundred metres.

Description

The assemblage FA3 (Fig. 3) consists mainly of lithofacies Mm, Ml and Hm, interspersed with thin sandstone sheets of lithofacies Sr (Table 1, Fig. 6F, I). The sandstone beds are very fine- to fine-grained and locally up to 20 cm thick, but are mainly thinner than 5 cm and commonly discontinuous, composed of isolated lenses with a lateral extent of 10 cm to several metres. The boundaries of sandstone beds are sharp, but the bases are seldom recognizably erosional and the tops show well-preserved ripple forms. Ripple crests are trending mainly SE, and the ripple cross-laminae sets in some beds show mud drapes, occasionally rich in carbonaceous plant detritus.

FA3 in its lowest stratigraphic occurrence (Fig. 12), particularly in its basal part, is distinctly less burrowed and shows a much lower diversity of trace fossils than in the higher occurrences. Moderate to high bioturbation occurs in thickness intervals of 1 m to a few metres, particularly in lithofacies Hm. There are isolated horizons of intense burrowing as well as random solitary burrows. High bioturbation (BI = 5–6) prevails in the FA3 package at 40–55 m above the base of the formation.

Trace fossils include *Helminthopsis* isp. and some other *Phycosiphon*-like ichnotaxa, *Asterosoma* isp., *Planolites* isp., *Thalassinoides* isp., *Teichichnus rectus*, *Palaeophycus* isp., *Siphonichnus* isp., ?*Cylindrichnus concentricus* and *Rosselia* isp., accompanied by sporadic *Diplocraterion* ?div. isp., ?*Lingulichnus* isp. and undetermined cup-shaped, funnel-shaped and fringed U-shaped burrows (Table 2). Ichnofabric is dominated by *Phycosiphon*-like burrows, locally with *Asterosoma, Planolites*, *Thalassinoides* and *Teichichnus*. *Asterosoma* is characteristic of the sand-richer parts of FA3 packages. The lowermost stratigraphic package of FA3 (Fig. 12), particularly at its transition from the underlying FA4, shows only ?*Phycosiphon isp*., *Schaubcylindrichnus freyi* and some sand-filled thin pipes reminiscent of *Planolites*. Overall, the FA3 deposits bear a trace-fossil assemblage of the *Cruziana* ichnofacies, mainly its distal variety (cf. Savrda et al. 2001; MacEachern et al. 2007a).

Interpretation

The differences in lithofacies and ichnofauna and the stratigraphic relationship between lithofacies association FA2 and mud-dominated FA3 indicate that the latter is a more distal seaward equivalent of the former. The isolated thin sandstone beds are thought to be distal tempestites, deposited at water depths where only the strongest storm-generated currents were delivering fine sand and where the sand was fully reworked by storm waves with mainly low near-bottom orbital velocities (Komar and Miller 1975; Clifton 1981; Clifton and Dingler 1984). Ripple mud drapes indicate brief

rhythmic detachments of the wave base from the seafloor, which may reflect pulsating storms or the impact of tides on the wave base during storms lasting for several days. The pinch-and-swell geometry of thin sandstone beds, on the scale of ripples or small groups of ripples, indicates sand-starved seafloor conditions. The lenticularity of thicker beds, on a lateral scale of several tens to hundreds of metres (Nøttvedt and Kreisa 1987), reflects the inherently patchy pattern of spatial sand distribution by storms (cf. Bentley et al. 2002; Keen et al. 2004).

The evidence as a whole indicates deposition in the distal offshore-transition zone, below the mean storm-wave base (Howard and Reineck 1981; Reading and Collinson 1996; Hampson 2000). This interpretation is consistent with a distal *Cruziana* ichnofacies, dominated by traces of deposit-feeding, dwellings and grazing fauna. The general lack of suspension-feeders reflects the sparsity and infrequent availability of sandy substrate.

The poor assemblage of ichnofauna in the stratigraphically lowest package of FA3, at its transition from the underlying FA4, apparently reflects a benthic ecological change from an unhospitable (anoxic?) muddy environment to a more hospitable environment with episodic delivery of sand and improved seafloor oxygenation. A similar ichnological case was reported, for example, by Savrda et al. (2001) from the Pleistocene shelf of New Jersey.

FA4: Offshore deposits

Lithofacies association FA4 occurs only in the basal part of the succession (Figs. 3, 12), where these muddy deposits form a unit ranging in thickness from ~ 2 m in wells Dh1/Dh2 to 5 m in wells Dh3/Dh4 (Figs. 1C, 3) and to nearly 15 m in the southern outcrops more distal from the inferred palaeoshoreline (Midtkandal et al. 2016). This muddy unit is underlain by a solitary erosional conglomeratic sheet (wells Dh1 to Dh3) or locally by a correlative erosional bypass surface (well Dh4). The conglomeratic layer, although laterally discontinuous, is a regionally widespread feature (Birkenmajer 1966) considered in mapping to mark the base of the Carolinefjellet Formation (Parker 1967; Nagy 1970; Mørk et al. 1999). Similarly widespread is the basal mudshale unit, which apparently extends beyond the coastal outcrops in SE Spitsbergen (Nemec et al. 1988; Århus 1991).

Description

This lithofacies association consists chiefly of the blackish grey, parallel-laminated clayey to silty mudshales of lithofacies Ml (Fig. 6F) interspersed towards the top with sporadic thin (< 1 cm) and mainly discontinuous, pinch-and-swell sheets of very fine-grained sandstone lithofacies Sp and/or Sr. Ripple cross-laminae sets in lithofacies S4 occasionally show carbonaceous mud drapes. The underlying polymict conglomeratic sheet consists of poorly sorted lithofacies C, generally no more than 10 cm thick, alternating laterally between massive and faintly planar stratified (Table 1, Figs. 3, 5A, 12). The conglomerate layer contains intraformational mudclasts and has an uneven erosional base and a flat top locally covered with a thin discontinuous layer of lithofacies Sr.

Lithofacies association FA4, although the most muddy (Table 1), generally lacks bioturbation. Sporadic tiny sand spots (~ 1 mm in diameter) occur on the non-slabbed core surfaces, but it is unclear if these are some sand-filled very thin burrowing pipes or rather floating tiny aggregates (intraclasts) of very fine-grained sand.

Interpretation

The unit of muddy lithofacies Ml intercalated with sporadic very thin sheets of finest-grained sand indicates deposition in an offshore zone, where only some of the strongest storms would occasionally spread sparse sand (Howard and Reineck 1981; Reading and Collinson 1996; Hampson 2000). Non-bioturbated black mudshales may indicate either a prolonged episode of sand-starved anoxic seafloor conditions or a high-rate deposition of ubiquitous mud rich in organic carbon. The widespread occurrence of these muddy deposits directly above the gravel-lain erosional surface indicates an abrupt ultimate drowning of the retreating fluvio-deltaic system of the Helvetiafjellet Formation (Fig. 2C). Therefore, the discontinuous basal conglomerate sheet has been interpreted in the regional stratigraphy to be a transgressive lag, with the sand and gravel fraction derived by erosional reworking of the fluvio-deltaic substrate (Nemec et al. 1988; Gjelberg and Steel 1995).

The basal muddy unit (Fig. 12), recording the global episode OAE1a (Midtkandal et al. 2016, Fig. 3), was deposited in environmental continuity with the increasingly anoxic Svalbard lagoonal embayment of the topmost Helvetiafjellet Formation (Fig. 2C, D). The retreating broad Barremian delta of the Helvetiafjellet Formation (Gjelberg and Steel 1995) accumulated abundant organic-rich black mud (TOC 2−5%) in its interdistributary bays and back-barrier lagoon (Fig. 2C; Nemec et al. 1988; Nemec 1992). The abrupt marine invasion probably resuspended the latest of these deposits and spread anoxia unhospitable to benthic fauna in the resulting Svalbard embayment (Fig. 2D), while increasing its bulk water energy, sparse sand delivery and aeration. The mud deposition at this stage may have involved resedimentation of bottom fluid mud, flowing in accordance to the local seafloor gradients (Allison et al. 2000; Traykovski et al. 2000; Sheremet et al. 2005; Ichaso and Dalrymple 2009). Large volumes of mobile seafloor mud might thus be gravitationally redeposited within the Svalbard embayment

avoiding bioturbation (Mehta 1991; Trowbridge and Kineke 1994). The volumetric concentration of clay aggregates in fluid mud may reach 95% (Wells 1989), which allows the flow to carry silt particles and possibly tiny clumps of fine sand grains in its rigid-plug zone (Baas et al. 2009). Thin rhythmic sets of graded silty to clayey mud layers (Fig. 6F) may be due to a pulsating downward flux of sediment settling from storm-generated suspension plumes, caused by the depletion of their unstable density gradient by deposition-driven convection (Kerr 1991; Nemec 1995).

Discussion

Shelf sedimentation conditions

The present study concurs with the regional reconstructions postulating Barremian major palaeogeographic changes in Svalbard (Figs. 1D, 2), with the Aptian–Albian sourcing shoreline in the midst of Svalbard and trending approximately NW–SE (Birkenmajer 1966; Århus 1991; Dypvik et al. 2002; Blakey 2011). The opposite shoreline of the Svalbard Aptian–Albian seaway was in NE Greenland (Fig. 2D), but its relative regional position had been changed by the Palaeogene opening of the North Atlantic and Arctic Ocean.

The present study is limited to the Dalkjegla Member of the Carolinefjellet Formation (Fig. 1D), but a similar range of lithofacies characterizes its higher stratigraphic members (Grundvåg et al. 2017, 2019, 2021). The sand-rich lithofacies association FA1 of the Dalkjegla Member is considered as deposited within the maximum reaches of a fairweather wave base, but the majority of the isolated or amalgamated sandstone beds in FA1 and all the sandstone sheets in lithofacies associations FA2 to FA4 are tempestites—as originally postulated by Nøttvedt and Kreisa (1987). The large-scale lateral discontinuity of tempestites apparently reflects the inherently patchy style of sand distribution by storms on an inner shelf (cf. Bentley et al. 2002; Keen et al. 2004). The mounded geometry of thick tempestite beds, mainly composite (Fig. 4B−D), is thought to reflect large hummocks and their common stacking into some kind of storm bars by vertical and/or lateral accretion, the latter directed variably seawards or landwards (Fig. 4E, F; Jelby et al. 2020; Grundvåg et al. 2021).

The abundance and considerable thicknesses of both solitary and amalgamated sandstone tempestites in the study area, several tens of kilometres away from the inferred northeastern palaeoshoreline, imply high-frequency severe storms with a magnitude commonly exceeding that of the world's largest modern storms. For comparison, the largest modern hurricane storms in the Gulf of Mexico deposited relatively thin and very fine-grained sand layers on the shelf, only locally reaching a thickness of 10−20 cm (Snedden et al. 1988; Bentley et al. 2002; Keen et al. 2004, 2006; Allison et al. 2005). The single sandstone tempestites in the present case are up 100 cm thick and their amalgamated stacks are up to 350 cm (cf. Grundvåg et al. 2021). Sandstone tempestites of similar thickness have also been reported from other stormy Cretaceous shelves (Burgeois 1980; Duke 1985; Århus 1991; Arnott 1993b; Midtgaard 1996), which seems to support the notion that a major global climatic change triggers extreme weather phenomena (Easterling et al. 2000; Meehl et al. 2000; Rosenzweig et al. 2001; Francis and Vavrus 2012). This notion has important stratigraphic palaeoenvironmental implications in the context of the Earth history of cyclic changes between icehouse and greenhouse climatic conditions (Scotese et al. 2021). It also serves as a predictive warning for the impending modern climate change, as shown by the recent increase in the frequency and magnitude of Atlantic hurricanes and Pacific typhoons (Johnson et al. 2018, 2020).

As pointed out by Leckie and Krystinik (1989), the vast majority of reported ancient shelves show storm-generated compensation currents flowing orthogonally away from the shoreline, rather than being strongly deviated subparallel to the shore by the Coriolis effect and turned into classic theoretical geostrophic currents (Walker 1984b). The Early Cretaceous shelf of Svalbard and NE Greenland (Midtgaard 1996), with the storm-driven currents directed at ~ 70° away from the inferred shoreline, would be among the relatively few ancient cases where typical geostrophic currents have been recognized (cf. Duke 1985). Could the Svalbard shelf be somehow unique? Its high latitude and palaeogeographic setting must be taken into account. First, the horizontal deflection of storm compensation currents by the Coriolis effect is greatest near the pole and smallest at the equator. Second, this subarctic shelf was within a relatively narrow seaway, where the axial tidal currents—enhanced by confinement—could impose their action on the storm compensation flows.

It is by no means certain that the iron ooids found in the Dalkjegla Member are of lagoonal origin, as suggested by Mutrux et al. (2008), even though a dysoxic brackish lagoon formed in Spitsbergen during the Barremian marine transgression (Fig. 2C; Nemec 1992; cf. Boyd 2010). The Svalbard area in the Early Cretaceous was under the influence of the HALIP volcanic activity (Maher et al. 2004). Iron ooids could have formed by exhalative hydrothermal fluids rising to the seafloor (Heikoop et al. 1996) or by the alteration of volcanic ash (Sturesson et al. 1999, 2000), with possible mineralogical changes by diagenetic reactions. The iron ooids might thus not derive from the non-evidenced, hypothetical multiple coastal lagoons postulated by Mutrux et al. (2008), and could form in the early Aptian nearshore

or even offshore-transition zone affected by frequent storm wave action (Collin et al. 2005).

The stratigraphic organization of the Carolinefjellet Formation into five members (Fig. 1D) may reflect 3rd-order eurybatic sea level changes (sensu Haq 2014). The Carolinefjellet Formation has an estimated time span of about 20 Ma. Although its mud-rich Innkjegla and Zillerberget members are somewhat thicker than the sand-richer Dalkjegla, Langstakken and Schønrockfjellet members (Fig. 1D), these latter members abound in the internal surfaces of erosion and seaward sediment bypass. The five members might thus have had a roughly comparable time span of about 4 Ma.

The stratigraphic alternation of lithofacies associations FA1–FA4 within the Dalkjegla Member (Figs. 3, 4A, 12) may then be due to eurybatic 4th-order sea level changes, with a mean time span of ~ 0.45 Ma (cf. Plint 1991; Hampson and Storms 2003; Haq 2014), driven astronomically and affecting the shelf wave climate. Seismic and interpretive correlation sections (Grundvåg et al. 2017, 2021) show large-scale morphodynamic adjustments of the inner shelf profile with a repetitive low-angle (< 1°) clinoformal stacking of deposits, which may reflect eurybatic 4th-order sea level changes, expectedly accompanied by changes in the sediment supply and wave climate (Clifton 1981; Hampson 2000; Hampson and Storms 2003). The vertical changes of lithofacies associations (Figs. 4A, 12) may thus reflect a steepening of the shoreface–shelf profile during its early progradation and a maintenance of uniformly gentle profile during the later progradation (Swift et al. 1987; Hampson and Storms 2003). The seasonal peaks of stormy wave climate would keep the progradation in check.

The late Aptian–Albian net eustatic sea-level rise did not exceed 50 m (Fig. 1D; Haq 2014), and hence the succession of open-marine shelf deposits with a preserved compacted thickness of at least 1200 m implies considerable syndepositional tectonic subsidence. Pulses of subsidence may have reduced the record of eustatic sea level falls to an apparent normal regression (cf. Jervey 1988; Messina et al. 2007), with a gradual upward change from FA2 to FA1. A sharp erosional base of FA1 indicates cases of a forced regression non-compensated by subsidence and representing a bypass hiatus. Transgressive systems tracts FA1 → FA2 → FA3(→ FA4) imply depositional and highly aggradational transgressions, which can be attributed to the active tectonic subsidence with a high rate of sediment supply by coastal erosion and alongshore drift. The vertical changes of lithofacies associations may thus have important implications for the palaeoshoreline trajectory, reflecting an interplay of eustatic sea-level changes, tectonic subsidence and sediment supply (Hampson 2000; Hampson and Storms 2003; Haq 2014; Grundvåg et al. 2021).

Shelf ichnofauna ecology

Except for two minor stratigraphic intervals, the studied shelf succession shows a trace fossil assemblage of the *Cruziana* ichnofacies in its proximal to distal expression. However, it should be noted that the succession spans a relatively narrow bathymetric range and a limited range of shelf subenvironments from lower shoreface to offshore zone. The two exceptions are the non-bioturbated black mudshales in the basal part of the succession and the occurrence of a distal expression of the *Skolithos* ichnofacies in a thin package of amalgamated sandstone beds in the lower mid-part of the succession (Fig. 12). The black shales formed in anoxic conditions linked to the OAE1a flooding (Midtkandal et al. 2016), whereas the nature of the sandstone package with *Skolithos* ichnofacies is less clear. Considering its small thickness and isolated occurrence at the turnabout level of the succession regressive to transgressive trend (Fig. 12), this unit may represent a brief encroachment of middle shoreface conditions at the regression culmination.

The intensity of bioturbation varies in the succession profiles, but similar lithofacies associations show a comparable intensity throughout the stratigraphic succession (Figs. 3, 12), which implies an ichnofauna ecology controlled by the seafloor hydraulic regime and oxygenation, and hence mainly by the wave climate and eurybatic sea-level changes. The forcing mechanism could thus be climate combined with eustasy (Fig. 1D) and regional tectonism. The intensity of bioturbation was decreasing during periods of both elevated and lowered sea level. A rise of sea level would reduce the impact of storms on the seafloor, resulting in poorer sand supply and benthic water aeration, while allowing polar water incursions. A fall of sea level would increase the impact of storms and benthic aeration, while creating unstable, mobile sandy substrate. The optimal seafloor conditions for a markedly increased benthic fertility are recorded by the most borrowed stratigraphic interval 40–55 m above the formation base, dominated by FA3 deposits (Figs. 3, 12). This interval represents specific seafloor conditions attributed to a marine transgression in harsh subpolar wave climate, with increased bottom oxygenation and decreased frequency of sand incursions from the receding shoreline.

Some lateral variation in the bioturbation intensity was due to the seafloor uneven depositional morphology (cf. Bentley et al. 2002; Hampson and Storms 2003; Keen et al. 2004; Grundvåg et al. 2021). Storm-accreted elevated areas had a better-aerated and steadily sandy substrate, while the least aerated local depressions with an unsteady heterogeneous substrate were less hospitable to benthic fauna. The lack of bioturbation in the muddy FA4 (Figs. 3, 12) reflects probably a sparsity of seaward nutrient supply, which contrasts with the generally fertile prodelta

environments (Díaz et al. 1996; Ayranci et al. 2014) and supports the notion of a storm-dominated, non-deltaic inner shelf (cf. Hamblin and Walker 1979; Hampson 2000; Hampson and Storms 2003; Grundvåg et al. 2021). Small deltas undoubtedly existed, but their role was probably limited to the feeding of a wave-dominated shoreline subject to alongshore sediment drift.

The stratigraphic succession shows a trace-fossil assemblage of the *Cruziana* ichnofacies in its distal to proximal expression. The documented variation in its species composition and bioturbation intensity is limited to a relatively narrow bathymetric range and a narrow environmental systems tract spanning lower shoreface to offshore zone. The only recognizable exceptions are the non-bioturbated black shales of FA4 in the basal part of the succession and the thin correlative sandy package with a distal expression of the *Skolithos* ichnofacies ~ 20 m above the succession base (Figs. 3, 12). The shale unit is attributed to deposition in a dysoxic lagoon transformed into anoxic embayment by the early Aptian OAE1a (Fig. 2C, D; Midtkandal et al. 2016), and the sandstone unit to a brief encroachment of the sandy mid-shoreface zone at the culmination of the shelf regressive trend (Fig. 12).

Noteworthy in the *Cruziana* ichnofacies here is the lack of arthropod trackways, its denominative component, which may suggest an absence of epibenthic arthropods in the sedimentary environment or be simply an artefact of observations made mainly on drilling cores, where the recognition of epichnial traces and horizontal burrows is difficult. More certain is the lack of such ichnotaxa as *Ophiomorpha*, *Chondrites* and *Zoophycos*, which may indicate seafloor ecological conditions unhospitable to certain benthic animals. Despite the global greenhouse climate, the Svalbard shelf area was subject to the invasions of cold polar water (Wilkinson and Riding 2007; Herle et al. 2015; Vickers et al. 2019). As noted by Cadée (2001), the present-day Arctic and temperate coasts lack Callianassids and crabs, which are producers of *Ophiomorpha*, *Thalassinoides* and *Spongeliomorpha* traces. According to Dworschak (2000), the Thalassinideans today are unknown from nearshore deposits at latitudes higher than 70 ºN and 50 ºS. These observations had led Goldring et al. (2007) to a tentative suggestion that the occurrence of pellet-lined burrows, such as *Ophiomorpha*, in the shoreface, lower foreshore and estuarine sandy deposits is restricted to warm, tropical or subtropical environments. The lack of *Ophiomorpha*, *Chondrites* and *Zoophycos* in the present case may thus be due to the specific conditions of a highly unsteady and episodically polar-influenced seafloor. Notably, abundant *Ophiomorpha* are known from the more stable Santonian–Campanian environment of western Greenland (Pedersen and Bromley 2006) and the Palaeocene environment of Spitsbergen (Svinth 2013). Likewise, both *Chondrites* and *Zoophycos* are known from the late Palaeozoic shallow glaciomarine deposits (Netto et al. 2012).

The black to dark grey shales with a high TOC content imply a low-oxygen sediment pore waters, which should generally be suitable for at least the occurrence of *Chondrites*. The lack of *Chondrites*, *Ophiomorpha* and *Zoophycos* in the present regional case was thus probably due to the benthic anoxia combined with unstable and insufficient water salinity in the Spitsbergen lagoon transformed into embayment (Fig. 2C, D) surrounded by land-draining river outlets.

Apart from the basal unit of FA4 (Fig. 12), the distribution and intensity of bioturbation in the sedimentary succession was apparently controlled mainly by the time span of colonisation windows and the magnitude of sand-emplacing storm events. The colonisation windows were expectedly a function of the storm frequency and sea level, whereas the thickness of tempestites depended on the storm magnitude. Powerful storms eroded the substrate and covered it with a sediment layer too thick to be burrowed in continuity with the underlying pre-storm deposit. The deposition of the basal black shales in Spitsbergen area (Fig. 2C, D) could similarly be affected by rapid *en masse* emplacement of fluid-mud layers.

The ichnofauna assemblages in the studied succession are generally consistent with their hosting lithofacies association and hence vary with the sedimentary environment conditions. The environmental changes in the study area commenced with a transgressive invasion of anoxic offshore environment and were followed by fluctuations between offshore transition and lower shoreface subenvironments, with a brief encroachment of sandy mid-shoreface conditions at the turnaround of the shelf general regressive to transgressive trend (Fig. 12). The short-term environmental fluctuations and related ecological changes on the Svalbard shelf were probably a result of the interplay of 4th-order eustatic cycles (Haq 2014) and the active rifting at the Barents Shelf margins (Ziegler 1988; Maher 2001; Torsvik et al. 2002; Worsley 2008).

Conclusions

The lithofacies associations and ichnofauna assemblages in the studied part of the Carolinefjellet Formation, Spitsbergen, record important *in loco* changes of environment conditions at the western margin of the Barents Shelf, controlled by both the Cretaceous global greenhouse climate and the shelf local opening to a harsh wave climate of the Arctic Ocean. The Aptian shelf subenvironments ranged from lower shoreface to offshore zone, with a brief encroachment of mid-shoreface conditions at the culmination of regressive aggradational stratigraphic trend.

Sedimentological data indicate high-frequency storms, often exceeding the magnitude of largest modern hurricane events. While the individual lithofacies reflect short-term (annual?) weather changes in the shelf environment conditions, their varying associations record morphodynamic changes in the shelf topography driven by 4th-order eurybatic sea-level fluctuations. The formation's five lithostratigraphic members, alternatingly sand- and mud-dominated, probably represent 3rd-order eurybatic sea-level changes.

The deposits are rich in ichnofauna, but the bioturbation degree varies between none (BI = 0) and total (BI = 6). Free of burrows are the basal transgressive conglomerate layer and the overlying package of black mudshales, the majority of thick sandstone beds, and some units of recurring heterolithic deposits. Pervasive total bioturbation prevails in the mudshales and heterolithic deposits located at 40–55 m above the formation base, which apparently recorded the shelf optimal fertility conditions for benthic fauna: a modest sedimentation rate with high nutrient supply and water circulation allowing for a stable and moderately dysoxic benthic environment.

Thirty-eight ichnotaxa have been recognized, mainly on core surface, with fourteen of them uncertain. The trace fossils include vertical, inclined and horizontal burrows, mostly fondichnia and domichnia, produced by mobile benthic organisms. The Aptian succession as a whole shows trace fossils assemblages of the *Cruziana* ichnofacies in its proximal to distal expression, with ichnotaxa impoverishment indicating bathymetry generally shallower than that of the archetypal *Cruziana* ichnofacies. Exceptions are a solitary sandstone package with the *Skolithos* ichnofacies in its distal expression and the basal non-bioturbated unit of black mudshales. The basal mudshales represent an end-Barremian dysoxic estuarine Spitsbergen lagoon invaded by the anoxic waters of the global event OAE1a. The sandy deposits with the *Skolithos* ichnofacies were formed close to the maximum fairweather wave base at the mid-Aptian culmination of a eurybatic shelf regressive trend.

Acknowledgements This research was funded by the UNIS CO_2 Lab project. We thank the project leader, Alvar Braathen, for permission to publish our data. The University of Bergen funded the Open Access format of the publication. We thank the anonymous referees for their highly constructive reviews that helped to improve the manuscript.

Author contributions Conceptualization: WN, SL and MJW; methodology: SL, MJW and WN; investigation: SL, MJW and WN; visualization: MJW and SL; writing—original draft: SL, MJW and WN; writing—review and editing: WN, MJW and SL.

Funding Open access funding provided by University of Bergen (incl Haukeland University Hospital). This research was financed by UNIS, Norway, and conducted at the margin of the Longyearbyen CO2 Lab project sponsored by several companies and institutions (for details, see acknowlegements in Braathen et al. 2012).

Availability of data and materials The data that support the findings of this study are available from the corresponding author upon reasonable request.

Declarations

Conflict of interest The authors have no relevant financial or non-financial competing interests to declare.

References

Allen JRL (1982) Sedimentary structures: their character and physical basis. developments in sedimentology 30, 663 pp. Elsevier, Amsterdam

Allison MA, Kineke GC, Gordon ES, Goñi MA (2000) Development and reworking of an annual flood deposit on the inner continental shelf off the Atchafalaya River. Cont Shelf Res 20:2267–2294

Allison MA, Sheremet A, Goñi M, Stone GW (2005) Storm layer deposition on the Mississippi-Atchafalaya subaqueous delta generated by Hurricane Lili in 2002. Cont Shelf Res 25:2213–2232

Alpert SP (1974) Systematic review of the genus *Skolithos*. J Paleontol 48:661–669

Angulo S, Buatois LA (2012) Integrating depositional models, ichnology, and sequence stratigraphy in reservoir characterization: the middle member of the Devonian-Carboniferous Bakken formation of subsurface southeastern Saskatchewan revisited. AAPG Bull 96:1017–1043

Århus N (1991) Dinoflaggelate cyst stratigraphy of some Aptian to Albian sections from North Greenland, southeastern Spitsbergen and the Barents Sea. Cret Res 12:209–225

Arnott RWC (1993a) Sedimentological and sequence stratigraphic model of the Falher 'D' Pool, Lower Cretaceous, northwestern Alberta. Bull Can Petrol Geol 41:453–463

Arnott RWC (1993b) Quasi-planar laminated sandstone beds of the Lower Cretaceous Bootlegger Member, north-central Montana: evidence of combined-flow sedimentation. J Sed Petrol 63:488–494

Arnott RWC, Southard JB (1990) Exploratory flow-duct experiments on combined-flow bed configurations, and some implications for interpreting storm-event stratification. J Sed Petrol 60:211–219

Ayranci K, Dashtgard SE, MacEachern JA (2014) A quantitative assessment of the neoichnology and biology of a delta front and prodelta, and implications for delta ichnology. Palaeogeogr Palaeoclimatol Palaeoecol 409:114–134

Baas JH, Best JL, Peakall J, Wang M (2009) A phase diagram for turbulent, transitional, and laminar clay suspension flows. J Sed Res 7:162–183

Bann KL, Fielding CR (2004) An integrated ichnological and sedimentological comparison of non-deltaic shoreface and subaqueous delta deposits in Permian reservoir units of Australia. In: McIlroy D (ed) The application of ichnology to palaeoenvironmental and stratigraphic analysis. Geol Soc London Spec Publ 228:273–310

Bann KL, Fielding CR, MacEachern JA, Tye SC (2004) Differentiation of estuarine and offshore marine deposits using integrated ichnology and sedimentology: Permian Pebbley Beach Formation, Sydney Basin, Australia. In: McIlroy (ed) The application of ichnology to palaeoenvironmental and stratigraphic analysis. Geol Soc London Spec Publ 228:179–211

Bann KL, Tye SC, MacEachern JA, Fielding CR, Jones BG (2008) Ichnological and sedimentologic signatures of mixed wave- and storm-dominated deltaic deposits: examples from the early Permian Sydney Basin, Australia. In: Hampson GJ, Steel RJ, Burgess PM, Dalrymple RW (eds) Recent advances in models of Siliciclastic Shallow Marine Stratigraphy. SEPM Spec Publ 90:293–332

Bednarz M, McIlroy D (2009) Three-dimensional reconstruction of 'phyconiform' burrows: implications for identification of trace fossils in core. Palaeont Electr 12:1–15

Bednarz M, McIlroy D (2012) Effect of phycosiphoniform burrows on shale hydrocarbon reservoir quality. AAPG Bull 96:1957–1980

Belaústegui Z, de Gibert JM (2013) Bow-shaped, concentrically laminated polychaete burrows: a *Cylindrichnus concentricus* ichnofabric from the Miocene of Tarragona, NE Spain. Palaeogeogr Palaeoclimatol Palaeoecol 381–382:119–127

Bentley SJ, Keen TR, Blain CA, Vaughan WC (2002) The origin and preservation of a major hurricane event bed in the northern Gulf of Mexico: Hurricane Camille, 1969. Mar Geol 186:423–446

Bertling M, Braddy SJ, Bromley RG, Demathieu GR, Genise J, Mikulaš R, Nielsen JK, Nielsen KSS, Rindsberg AK, Schlirf M, Uchman A (2006) Names for trace fossils: a uniform approach. Lethaia 39:265–286

Bertling M, Buatois LA, Knaust D, Laing B, Mángano MG, Meyer N, Mikuláš R, Minter NJ, Neumann C, Rindsberg AK, Uchman A, Wisshak M (2022) Names for trace fossils 2.0: theory and practice in ichnotaxonomy. Lethaia 55:1–19

Bhattacharya JP, Walker RG (1992) Deltas. In: Walker RG, James NP (eds) Facies models: response to sea-level change. Geological Association of Canada, St John's, pp 157–177

Birkenmajer K (1966) Lower Cretaceous tidal deposits of central Vestspitsbergen. Norsk Polarinst Årbok 1964:73–85

Blakey R (2011) Library of Paleogeography. Website http://cpgeosystems.com/paleomaps.html [accessed 15 May 2016]

Bourgeois J (1980) A transgressive shelf sequence exhibiting hummocky stratification: the Cape 961 Sebastian Sandstone (Upper Cretaceous), southwestern Oregon. J Sed Petrol 50:681–702

Boyd R (2010) Transgressive wave-dominated coasts. In: James NP, Dalrymple RW (eds) Facies models 4. Geological Association of Canada, St. John's, pp 265–294

Boyd R, Darlymple R, Zaitlin BA (1992) Classification of clastic coastal depositional environments. Sed Geol 80:139–150

Braathen A, Bælum K, Christiansen HH, Dahl T, Eiken O, Elvebakk H, Hansen F, Hanssen TH, Jochman M, Johansen TA, Johnsen H, Larsen L, Lie T, Mertes J, Mørk A, Mørk MB, Nemec W, Olaussen S, Oye V, Rød K, Titlestad GO, Tveranger J, Vagle K (2012) The Longyearbyen CO_2 Lab of Svalbard, Norway—initial assessment of the geological conditions for CO_2 sequestration. Norw J Geol 92:353–376

Brekke H, Sjulstad HI, Magnus C, Williams RW (2001) Sedimentary environments offshore Norway—an overview. In: Martinsen OJ, Dreyer T (eds) Sedimentary Environments Offshore Norway—Palaeozoic to Recent Norw Petrol Soc Spec Publ 10:571–593. Elsevier, Amsterdam

Brenchley PJ (1985) Storm influenced sandstone beds. Modern Geol 9:369–396

Bromley RG (1990) Trace fossils: biology and taphonomy. Unwin Hyman, London, p 280

Bromley RG, Asgaard U (1972) Notes on Greenland trace fossils. Grønl Geol Unders 49:23–30

Bromley RG, Uchman A (2003) Trace fossils from the lower and middle Jurassic marginal marine deposits of the Sorthat Formation, Bornholm. Denmark Bull Geol Soc Denmark 52:185–208

Buatois LA, Angriman AOL (1991) Ichnologia de la Formacion Whisky Bay (Cretacico, Isla James Ross, Antarctida): implicancias paleoecologicas y paleoambientales. Ameghiniana 28:75–88

Buatois LA, Mángano MG (2011) Ichnology: organism-substrate interactions in space and time. Cambridge University Press, Cambridge, p 358

Buatois LA, Gingras MK, MacEachern J, Mángano MG, Zonneveld J-P, Pemberton SG, Netto RG, Martin A (2005) Colonization of brackish-water systems through time: evidence from the trace-fossil record. Palaios 20:321–347

Buatois LA, Santiago N, Parra K, Steel L (2008) Animal-substrate interactions in an Early Miocene wave-dominated tropical delta: Delineating environmental stresses and depositional dynamics (Tácata field, eastern Venezuela). J Sed Res 78:458–479

Cabrera MIL, Olivero EB, Carmona NB, Ponce JJ (2008) Cenozoic trace fossils of the *Cruziana*, *Zoophycos* and *Nereites* ichnofacies from the Fuegian Andes, Argentina. Ameghiniana 45:377–392

Cattaneo A, Steel RJ (2003) Transgressive deposits: a review of their variability. Earth-Sci Rev 62:187–228

Cheel RJ, Leckie DA (1992) Coarse-grained storm beds of the Upper Cretaceous Chungo Member (Wapiabi Formation), southern Alberta. Canada J Sed Res 62:933–945

Clifton HE (1976) Wave-formed sedimentary structures—a conceptual model. In: Davis RA Jr, Ethington RL (eds) Beach and Nearshore Sedimentation. SEPM Spec Publ 24:126–148

Clifton HE (1981) Progradational sequences in Miocene shoreline deposits, southeastern Caliente Range, California. J Sed Petrol 51:165–184

Clifton HE, Dingler JR (1984) Wave-formed structures and paleoenvironmental reconstruction. Mar Geol 60:165–198

Clifton HE, Hunter RE, Phillips RL (1971) Depositional structures and processes in the non-barred high-energy nearshore. J Sed Petrol 44:651–670

Coates L, MacEachern JA (2007) The ichnological signatures of river- and wave-dominated delta complexes: differentiating deltaic and non-deltaic shallow marine successions, Lower Cretaceous Viking Formation and Upper Cretaceous Dunvegan Formation, West-Central Alberta. In**:** MacEachern JA, Bann KL, Gingras MK, Pemberton SG (eds) Applied Ichnology. SEPM Short Course Lecture Notes 52:227–254

Collin PY, Loreau JP, Courville P (2005) Depositional environments and iron ooid formation in condensed sections (Callovian–Oxfordian, south-eastern Paris Basin, France). Sedimentology 52:969–985

Collinson JD, Mountney NP, Thompson DB (2006) Sedimentary Structures, 3rd edn. Terra Publishing, Harpenden, p 292

Dallmann W (1999) Lithostratigraphic Lexicon of Svalbard. Norwegian Polar Institutt, Tromsø, pp 318

Dashtgard SE, MacEachern A, Frey SE, Gingras MK et al (2012) Tidal effects on the shoreface: towards a conceptual framework. Sed Geol 279:42–61

Davies DK, Ethridge FG, Berg RR (1971) Recognition of barrier environments. AAPG Bull 55:550–565

Davison JEA, MacEachern JA (2007) Ichnological variations in brackish-water central basin complexes of wave-dominated estuarine incised-valley fills, Lower Cretaceous Viking Formation, Central Alberta. In: MacEachern JA, Bann KL, Gingras MK, Pemberton SG (eds) Applied Ichnology. SEPM Short Course Lecture Notes 52:273–289

de Gibert JM, Benner JS (2002) The trace fossil *Gyrochorte*: ethology and paleoecology. Rev Esp Paleontol 17:1–12

De Lurio J, Frakes LA (1999) Glendonites as a paleoenvironmental tool: implications for early Cretaceous high latitude climates in Australia. Geochim Cosmochim Acta 63:1039–1048

De Raaf JFM, Boersma JR, Van Gelder A (1977) Wave-generated structures and sequences from a shallow marine succession, Lower Carboniferous, County Cork, Ireland. Sedimentology 24:451–483

Doré AG (1991) The structural foundation and evolution of Mesozoic seaways between Europe and the Arctic. Palaeogeogr Palaeoclim Palaeoecol 87:441–492

Dott RJ, Bourgeois J (1982) Hummocky stratification: Significance of its variable bedding sequences. Geol Soc Am Bull 93:663–680

Duke WL (1985) Hummocky cross-stratification, tropical hurricanes, and intense winter storms. Sedimentology 32:167–194

Dumas S, Arnott RWC (2006) Origin of hummocky and swaley cross-stratification—The controlling influence of unidirectional current strength and aggradation rate. Geology 34:1073–1076

Dumas S, Arnott RWC, Southard JB (2005) Experiments on oscillatory-flow and combined-flow bed forms: implications for interpreting parts of the shallow-marine sedimentary record. J Sed Res 75:501–513

Dworschak PC (2000) Global diversity in Thalassinidea (Decapoda). J Crust Biol 20:238–245

Dypvik H, Håkansson E, Heinberg C (2002) Jurassic and Cretaceous palaeogeography and stratigraphic comparisons in the North Greenland-Svalbard region. Polar Res 21:91–108

Easterling DR, Meehl GA, Parmesan C, Changnon SA, Karl TR, Mearns LO (2000) Climate extremes: observations, modelling, and impacts. Science 289:2068–2074

Edwards MB, Edwards R, Colbert EH (1978) Carnosaurian footprints in the Lower Cretaceous of Eastern Spitsbergen. J Paleontol 52:940–941

Embry AF (1991) Mesozoic history of the Arctic islands. In: Trettin HP (ed) Geology of the Innuitian Orogen and Arctic Platform of Canada and Greenland. Geol Can 3:371–433

Fielding CR, Bann KL, Trueman JD (2007) Resolving the architecture of a complex, low accommodation unit using high-resolution sequence stratigraphy and ichnology: the Late Permian Freitag Formation in the Dension trough, Queensland, Australia. In: MacEachern JA, Bann KL, Gingras MK, Pemberton SG (eds) Applied Ichnology. SEPM Short Course Lecture Notes 52:179–208

Fillion D, Pickerill RK (1990) Ichnology of the Upper Cambrian? to Lower Ordovician Bell Island and Wabana groups of eastern Newfoundland. Canada Paleontograph Can 7:1–119

Fischer AG (1981) Climatic oscillations in the biosphere. In: Nitecki MH (ed) Biotic crises in ecological and evolutionary time. Academic Press, New York, pp 103–131

Folk RL (1980) Petrology of sedimentary rocks, 2nd edn. Austin, Hemphill, p 195

Francis JA, Vavrus SJ (2012) Evidence linking Arctic amplification to extreme weather in mid-latitudes. Geophys Res Lett. https://doi.org/10.1029/2012GL051000

Frebold H (1930) Verbreitung und Ausbildung des Mesozoikums in Spitzbergen (Nebst einer Revision der Stratigraphie des Jura und der Unterkreide in Nowaja Semlja und cinem Entwurf der mesozoischen Fntwiklungseschichte des Barentsseeschelfes). Skr Svalb Ishhav 31, 126 pp

Frebold H (1931) Fazielle Verhältnisse des Mesozoikums im Eisfjordgebiet Spitzbergens (Ein Beitrag zur Entwicklungsgeschichte des Skandiks). Skr. Svalb. Ishhav. 37, 94 pp

Frey RW (1990) Trace fossils and hummocky cross-stratification, Upper Cretaceous of Utah. Palaios 5:203–218

Frey RW, Howard JD (1981) *Conichnus* and *Schaubcylindrichnus*: redefined trace fossils from the Upper Cretaceous of the Western Interior. J Paleontol 56:800–804

Frey RW, Howard JD (1990) Trace fossils and depositional sequences in a clastic shelf setting, Upper Cretaceous of Utah. J Paleontol 64:803–820

Frey RW, Pemberton SG (1985) Biogenic structures in outcrops and cores, I. Approaches to ichnology. Bull Can Petrol Geol 33:72–115

Frey RW, Curran AH, Pemberton GS (1984) Tracemaking activities of crabs and their environmental significance: the ichnogenus *Psilonichnus*. J Paleontol 58:511–528

Frey RW, Pemberton SG, Saunders TDA (1990) Ichnofacies and bathymetry: a passive relationship. J Paleontol 64:155–158

Fu S (1991) Funktion, Verhalten und Einteilung fucoider und lophoctenoider Lebensspuren. Cour Forsch Inst Senckenb 135:1–79

Gani MR, Bhattacharya JP, MacEachern JA (2007) Using ichnology to determine the relative influence of waves, storms, tides, and rivers in deltaic deposits: examples from Cretaceous western interior seaway, USA. In: MacEachern JA, Bann KL, Gingras MK, Pemberton SG (eds) Applied Ichnology. SEPM Short Course Lecture Notes 52:209–225

Ganino C, Arndt NT (2009) Climate changes caused by degassing of sediments during the emplacement of large igneous provinces. Geology 37:323–326

Gingras MK, Pemberton SG, Saunders T, Clifton HE (1999) The ichnology of modern and Pleistocene brackishwater deposits at Willapa Bay, Washington: variability in estuarine settings. Palaios 14:352–374

Gingras MK, Dashtgard SE, MacEachern JA, Pemberton SG (2008) Biology of shallow marine ichnology: a modern perspective. Aq Biol 2:255–268

Gjelberg J, Steel RJ (1995) Helvetiafjellet Formation (Barremian–Aptian), Sptsbergen: characteristics of a transgressive succession. In: Steel RJ, Felt VL, Johannessen EP, Mathieu C (eds) Sequence Stratigraphy on the Northwest European Margin. Norw Petrol Soc Spec Publ 5:571–593. Elsevier, Amsterdam

Goldring R, Cadée GC, D'Alessandro A, Gibert JM de, Jenkins R, Pollard JE (2004) Climatic control on trace fossil distribution in the marine realm. In: McIlroy D (ed) The Application of Ichnology to Palaeoenvironmental and Stratigraphic Analysis. Geol Soc London Spec Publ 228:77–92

Goldring R, Cadée GC, Pollard JE (2007) Climatic control of marine trace fossil distribution. In: Miller W (ed) Trace fossils: concepts, problems, prospects. Elsevier, Amsterdam, pp 159–171

Gouramanis C, Webb JA, Warren AA (2003) Fluviodeltaic sedimentology and ichnology of part of the Grampians Group, Western Victoria. Aust J Earth Sci 50:811–825

Grundvåg S-A, Olaussen S (2017) Sedimentology of the Lower Cretaceous at Kikutodden and Keilhaufjellet, southern Spitsbergen: implications for an onshore–offshore link. Polar Res 36:1302124. https://doi.org/10.1080/17518369.2017.130212

Grundvåg S-A, Marin D, Kairanov B, Śliwińska KK, Nøhr-Hansen H, Jelby ME, Escalona A, Olaussen S (2017) The Lower Cretaceous succession of the northwestern Barents Shelf: onshore and offshore correlations. Mar Petrol Geol 86:834–857

Grundvåg S-A, Jelby ME, Śliwińska KK, Nøhr-Hansen H, Aadland T, Sandvik SE, Tennvassås I, Engen T, Olaussen S (2019) Sedimentology and palynology of the Lower Cretaceous succession of central Spitsbergen: integration of subsurface and outcrop data. Norw J Geol 99:253–283

Grundvåg S-A, Jelby ME, Olaussen S, Śliwińska KK (2021) The role of shelf morphology on storm-bed variability and stratigraphic architecture, Lower Cretaceous, Svalbard. Sedimentology 68:196–237

Gruszczyński M, Rudowski S, Semil J, Słomiński J, Zrobek J (1993) Rip currents as geological tool. Sedimentology 40:217–236

Haldeman SS (1840) Supplement to number one of 'A monograph of the Limniades, or freshwater univalve shells of North America', containing descriptions of apparently new animals in different classes, and the names and characters of the subgenera in *Paludina* and *Anculosa*. Privately printed, Philadelphia, p 3

Hamblin AP, Walker RG (1979) Storm-dominated shallow marine deposits: the Fernie-Kootenay (Jurassic) transition, southern Rocky Mountains. Can J Earth Sci 16:1673–1690

Hampson GJ (2000) Discontinuity surfaces, clinoforms, and facies architecture in a wave-dominated, shoreface–shelf parasequence. J Sed Res 70:325–340

Hampson GJ, Storms JE (2003) Geomorphological and sequence stratigraphic variability in wave-dominated shoreface–shelf parasequences. Sedimentology 50:667–701

Hampson GJ, Howell JA (2005) Sedimentologic and geomorphic characterization of ancient wave-dominated shorelines: examples from the Late Cretaceous Blackhawk Formation, Book Cliffs, Utah. In: Bhattacharya JP, Giosan L (eds) River deltas–concepts, models and examples. SEPM special publication, vol 83, pp 133–154

Han Y, Pickerill RK (1995) Taxonomic revision of the ichnogenus *Helminthopsis* Heer 1877 with a statistical analysis of selected ichnospecies. Ichnos 4:83–118

Hansen CD, MacEachern JA (2007) Application of the asymmetric delta model to along-strike facies variations in a mixed wave- and river-influenced delta lobe, Upper Cretaceous Basal Belly River Formation, Central Alberta. In: MacEachern JA, Bann KL, Gingras MK, Pemberton SG (eds) Applied Ichnology. SEPM Short Course Lecture Notes 52:255–271

Haq BU (2014) Cretaceous eustasy revisited. Glob Planet Change 113:44–58

Harland WB (ed) (1997) The Geology of Svalbard. Geol. Soc. London Memoir 17, 514 pp

Harms JC, Southard JB, Spearing DR, Walker RG (1975) Depositional Environments as interpreted from Primary Sedimentary Structures and Stratification Sequences. SEPM Short Course Lecture Notes 2, 161 pp

Harms JC, Southard JB, Walker RG (1982) Structures and Sequences in Clastic Rocks. SEPM Short Course Lecture Notes 9, 250 pp

Heikoop JM, Tsujita CJ, Risk MJ, Tomascik T, Mah AJ (1996) Modern iron ooids from a shallow-marine volcanic setting: Mahengetang, Indonesia. Geology 24:759–762

Heintz N (1963) Dinosaur-footprints and polar wandering. Norsk Polarinst Årbok 1962:35–43

Herrle JO, Schroder-Adams CJ, Davis W, Pugh AT, Galloway JM, Fath J (2015) Mid-Cretaceous High Arctic stratigraphy, climate, and Oceanic Anoxic Events. Geology 43:403–406

Hjelle A (1993) The geology of Svalbard. Norsk Polarinstitutt, Oslo, p 163

Howard JD (1975) The sedimentological significance of trace fossils. In: Frey RW (ed) The study of trace fossils: a synthesis of principles, problems, and procedures in ichnology. Springer-Verlag, New York, pp 131–146

Howard JD, Frey RW (1984) Characteristic trace fossils in nearshore to offshore sequences, Upper Cretaceous of east-central Utah. Can J Earth Sci 21:200–219

Howard JD, Reineck H-E (1981) Depositional facies of a high-energy beach-to-offshore sequence: comparison with low-energy sequence. AAPG Bull 65:807–830

Huang Y, Yang G, Wang C, Wu H (2012) The stabilisation of long-term Cretaceous greenhouse climate: contribution from the semi-periodical burial of phosphorus in the ocean. Cret Res 38:7–15

Hurum J, Milan J, Hammer Ø, Midtkandal I, Amundsen H, Sæther B (2006) Tracking polar dinosaurs—new finds from the Lower Cretaceous of Svalbard. Norw J Geol 86:397–402

Ichaso AA, Dalrymple RW (2009) Tide- and wave-generated fluid mud deposits in the Tilje Formation(Jurassic), offshore Norway. Geology 37:539–542

Jelby ME, Grundvåg S-A, Helland-Hansen W, Olaussen S, Stemmerik L (2020) Tempestite facies variability and storm-depositional processes across a wide ramp: towards a polygenetic model for hummocky cross-stratification. Sedimentology 67:742–781

Jervey MT (1988) Quantitative geological modeling of siliciclastic rock sequences and their seismic expression. In: Wilgus CK, Hastings BS, Posamentier HW, Van Wagoner JC, Ross CA, Kendall CGSC (eds) Sea-Level Changes: An Integrated Approach. SEPM Spec Publ 42:47–69

Johansson L, Zahirovic S, Müller D (2018) The interplay between the eruption and weathering of large igneous provinces and the deep-time carbon cycle. Geophys Res Lett 45:5380–5389

Johnson ME, Ledesma-Vázques J, Guardado-France R (2018) Coastal geomorphology of a Holocene hurricane deposit on a Pleistocene marine terrace from Isla Carmen (Baja California Sur, Mexico). J Mar Sci Eng 6:108. https://doi.org/10.3390/jmse6040108

Johnson ME, Johnson EM, Guardado-France R, Ledesma-Vázques J (2020) Holocene Hurricane Deposits Eroded as Coastal Barriers from Andesite Sea Cliffs at Puerto Escondido (Baja California Sur, Mexico). J Mar Sci Eng 8:75. https://doi.org/10.3390/jmse8020075

Keen TR, Bentley SJ, Vaughan WC, Blain CA (2004) The generation and preservation of multiple hurricane beds in the northern Gulf of Mexico. Mar Geol 210:79–105

Keen TR, Furukawa Y, Bentley SJ, Slingerland RL, Teague WJ, Dykes JD, Rowley CD (2006) Geological and oceanographic perspectives on event bed formation during Hurricane Katrina. Geophys Res Lett. https://doi.org/10.1029/2006GL027981

Kerr RC (1991) Erosion of a stable density gradient by sedimentation-driven convection. Nature 353:423–425

Kessels K, Mutterlose J, Michalzik D (2006) Early Cretaceous (Valanginian–Hauterivian) calcareous nannofossils and isotopes of the northern hemisphere: proxies for the understanding of Cretaceous climate. Lethaia 39:157–172

Knaust D (2015) Siphonichnidae (new ichnofamily) attributed to the burrowing activity of bivalves: Ichnotaxonomy, behaviour and palaeoenvironmental implications. Earth-Sci Rev 150:497–519

Komar PD, Miller MC (1975) The initiation of oscillatory ripple marks and the development of plane-bed at high shear stresses under waves. J Sed Petrol 45:697–703

Kotake N (2003) Ethologic and ecologic interpretation of complex stellate structures in Pleistocene deep-sea sediments (Otadai Formation), Boso Peninsula, central Japan. Palaeogeogr Palaeoclim Palaeoecol 192:143–155

Kotlarczyk J, Uchman A (2012) Integrated ichnological and ichthyological analysis of oxygenation changes in the Menilite Formation during Oligocene, Skole and Subsilesian nappes, Polish Carpathians. Palaeogeogr Palaeoclim Palaeoecol 331–332:104–118

Krajewski KP, Luks B (2003) Origin of 'cannon-ball' concretions in the Carolinefjellet Formation (Lower Cretaceous, Spitsbergen). Pol Polar Res 24:217–242

Kranenburg C, Winterwerp JC (1997) Erosion of fluid mud layers. I: Entrainment model. J Hydr Eng 123:504–511

Kreisa RD (1981) Storm-generated sedimentary structures in subtidal marine facies with examples from the Middle and Upper Ordovician of southwestern Virginia. J Sed Petrol 51:823–848

Leckie D (1988) Wave-formed, coarse-grained ripples and their relationship to hummocky cross-stratification. J Sed Petrol 58:607–622

Leckie D, Krystinik LF (1989) Is there evidence of geostrophic currents preserved in the sedimentary record of inner to middle-shelf deposits? J Sed Res 59:862–870

Lettley CD, Gingras MK, Pearson NJ, Pemberton SG (2007) Burrowed stiffgrounds on estuarine point bars: modern and ancient examples, and criteria for their discrimination from firmgrounds developed along omission surfaces**.** In: MacEachern JA, Bann KL, Gingras MK, Pemberton SG (eds) Applied Ichnology. SEPM Short Course Lecture Notes 52:325–333

MacEachern JA, Bann KL (2008) The role of ichnology in refining shallow marine facies *models*. In: Hampson GJ, Steel RJ, Burgess PM, Dalrymple RW (eds) Recent Advances in Models of Siliciclastic Shallow-Marine Stratigraphy. SEPM Spec. Publ. 90:73–116

MacEachern JA, Løseth TM (2003) Sedimentology and ichnology of a transgressively back-stepped wave-dominated deltaic reservoir: Middle Jurassic Tarbert and Heather formations, North Sea, Norway. Abstract A110, AAPG Annual Convention, Salt Lake City

MacEachern JA, Pemberton SG (1992) Ichnological aspects of Cretaceous shoreface successions and shoreface variability in the Western Interior Seaway of North America. In: Pemberton SG (ed) Applications of Ichnology to Petroleum Exploration. SEPM Core Workshop 17:57–84

MacEachern JA, Pemberton SG (1994) Ichnological aspects of incised valley fill systems from the Viking Formation of the Western Canada Sedimentary Basin, Alberta, Canada. In: Boyd R, Dalrymple RW, Zaitlin B (eds), Incised-Valley Systems: Origin and Sedimentary Sequences. SEPM Spec Publ 51:129–157

MacEachern JA, Raychaudhuri I, Pemberton SG (1992) Stratigraphic applications of the *Glossifungites* ichnofacies: delineating discontinuities in the rock record. In: Pemberton SG (ed) Applications of Ichnology to Petroleum Exploration. SEPM Core Workshop 17:169–198

MacEachern JA, Stelck CR, Pemberton SG (1999a) Marine and marginal marine mudstone deposition: Paleoenvironmental interpretations based on the integration of ichnology, palynology and foraminiferal paleoecology. In: Bergman KM, Snedden JW (eds) Isolated Shallow Marine Sand Bodies: Sequence Stratigraphic and Sedimentologic Interpretation. SEPM Spec Publ 64:205–225

MacEachern JA, Zaitlin BA, Pemberton SG (1999b) A sharp-based sandstone succession of the Viking Formation, Joffre Field, Alberta, Canada: Criteria for recognition of transgressively incised shoreface complexes. J Sed Res 69:876–892

MacEachern JA, Bann KL, Bhattacharya JP, Howell CD (2005) Ichnology of deltas: organism responses to the dynamic interplay of rivers, waves, storms and tides. In: Giosan L, Bhattacharya JP (eds) River Deltas—Concepts, Models, and Examples. SEPM Spec Publ 83:45–85

MacEachern JA, Bann KL, Pemberton SG, Gingras MK (2007a) The ichnofacies paradigm: High-resolution paleoenvironmental interpretation of the rock record. In: MacEachern JA, Bann KL, Gingras MK, Pemberton SG (eds) Applied Ichnology. SEPM Short Course Lecture Notes 52:27–64

MacEachern JA, Gingras MK, Bann KL, Dafoe LT, Pemberton SG (2007b) Applications of ichnology to high-resolution genetic stratigraphic paradigms. In: MacEachern JA, Bann KL, Gingras MK, Pemberton SG (eds) Applied Ichnology. SEPM Short Course Lecture Notes 52:95–129

MacEachern JA, Pemberton SG, Bann KL, Gingras MK (2007c) Departures from the archetypal ichnofacies: Effective recognition of physico-chemical stresses in the rock record. In: MacEachern JA, Bann KL, Gingras MK, Pemberton SG (eds) Applied Ichnology. SEPM Short Course Lecture Notes 52:65–93

MacEachern JA, Pemberton SG, Gingras MK, Bann KL (2007d) The ichnofacies concept: a fifty-year retrospective. In: Miller W (ed) Trace fossils: concepts, problems, prospects. Elsevier, Amsterdam, pp 50–75

MacEachern JA, Bann KL, Gingras MK, Zonneveld J-P, Dashtgard SE, Pemberton SG (2012) The ichnofacies paradigm. In: Knaust D, Bromley RG (eds) Trace Fossils as Indicators of Sedimentary Environments. Developments in Sedimentology 64:103–138. Elsevier, Amsterdam

Maher HD Jr (2001) Manifestations of the Cretaceous High Arctic Large Igneous Province in Svalbard. J Geol 109:91–104

Maher HD Jr, Hays T, Shuster RD, Mutrux J (2004) Petrography of Lower Cretaceous sandstones on Spitsbergen. Polar Res 23:142–165

Männil RM (1966) O vertikalnykh norkakh zaryvanija v ordovikskikh izvestnjakakh Pribaltiki. In: Organizm i Sreda v Geologicheskom Proshlom, pp. 200–207. Nauka, Moskva [In Russian, with English abstract.]

Mathers S, Zalasiewicz J (1996) A gravel beach-rip channel system: the Westleton Beds (Pleistocene) of Suffolk. England Proc Geol Assoc 107:57–67

McIlroy D (ed) (2004) The Application of Ichnology to Palaeoenvironmental and Stratigraphic Analysis. Geol Soc London Spec. Publ. 228, 490 pp

Meehl GA, Zwiers F, Evans J, Knutson T, Mearns L, Whetton P (2000) Trends in extreme weather and climate events: issues related to modelling extremes in projections of future climate change. Am Meteo Soc Bull 81:427–436

Mehta AJ (1991) Understanding fluid mud in a dynamic environment. Geo-Mar Lett 11:113–118

Messina C, Rosso A, Sciuto F, Di Geronimo I, Nemec W, Di Dio T, Di Geronimo R, Maniscalco R, Sanfilippo R (2007) Anatomy of a transgressive systems tract revealed by integrated sedimentological and palaeoecological study: the Barcellona P.G. Basin, northeastern Sicily, Italy. In: Nichols G, Paola C, Williams EA (eds) Sedimentary Environments, Processes and Basins – A Tribute to Peter Friend. IAS Spec Publ 38:367−400

Midtgaard HH (1996) Inner-shelf to lower-shoreface hummocky sandstone bodies with evidence for geostrophic influenced combined flow, Lower Cretaceous, west Greenland. J Sed Res 66:343–353

Midtkandal I, Nystuen JP, Nagy J, Mørk A (2008) Lower Cretaceous lithostratigraphy across a regional subaerial unconformity in Spitsbergen: the Rurikfjellet and Helvetiafjellet formations. Norw J Geol 88:297–304

Midtkandal I, Svensen HH, Planke S, Corfu F, Polteau S, Torsvik TH, Faleide JI, Grundvåg S-A, Selnes H, Kürschner W, Olaussen S (2016) The Aptian (Early Cretaceous) oceanic anoxic event (OAE1a) in Svalbard, Barents Sea, and the absolute age of the Barremian-Aptian boundary. Palaeogeogr Palaeoclim Palaeoecol 463:126–135

Midtkandal I (2007) Depositional Dynamics of an Epicontinental Basin; Lower Cretaceous on Svalbard. Unpubl. PhD Thesis, University of Oslo, 174 pp

Miller W III (1995) '*Terebellina*' (= *Schaubcylindrichnus freyi* ichnosp. nov.) in Pleistocene outer shelf mudrocks of northern California. Ichnos 4:141–149

Miller W III, Aalto KR (2008) *Rosselia* ichnofabric in the Miocene Pullen Formation, northwestern California: implications for the interpretation of regional tectonics. Palaios 23:329–335
Moriya K (2011) Development of the Cretaceous greenhouse climate and the oceanic thermal circulation. Paleontol Res 15:77–88
Mørk A, Dallmann WK, Dypvik H, Johannessen EP, Larssen GB, Nagy J, Nøttvedt A, Olaussen S, Pčelina TM, Worsley D (1999) Mesozoic lithostratigraphy. In: Dallmann WK (ed) Lithostratigraphic Lexicon of Svalbard. Norsk Polarinstitutt, Tromsø, pp 127–214
Mosar J, Eide EA, Osmundsen PT, Sommaruga A, Torsvik TH (2002) Greenland-Norway separation: A geodynamic model for the North Atlantic. Norw J Geol 82:281–298
Müller RD, Zahirovic S, Williams SE, Cannon J, Seton M, Bower DJ, Gurnis M (2019) A global plate model including lithospheric deformation along major rifts and orogens since the Triassic. Tectonics. https://doi.org/10.1029/2018TC005462
Mutrux J, Maher H, Shuster R, Hays T (2008) Iron ooid beds of the Carolinefjellet Formation, Spitsbergen. Norway Polar Res 27:28–43
Naafs BDA, Castro JM, De Gea GA, Quijano ML, Schmidt DN, Pancost RD (2016) Gradual and sustained carbon dioxide release during Aptian oceanic anoxic event 1a. Nat Geosci 9:1–5
Nagy J (1970) Ammonite faunas and stratigraphy of Lower Cretaceous (Albian) rocks in southern Spitsbergen. Norsk Polarinst Skrift 152:1–58
Nara M (2006) Reappraisal of *Schaubcylindrichnus*: a probable dwelling/feeding structure of a solitary funnel feeder. Palaeogeogr Palaeoclim Palaeoecol 240:439–452
Nemec W (1992) Depositional controls on plant growth and peat accumulation in a braidplain delta environment: Helvetiafjellet Formation (Barremian–Aptian), Svalbard. In: McCabe PJ, Parrish JT (eds) Controls on the Distribution and Quality of Cretaceous Coals. Geol Soc Am Spec Paper 267:209–226
Nemec W (1995) The dynamics of deltaic suspension plumes. In: Oti MN, Postma G (eds) Geology of Deltas. Balkema, Rotterdam, pp 31–93
Nemec W, Steel RJ, Gjelberg J, Collinson JD, Prestholm E, Øxnevad IE (1988) Anatomy of collapsed and re-established delta front in Lower Cretaceous of eastern Spitsbergen: gravitational sliding and sedimentation processes. AAPG Bull 72:454–476
Netto RG, Buatois LA, Mángano MG (2007) *Gyrolithes* as multipurpose burrow: an ethologic approach. Rev Bras Paleontol 10:157–168
Netto RG, Benner JS, Buatois LA, Uchman A, Mángano MG, Ridge JC, Kazakauskas V, Gaigalas A (2012) Glacial environments. In: Knaust D, Bromley RG (eds) Trace Fossils as Indicators of Sedimentary Environments. Developments in Sedimentology 64:299–327. Elsevier, Amsterdam
Nøhr-Hansen H (1993) Dinoflagellate cyst stratigraphy of the Barremian to Albian, Lower Cretaceous, North-East Greenland. Bull Grønl Geol Unders 166:1–171
Nøttvedt A, Cecchi M, Gjelberg JG, Kristensen SE, Lønøy A, Rasmussen A, Rasmussen E, Skott PH, Van Veen PM (1992) Svalbard–Barents Sea correlation: a short review. In: Vorren TO, Bergsager E, Dahl-Stamnes ØA, Holter E, Johansen E, Lie E, Lund TB (eds) Arctic Geology and Petroleum Potential. Norw. Petrol Soc Spec Publ 2:363–375. Elsevier, Amsterdam
Nøttvedt A, Kriesa RD (1987) Model for the combined-flow origin of hummocky cross-stratification. Geology 15:357–361
Nysæther E (1966) Petrografisk undersøkelse av sedimentærebergarter fra tidsperioden kritt-tertiær i Nathorst Land, Vest Spitsbergen. Unpubl. Cand. Real. Thesis, University of Bergen, 167 pp
Owen HG (1988) Correlation of ammonite faunal provinces in the Lower Albian (mid-Cretaceous). In: Wiedmann J, Kullmann J (eds) Cephalopods – Present and Past. Swietzerbartsche Verlagsbuchhandlung, Stuttgart, pp 477–489
Pacześna J (2010) Ichnological record of the activity of Anthozoa in the early Cambrian succession of the Upper Silesian Block (southern Poland). Acta Geol Pol 60:93–103
Parker JR (1967) The Jurassic and Cretaceous sequence in Spitsbergen. Geol Mag 104:487–505
Pedersen GK, Bromley RG (2006) *Ophiomorpha irregulaire*, rare trace fossil in shallow marine sandstones, Cretaceous Atane Formation, West Greenland. Cret Res 27:964–972
Pemberton SG, Frey RW (1982) Trace fossil nomenclature and the *Planolites-Palaeophycus* dilemma. J Paleontol 56:843–881
Pemberton SG, Frey RW (1984) Ichnology of storm-influenced shallow marine sequence: Cardium Formation (Upper Cretaceous) at Seebe, Alberta. In: Stott DF, Glass DJ (eds) The Mesozoic of Middle North America. Can Soc Petrol Geol Memoir 9:281–304
Pemberton SG, MacEachern JA (1995) The sequence stratigraphic significance of trace fossils: examples from the Cretaceous foreland basin of Alberta. In: Van Wagoner JC, Bertram G (eds) Sequence Stratigraphy of Foreland Basin Deposits: Outcrop and Subsurface Examples from the Cretaceous of North America. AAPG Memoir 64:429–470
Pemberton SG, MacEachern JA (1997) The ichnological signature of storm deposits: the use of trace fossils in event stratigraphy. In: Brett CE, Baird GC (eds) Paleontological Event Horizons: ecological and evolutionary implications. Columbia University Press, New York, pp 73–109
Pemberton SG, Frey RW, Bromley RG (1988) The ichnotaxonomy of *Conostichus* and other plug-shaped ichnofossils. Can J Earth Sci 25:866–892
Pemberton SG, Wighman DM (1992) Ichnological characteristics of brackish water deposits. In: Pemberton SG (ed) Applications of Ichnology to Petroleum Exploration. SEPM Core Workshop 17:141–167
Pemberton SG, MacEachern JA, Frey RW (1992a) Trace fossil facies models: environmental and allostratigraphic significance. In: Walker RG, James NP (eds) Facies Models: Response to Sea Level Change, pp. 47–72. Geological Association of Canada, St. John's
Pemberton SG, MacEachern JA, Frey RW (1992b) Ichnology and event stratigraphy: The use of trace fossils in recognizing tempestites. In: Pemberton SG (ed) Applications of Ichnology to Petroleum Exploration. SEPM Core Workshop 17:85–117
Pemberton SG, MacEachern JA, Saunders, T (2004) Stratigraphic applications of substrate-specific ichnofacies: delineating discontinuities in the rock record. In: McIlroy D (ed) The Application of Ichnology to Palaeoenvironmental and Stratigraphic Analysis. Geol Soc London Spec Publ 228:29–62
Pemberton SG, MacEachern JA, Dashtgard SE, Bann KL, Gingras MK, Zonneveld J-P (2012) Shorefaces. In: Knaust D, Bromley RG (eds) Trace Fossils as Indicators of Sedimentary Environments. Developments in Sedimentology 64:563–603. Elsevier, Amsterdam
Perillo MM, Best JL, Yokokawa M, Sekiguchi T, Takagawa T, Garcia MH (2014) A unified model for bedform development and equilibrium under unidirectional, oscillatory and combined-flows. Sedimentology 61:2063–2085
Plint AG (1991) High-frequency relative sea-level oscillations in Upper Cretaceous shelf clastics of the Alberta foreland basin: possible evidence of glacio-ustatic control? In: Macdonald DIM (ed) Sedimentation, Tectonics and Eustasy. IAS Spec Publ 12:409–428
Pollard JE, Goldring R, Buck SG (1993) Ichnofabrics containing *Ophiomorpha:* significance in shallow-water facies interpretation. J Geol Soc London 150:149–164
Polteau S, Hendriks BWH, Planke S, Ganerød M, Corfu F, Faleide JI, Midtkandal I, Svensen HS, Myklebust R (2016) The Early Cretaceous Barents Sea sill complex: distribution, 40Ar/39Ar

geochronology, and implications for carbon gas formation. Palaeogeogr Palaeoclimatol Palaeoecol 441:83–95
Price GD, Nunn EV (2010) Valanginian isotope variation in glendonite and belemnites from Arctic Svalbard: Transient flacial temperatures during the Cretaceous greenhouse. Geology 38:251–254
Price GD, Passey BH (2013) Dynamic polar climates in a greenhouse world: Evidence from clumped isotope thermometry of Early Cretaceous belemnites. Geology 41:923–926
Rampino MR, Self S (2015) Large igneous provinces and biotic extinctions. In: Sigurdsson H, Houghton B, Rymer H, Stix J, McNutt S (eds) The Encyclopedia of Volcanoes, 2nd edn. Elsevier, Amsterdam, pp 1049–1158
Raychaudhuri I, Pemberton SG (1992) Ichnologic and sedimentologic characteristics of open marine to storm dominated restricted marine settings within the Viking/Bow Island formations, south-central Alberta. In: Pemberton SG (ed) Applications of Ichnology to Petroleum Exploration. SEPM Core Workshop 17:119–139
Reading HG, Collinson JD (1996) Clastic coasts. In: Reading HG (ed) Sedimentary environments: processes, facies and stratigraphy. Blackwell Science, Oxford, pp 154–231
Reineck H-E, Singh IB (1975) Depositional sedimentary environments, 2nd edn. Springer-Verlag, Berlin, p 439
Rosenzweig C, Iglesias A, Yang XB, Epstein PR, Chivian E (2001) Climate change and extreme weather events: Implications for food production, plant diseases, and pests. Glob Chan Hum Health 2:90–104
Savrda CE (1992) Trace fossils and benthic oxygenation. In: Maples CG, West RR (eds) Trace Fossils. Paleontol Soc Short Course Lecture Notes 5:172–196
Savrda CE (1995) Ichnologic applications in paleoceanographic, paleoclimatic, and sea level studies. Palaios 10:565–577
Savrda CE, Bottjer DJ (1987) The exaerobic zone: a new oxygen deficient marine biofacies. Nature 327:54–56
Savrda CE, Bottjer DJ (1989) Trace fossil model for reconstructing oxygenation histories of ancient marine bottom waters: application to Upper Cretaceous Niobrara Formation. Colorado Palaeogeogr Palaeoclim Palaeoecol 74:49–74
Savrda CE, Bottjer DJ (1991) Oxygen-related biofacies in marine strata: an overview and update. In: Tyson RV, Pearson TH (eds) Modern and Ancient Continental Shelf Anoxia. Geol Soc London Spec Publ 58:201–219
Savrda CE, Krawinkel H, McCarthy FMG, McHugh CMG, Olson HC, Mountain G (2001) Ichnofabrics of a Pleistocene slope succession, New Jersey margin: relations to climate and sea-level dynamics. Palaeogeogr Palaeoclim Palaeoecol 171:41–61
Schlirf M, Uchman A (2005) Revision of the ichnogenus *Sabellarifex* Richter, 1921, and its relationship to *Skolithos* Haldeman, 1840, and *Polykladichnus* Fürsich, 1981. J Syst Palaeontol 3:115–131
Scotese CR, Song H, Mills BJW, van der Meer DG (2021) Phanerozoic paleotemperatures: the Earth's changing climate during the last 540 million years. Earth-Sci Rev. https://doi.org/10.1016/j.earscirev.2021.103503
Seilacher A (1955) *Spuren und Fazies* im Unterkambrium. In: Schindewolf O, Seilacher A (eds) Beiträge zur Kenntnis des Kambriums in der Salt Range (Pakistan). Akad. Wissensch. Literat. Mainz, Abh. Math.-naturwissensch, 10:261–446
Seilacher A (1964) Biogenic sedimentary structures. In: Imbrie J, Newell N (eds) Approaches to paleoecology. Wiley, New York, pp 296–316
Seilacher A (1967) Bathymetry of trace fossils. Mar Geol 5:413–428
Seilacher A (2007) Trace fossil analysis. Springer-Verlag, Berlin, p 226
Sheremet A, Mehta AJ, Liu B, Stone GW (2005) Wave-sediment interaction on a muddy inner shelf during Hurricane Claudette. Estuar Coast and Shelf Sci 63:225–233
Šimo V, Olšavský M (2007) *Diplocraterion parallelum* Torell, 1870, and other trace fossils from the Lower Triassic succession of the Drienok Nappe in the Western Carpathians. Slovakia Bull Geosci 82:165–173
Snedden JW, Nummedal D, Amos AF (1988) Storm- and fair-weather combined flow on the central Texas continental shelf. J Sed Petrol 58:580–595
Stanistreet IG, Le Blanc SG, Cable AB (1980) Trace fossils as sedimentological and paleoenvironmental indices in the Ecca Group (Lower Permian) of the Transvaal. Trans Geol Soc South Africa 83:333–344
Steel RJ, Gjelberg J, Helland-Hansen W, Kleinspehn KL, Nottvedt A, Larsen MR (1985) The Tertiary strike-slip basins and orogenic belt of Spitsbergen. In: Biddle KT, Christie-Blick N (eds) Strike-Slip Deformation, Basin Formation and Sedimentation. SEPM Spec Publ 37:339–359
Steel RJ, Worsley D (1984) Svalbard's post-Caledonian strata; an atlas of sedimentation patterns and palaeogeographic evolution. In: Spencer AM (ed) Petroleum geology of the North European Margin. Graham and Trotman, London, pp 109–135
Stone GW, Xu JP, Zhang X (1995) Estimation of the wave field during Hurricane Andrew and morphological change along the Lousiana coast. J Coast Res 21:234–253
Sturesson U, Dronov A, Saadre T (1999) Lower Ordovician iron ooids and associated oolitic clays in Russia and Estonia: a clue to the origin of iron oolites? Sed Geol 123:63–80
Sturesson U, Heikoop JM, Risk MJ (2000) Modern and Palaeozoic iron ooids—a similar volcanic origin. Sed Geol 136:137–146
Swift DJP, Hudelson PM, Brenner RL, Thompson P (1987) Shelf construction in a foreland basin: storm beds, shelf sandbodies, and shelf-slope depositional sequences in the Upper Cretaceous Mesaverde Group, Book Cliffs, Utah. Sedimentology 34:423–457
Swinth AAG (2013) A Sedimentological and Petrographical Investigation of the Todalen Member and the Boundary Beds of the Endalen Member within the Firkanten Formation (Paleocene) in the Central Basin of Spitsbergen, Svalbard. Unpubl. PhD Thesis, Norwegian University of Science and Technology, Trondheim, 163 pp
Tarduno JA, Brinkman DB, Renne PR, Cottrell RD, Scher H, Castillo P (1998) Evidence for extreme climatic warmth from Late Cretaceous Arctic vertebrates. Science 282:2241–2244
Taylor AM, Goldring R (1993) Description and analysis of bioturbation and ichnofabric. J Geol Soc London 150:141–148
Taylor AM, Goldring R, Gowland S (2003) Analysis and application of ichnofabrics. Earth-Sci Rev 60:227–259
Tillman RW (1985) The Tocito and Gallop Sandstones, New Mexico: a comparison. In: Tillman RW, Swift DJP, Walker RG (eds) Shelf Sands and Sandstone Reservoirs. SEPM Short Course Lecture Notes 13:135–241
Torsvik TH, Carlos D, Mosar J, Cocks RM, Malme TN (2002) Global reconstructions and North Atlantic paleogeography 440 Ma to recent. In: Eide EA (ed) BATLAS – Mid-Norway Plate Reconstruction Atlas with Global and Atlantic Perspectives, pp. 18–39. Geological Survey of Norway (NGU), Trondheim
Torsvik TH, Smethurst MA, Burke K, Steinberger B (2006) Large igneous provinces generated from the margins of the large low-velocity provinces in the deep mantle. Geophys J Int 167:1447–1460
Torsvik TH, Müller RD, Van der Voo R, Steinberger B, Gaina C (2008) Global plate motion frames: Toward a unified model. Rev Geophys 46:RG3004. https://doi.org/10.1029/2007RG000227
Traykovski P, Geyer WR, Irish JD, Lynch JF (2000) The role of wave-induced density-driven fluid mud flows for crossshelf transport on the Eel River continental shelf. Cont Shelf Res 20:2113–2140

Trowbridge JH, Kineke GC (1994) Structure and dynamics of fluid muds on the Amazon continental shelf. J Geophys Res 99:865–874

Uchman A (1995) Taxonomy and palaeoecology of flysch trace fossils: The Marnoso Arenacea Formation and associated facies (Miocene, Northern Apennines, Italy). Beringeria 15:115–115

Uchman A (1998) Taxonomy and ethology of flysch trace fossils: a revision of the Marian Książkiewicz collection and studies of complementary material. Ann Soc Geol Pol 68:105–218

Uchman A (2009) The *Ophiomorpha rudis* ichnosubfacies of the *Nereites* ichnofacies: characteristics and constraints. Palaeogeogr Palaeoclim Palaeoecol 276:107–119

Uchman A, Nemec W, Ilgar A, Messina C (2007) Lacustrine trace fossils and environmental conditions in the early Miocene Ermenek Basin, southern Turkey. Ann Soc Geol Pol 77:123–139

Uchman A, Bąk K, Rodrígues-Tovar FJ (2008) Ichnological record of deep-sea palaeoenvironmental changes around the Oceanic Anoxic Event 2 (Cenomanian–Turonian boundary): an example from the Barnasiówka section, Polish Outer Carpathians. Palaeogeogr Palaeoclim Palaeoecol 262:61–71

Vickers ML, Price GD, Jerrett RM, Sutton P, Watkinson MP, FitzPatrick M (2019) The duration and magnitude of Cretaceous cool events: evidence from the northern high latitudes. GSA Bull. https://doi.org/10.1130/B35074.1

Vossler SM, Pemberton SG (1988) *Skolithos* in the Upper Cretaceous Cardium Formation: an ichnofossil example of opportunistic ecology. Lethaia 21:351–362

Vossler SM, Pemberton SG (1989) Ichnology and paleoecology of offshore siliciclastic deposits in the Cardium Formation (Turonian, Alberta, Canada). Palaeogeogr Palaeoclim Palaeoecol 74:217–229

Walker RG (1984a) General introduction: facies, facies sequences and facies models. In: Walker RG (ed) Facies Models. 2nd edn, Geosci Can Repr Ser 1:1–9

Walker RG (1984b) Shelf and shallow marine sands. In: Walker RG (ed) Facies Models. 2nd edn, Geosci Can Repr Ser 1:141–170

Wang T, 11 co-authors (2022) Ice sheet expansion in the Cretaceous greenhouse world. Paleoelev Paleoenvir. https://doi.org/10.21203/rs.3.rs-1755905/v1

Weissert H, Lini A (1991) Ice age interludes during the time of Cretaceous greenhouse climate. In: Müller DW, McKenzie JA, Weissert H (eds) Controversies in Modern Geology. Academic Press, London, pp 173–191

Wells JT (1989) *In situ* measurements of large aggregates over a fluid mud bed. J Coast Res SI5:75–86

Wetzel A, Bromley RG (1994) *Phycosiphon incertum* revisited: *Anconichnus horizontalis* is junior subjective synonym. J Paleontol 68:1396–1402

Wilkinson I, Riding J (2007) The Cretaceous greenhouse world. Earthwise 24:32–33

Worsley D (2008) The post-Caledonian development of Svalbard and the western Barents Sea. Polar Res 27:298–317

Yokokawa M, Masuda F, Endo N (1995) Sand particle movement on migrating combined-flow ripples. J Sed Res A65:40–44

Ziegler AM, Raymond AL, Gierlowski TC, Horrell MA, Rowley DB, Lottes AL (1987) Coal, climate and terrestrial productivity: The present and Early Cretaceous compared. In: Scott AC (ed) Coal and Coal-bearing Strata. Geol Soc London Spec Publ 32:25−49

Ziegler PA (1988) Evolution of the Arctic–North Atlantic and the Western Tethys. AAPG Memoir 43, 198 pp

Zonneveld J-P, Gingras MK (2013) The ichnotaxonomy of vertically oriented, bivalve-generated equilibrichnia. J Paleontol 87:243–253

Zonneveld J-P, Pemberton SG (2003) Ichnotaxonomy and behavioral implications of Lingulide-derived trace fossils from the Lower and Middle Triassic of Western Canada. Ichnos 10:25–39

Zonneveld J-P, Beatty TW, Pemberton SG (2007) *Lingulide* brachiopods and the trace fossil *Lingulichnus* from the Triassic of western Canada: implications for faunal recovery after the End-Permian mass extinction. Palaios 22:74–79